energies

Special Issue Reprint

Sustainable Shared Mobility

Current Status and Future Prospects

Edited by
Katarzyna Turoń

mdpi.com/journal/energies

MDPI

Sustainable Shared Mobility: Current Status and Future Prospects

Sustainable Shared Mobility: Current Status and Future Prospects

Editor

Katarzyna Turoń

MDPI

Basel • Beijing • Wuhan • Barcelona • Belgrade • Novi Sad • Cluj • Manchester

Editor
Katarzyna Turoń
Silesian University of Technology
Katowice
Poland

Editorial Office
MDPI
St. Alban-Anlage 66
4052 Basel, Switzerland

This is a reprint of articles from the Special Issue published online in the open access journal *Energies* (ISSN 1996-1073) (available at: https://www.mdpi.com/journal/energies/special_issues/Sustainable_Shared_Mobility).

For citation purposes, cite each article independently as indicated on the article page online and as indicated below:

Lastname, A.A.; Lastname, B.B. Article Title. *Journal Name* **Year**, *Volume Number*, Page Range.

ISBN 978-3-0365-8908-4 (Hbk)
ISBN 978-3-0365-8909-1 (PDF)
doi.org/10.3390/books978-3-0365-8909-1

Contents

About the Editor

Katarzyna Turoń

Katarzyna Turoń, Ph.D., is an Assistant Professor in the Department of Road Transport, Faculty of Transport and Aviation Engineering, Silesian University of Technology, Katowice, Poland. She is the author and co-author of over one hundred scientific publications as well as the laureate of numerous awards and scholarships, e.g., Division IV (Engineering Sciences) Award of the Polish Academy of Sciences, University of Oxford—Global Challenges in Transport Program Scholarship, iRAP Women in Engineering Training Grant and Visegrad Fund Scholarships. She has also been a participant in international internships at the following universities: Shanghai Jiao Tong University, Comenius University Bratislava, Budapest University of Technology and Economics. Her scientific interests combine the issues of sustainable development in transport, in particular shared mobility, and issues of mobility management and innovation.

Preface

The sustainable new mobility market is changing very rapidly. In recent years, a great number of solutions related to new mobility such as shared mobility systems, implementing and using vehicles with alternative drives or modern systems based on advanced digitization of mobility as a service have appeared in cities. With the emergence of new transport services, numerous problems began to arise related to their proper adaptation to both the current transport systems and the requirements of society. In response to this, large imbalances appeared between the offered mobility systems, service providers and scales of the range of the offered solutions. However, in connection with the trend of sustainable transport advancement, electromobility development and the need to change behavior in the mobility of society, there is a need for constant monitoring, improvement, and optimization of services operating in a new mobility market. This need and the related challenges and research gaps regarding new mobility have been addressed by the authors of the works that make up this book. This book provides a valuable resource for researchers, practitioners, and policymakers who are interested in the challenges and opportunities associated with the development of new mobility solutions, especially shared mobility systems.

Katarzyna Turoń
Editor

energies

MDPI

Article

E-Scooter Micro-Mobility Application for Postal Service: The Case of Turkey for Energy, Environment, and Economy Perspectives

Yunus Emre Ayözen [1], Hakan İnaç [2], Abdulkadir Atalan [3,*] and Cem Çağrı Dönmez [4]

[1] Strategy Development Department, Ministry of Transport and Infrastructure, 06338 Ankara, Turkey
[2] Investment Management & Control Department, Strategy Development Department, Ministry of Transport and Infrastructure, 06338 Ankara, Turkey
[3] Faculty of Engineering, Gaziantep Islam Science and Technology University, 27260 Gaziantep, Turkey
[4] Department of Industrial Engineering, Marmara University, 34722 Istanbul, Turkey
* Correspondence: abdulkadiratalan@gmail.com

Abstract: In this research, the advantages of the e-scooter tool used in the mail or package delivery process were discussed by considering the Turkish Post Office (PTT) data in the districts of Istanbul (Kadıköy, Üsküdar, Kartal, and Maltepe) in Turkey. The optimization Poisson regression model was utilized to deliver the maximum number of packages or mails with minimum cost and the shortest time in terms of energy consumption, cost, and environmental contribution. Statistical and optimization results of dependent and independent variables were calculated using numerical and categorical features of 100 e-scooter drivers. The Poisson regression analysis determined that the e-scooter driver's gender ($p \mid 0.05 < 0.199$) and age ($p \mid 0.05 < 0.679$) factors were not effective on the dependent variable. We analysed that the experience in the profession (tenure), the size of the area responsible, and environmental factors is effective in the e-scooter distribution activity. The number of packages delivered was 234 in a day, and the delivery cost per package was calculated as 0.51 TL (Turkish Lira) for the optimum values of the dependent variables. The findings show that the choice of e-scooter vehicle in the mail or package delivery process is beneficial in terms of time, cost, energy, and environmental contribution in districts with higher population density. As the most important result, the operation of e-scooter vehicles with electrical energy shows that it is environmentally friendly and has no CO_2 emission. The fact that the distribution of packages or mail should now turn to micro-mobility is emerging with the advantages of e-scooter vehicles in the mail and package delivery. Finally, this analysis aims to provide a model for integrating e-scooters in package or mail delivery to local authorities, especially in densely populated areas.

Keywords: micro-mobility; e-scooter; postal service; Poisson regression; optimization; energy; cost; environment

Citation: Ayözen, Y.E.; İnaç, H.; Atalan, A.; Dönmez, C.Ç. E-Scooter Micro-Mobility Application for Postal Service: The Case of Turkey for Energy, Environment, and Economy Perspectives. *Energies* **2022**, *15*, 7587. https://doi.org/10.3390/en15207587

Academic Editor: Katarzyna Turoń

Received: 22 September 2022
Accepted: 11 October 2022
Published: 14 October 2022

1. Introduction

Micro-mobility seems to be a useful strategy for cities that want to reduce single-person vehicle journeys and improve multimodal amenities [1]. Since the micro-mobility revolution is still in its infancy, it is an important topic of discussion in the literature, especially with the mobility sector changing rapidly and moving away from trend vehicle ownership, causing uncertainty about how this sector will develop to arise [2,3].

Entrepreneurs and authorized institutions are constantly searching for package and postal transportation vehicles. In particular, traffic density, one of the big cities' most significant problems, negatively affects package and mail delivery [4,5]. Significant congestion and dense urban structuring considerably impact distribution operations. To overcome such problems, although there are different opinions on the choice of distribution vehicles, enterprises and authorized institutions generally adopt scooter vehicles that are considered

within the scope of micro-mobility and work with electric energy [6]. The advantages and disadvantages of e-scooters in various aspects, such as social, environmental, economic, and energy effects, have been studied in the literature [7,8]. This study deals with the energy, economy, and ecological factors of e-scooter vehicle preference in package and mail delivery activities.

The latest strategy for city authorities that allows users to gain temporary access to modes of transport "as needed" is the use of delivery of a vehicle, bike, car, or another mode [9]. Electric micro-mobility systems such as e-scooters are used independently and as a shared service to provide sustainable mobility solutions for city logistics, particularly for certain classes of package delivery, user characteristics, and journey distances [10]. In particular, given the growth of e-commerce and the proliferation of new options for package delivery, it helps spread new alternatives such as e-scooters and speed delivery operations (such as bulk shipping) [10]. Conventional vehicles constitute 8–18% of urban traffic flows, significantly affecting the traditional vehicles (combivan, pick-up, etc.) used in package and mail distribution in traffic jams. However, it has been determined that the current road capacity has been reduced by 30% with micro-mobility applications [11,12].

Many advantages of using vehicles within the scope of micro-mobility in postal and package service have been discussed in the literature [13,14]. The most important benefit is that it provides fast and timely delivery of packages or mail with micro-mobility vehicles [15]. In one study, a project funded under the Smart Energy Europe program referred to micro-mobility tools for the fastest response in terms of time [16]. Another study mentioned the advantage of using e-scooter rides by calculating the average travel distance and running time of e-scooter journeys of 1.24 km and 7.55 min., respectively. However, another study determined that the time savings of e-scooter journeys in congested areas close to the city centre are limited, depending on the average cluster speed of e-scooter vehicles [17]. This study emphasizes that the time required to complete package and postal service operations is advantageous with the e-scooter [18].

Another advantage of using the e-scooter, which is among the micro-mobility tools, is that it keeps the energy consumption at a minimum level and reduces the distribution cost [19]. Most vehicles used in package or mail distribution activities need fuel energy [20]. Today, fuel type is more costly than electrical energy [21]. Gebhardt et al. argue that e-scooters used for package and mail delivery operations have lower land use consumption and significantly better energy efficiency than other motor vehicles [22]. In another study, it was determined that the e-scooter is more advantageous in terms of energy savings as a result of the test of e-scooter and other vehicles to estimate the amount of energy consumption in an area with a 0-degree slope [23]. In this study, the energy efficiency of the e-scooter delivery vehicle used in package and mail distribution is discussed in detail, especially in terms of cost.

Many studies explaining the effects of vehicles used for transportation or logistics purposes in many ways, especially in terms of environmental health and energy consumption, have been analysed with different methods. The common aspect of these studies draws attention to CO_2 emission, one of the environmental factors. A study aimed to overcome the many uncertainties and complexities in the mix of economy-energy-environment systems, random CO_2 emission, and water consumption control policies by integrating multi-objective programming, fuzzy linear programming, and multiple scenarios [24]. Another study focused on the environmental cost of CO_2 emissions, aiming to break the barrier of the CGE (the computable general equilibrium) model and provide researchers with a CGE model with available code and data [25]. As there is an important link between environmental factors and energy consumption, Miao et al. emphasized that CO_2 emissions, SO_2 emissions, and atmospheric environmental inefficiency caused by primary energy use are the main causes [26]. Another study applied a multi-sector and multi-site dynamic recursive computable general equilibrium model to reduce coal consumption in order to reduce CO_2 emissions to meet energy needs in the 2020–2030 period in China [27]. Using a multi-objective optimization model based on input–output analysis, Zhang et al.

investigated China's energy, water consumption, and CO_2 emissions values, including the high resolution of the country's electricity sector, in the period 2020–2030 [28]. Compared to studies dealing with the link between energy, cost, and environmental factors from different perspectives, this study also deals with the energy, cost, and environmental factors of e-scooter micro-mobility vehicle.

The environmental effects of e-scooter use are frequently discussed in the literature. At the beginning of environmental factors, the rate of CO_2 emission has been tested by researchers with a wide range. One study highlights that approximately 5.8 kt of CO_2 will be saved daily when e-scooter vehicles replace existing car trips [29]. Severengiz et al. investigated how using e-scooters for different purposes affect the crop greenhouse balance compared to alternative means of transportation by evaluating ecological factors [30]. Another study emphasizes that using e-scooters, among the smart mobility tools, will make urban life simpler, economical, and enjoyable with faster transportation, less congestion, and low CO_2 emissions. The same study found that e-scooters emit almost 45% less CO_2 than other vehicles, emphasizing that about 90% of people are exposed to air pollution [31]. According to the LCA results of personal e-scooter use, Moreau et al. calculated the environmental impact as approximately 67 g of CO_2 emissions [32]. In another study, the authors highlight a net reduction in environmental effects when the e-scooter vehicle replaces the personal automobile vehicle, finding with Monte Carlo simulation models that 65% of the life-cycle greenhouse gas emissions associated with e-scooter use were higher than the modified set of transport models. In this study, the effects of e-scooters and other delivery vehicles on the environment were investigated by using e-scooter vehicles for package and mail distribution by government units [33].

With temporary delivery due to the increase in volume transported, operations involving a key logistics player often require electric-powered vehicles [34]. Scientific studies emphasized that tricycles or e-scooter vehicles provide significant advantages [35–37]. However, in using these vehicles, they must operate within the framework of some rules following the rules of the people and society [6]. In particular, in cities with crowded settlements, the authority departments need to exchange information with e-scooter companies to guide many driving rules and regulations, such as driving in the wrong direction, right of way, and speed [14]. In general, it can be said that adopting e-scooter vehicles in package and mail delivery significantly impacts the delivery system [36]. If generalization is made with the following important advantages in e-scooter preference, e-scooter vehicles:

- are very suitable for providing transit first and last mile connections due to their low cost and high flexibility [38],
- almost minimizing delivery time as long as a parking option is available [38],
- have short charging cycles, which usually take place at night, and have the flexibility to recharge [39];
- the range distance is 30–90 km,
- easy supply of spare parts, such as additional provinces, so that distribution operation are not disrupted,

and offer many advantages. Another advantage of e-scooter vehicle preference is customer and rider satisfaction [14,40]. According to research conducted in northern European and North American countries over the last decade, user satisfaction with electric scooters and the service delivery process is high overall [41–43]. A study conducted in the Netherlands observed user satisfaction in the service delivery process. It was discovered that user happiness was associated with the length of actual waiting times [44]. Chinese customers seem to prefer e-scooters over public transport because of customers' demand for more flexible, comfortable, and enjoyable (at a reasonable price) mobility [45]. This has led to an increase in the production of e-scooter vehicles that has contributed to customer satisfaction in recent years [46]. All these results mean that micro-mobility vehicles such as e-scooters will have more of a place in human life [47].

Scientific studies investigating the many advantages of using micro-mobility vehicles for different purposes in terms of environmental, cost, and energy have used different

methods. Detailed information about the scientific studies in Table 1 is shared in order to reveal the difference between the Poisson optimization regression model method used in this study and other studies. The best statistical optimization model is the Poisson regression model method, especially for modelling situations that indicate the importance of the results of the objectives or output parameters in a subject [48]. In particular, we preferred methods for non-negative integer-valued variables that count information, such as specific counting data (such as the number of e-scooter vehicles and drivers) and the number of events occurring in a given time period (such as the number of packets delivered). Especially in a statistical or optimization model, if the values of the objective function or output parameter are positive and integer, the Poisson regression optimization model is preferred [49]. We contributed to obtaining numerical data of objective functions or output variables of micro-mobility vehicle applications (such as e-scooter, e-bike) with certain parameters with the statistical optimization model developed.

Table 1. Detailed information about the aims, methods, and factors of studies related to micro-mobility approaches and this study.

Source	Purpose (s)	Factor (s)	Method (s)
[50]	To investigate the factors affecting the use of electric scooter sharing service by university students	Intention, Perceived behaviour control, attitude, subjective norm, compatibility, environmental value, awareness–knowledge	Factor analysis and structural equation modelling
[51]	Adoption of shared micro-mobility in the city of Zurich	Person-specific socio-demographic, household-specific socio-demographic, person-specific mobility questions	Maximum simulated likelihood
[52]	Review of uses of a new micro-mobility service	Health and environmental impacts, policy implications	Literature review
[53]	Building a new multi-protocol tag switching (MPLS) based network architecture that implements micro-mobility	Tunnel-based, routing-based schemes	Label edge mobility agent
[54]	Creating a potential data source for micro-mobility research and applications	A range of temporal, spatial, and statistical mobility descriptors	Data processing framework
[55]	Investigating the impact of COVID-19 on micro-mobility	Relax, health, speed, price, availability	Independence test, correspondence analysis
[56]	Establish accessibility increase measures for micro-mobility services	General transit feed specification (GTFS), the locations of available of dockless vehicle, the empirical transit usage	Accessibility increment, spatiotemporal analyses
[57]	Exploring the energy limits of shared micro-mobility adoption	Energy impacts: age, time of day, trip purpose, area types, travel party size, tour mode restriction	Sensitivity statistical analysis
[19]	Design of a pilot device to study the energy conversion and storage achieved by converting a micro-mobility device to a stationary exercise bike with a piezoelectric generator	Energy, environmental factors, piezoelectric materials	The piezoelectric material
[58]	To clarify how the system, regime, and niche dynamics that make up the MLP are interrelated	Landscape, regime, niche	Sociotechnical transition and the multi-level perspective
This Study	To deliver the maximum number of packages or mails with minimum cost and the shortest time	Cost, energy, environmental aspects	Poisson regression optimization model

This study presents a case study of the advantages of using e-scooters vehicles in package and mail delivery services in Istanbul, Turkey. PTT provides package and mail distribution service with a total of 1915 vehicles throughout Istanbul megacity. Turkey postal service unit provides postal and package service, using approximately 1046 large vehicles (trucks, bus, van, combivans, minibus, etc.) and 655 motorbikes and other mobile vehicles. The use of e-scooters is used in four districts of Istanbul with a dense population. Around 161 e-scooters are allocated in these districts for postal and package services. The ratio of e-scooters to other vehicles is approximately 8.41% [59].

In this study, many independent parameters are considered to measure the effects of e-scooter vehicle choice in terms of environmental, economy (cost), and energy. These parameters are defined as the e-scooter driver's gender, age, professional experience, area of responsibility, and environmental factors. This study consists of five different sections. The literature review about the advantages and disadvantages of using e-scooter within the scope of micro-mobility is discussed in the introduction part of the study. The methodology developed for the study is discussed in the second section. The numerical results of the study are shared in the third section. Discussion of significant findings is debated in the fourth part of the study. The conclusion of the study is mentioned in the last part of the study.

2. Materials and Methods

This study aims to calculate the optimum values of the objective functions by developing optimization Poisson regression models using the data of the e-scooter application for package and mail distribution in four different regions of Istanbul with the highest population density. This part of the study consists of three main parts: data preparation, statistical analysis, and development of optimization models.

2.1. Data

PTT (International Logistics Services), which has been using the bicycle for years (one of the micro-mobility vehicles, which is an environmentally friendly and more efficient alternative in urban use), has started to use the e-scooter in urban distribution/delivery operations as of July 2021. Kadıköy, Üsküdar, Kartal, and Maltepe Postal Distribution Directorates affiliated with PTT Istanbul Regional Directorate were selected as pilots for the e-scooter, which is more suitable for the distribution of registered-unregistered mail and cargo-courier shipments under 2 kg/decis. The total population of these regions is approximately 2.02 million, constituting 12.73% of Istanbul's population as of 2021. The population density of these districts is 10,728 people per km squared. The pilot chosen areas for mail delivery with the e-scooter are illustrated in Figure 1.

One hundred e-scooters accompany one hundred drivers (each scooter belongs to only one driver, e-scooter vehicles are not shared between drivers) working in plot areas. The relationship between the age and occupational experience of 100 drivers employed in packages and mail delivery based on the delivery time by e-scooter is shown in Figure 2.

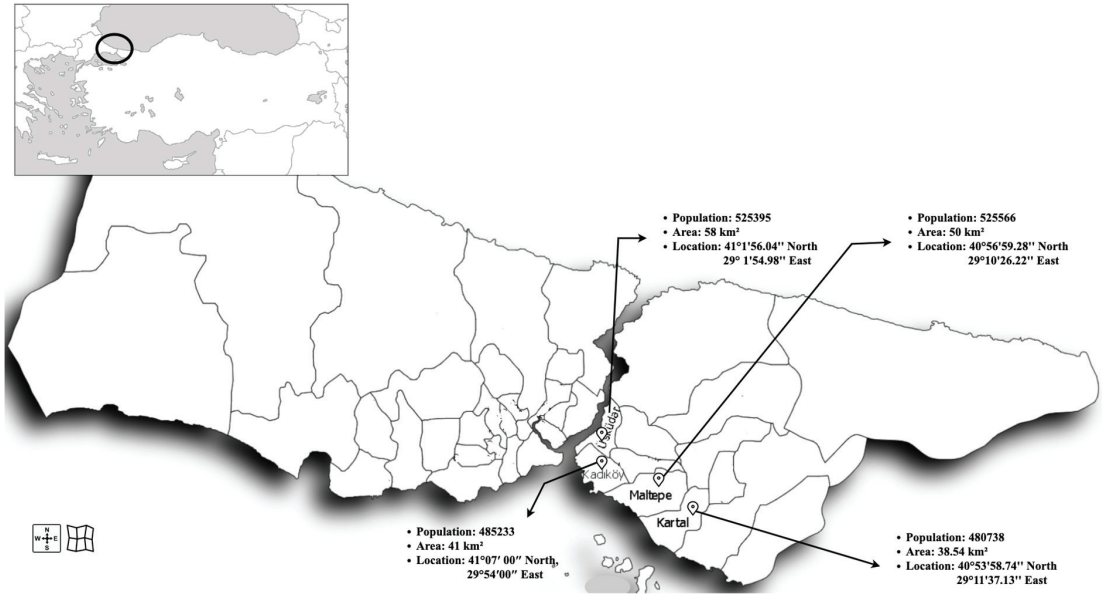

Figure 1. Plot zones selected for packages delivered with the e-scooter application.

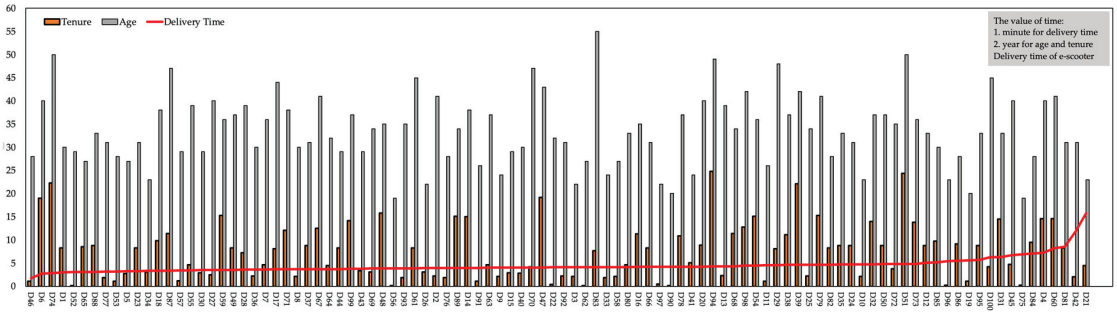

Figure 2. The sort of the delivery drivers based on the delivery time by e-scooter.

The technical specifications of the preferred e-scooter ranges for the distribution process are shared in Figure 3.

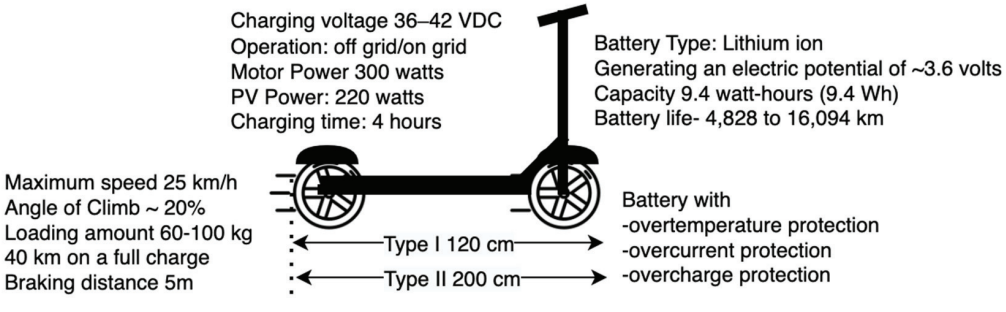

Figure 3. Technical specifications of the e-scooter.

A total of 3000 data points were used, taking into account the 30-day working time of each driver. The average daily distribution numbers of 100 riders with the e-scooter are shown in Figure A1 in Appendix A Section. During the period in which the data were taken into account, a total of 351.180 distributions were made using e-scooters. The maximum distribution amount was computed as 8454, and the minimum distribution amount was calculated as 915. The monthly average distribution amount of these drivers was computed as 3511.8 packages.

For this study, the economic, energy, and environmental factors of both the e-scooter and other vehicles are utilized to compare the e-scooter distribution vehicle with other distribution vehicles. The monthly rental price of the vehicles, the energy (fuel and electric) used, the distribution flow, CO_2 emission rates, and distance information are discussed in this study. The vehicles used in package distribution are given the combivan vehicle with a volume of 4 m^3, and the motorcycle and e-scooter vehicles were used in the distribution at the PTT. Although many factors affect the performance of drivers in distribution planning with e-scooters, seven different parameters are considered in this research. Qualitative information about each parameter, such as variable type, units, status of variables, notation, and descriptive expressions, is shared in Table 2.

Table 2. Indicators of the packages delivered by the e-scooters.

Variables	Units	Status	Notation	Description
Number of packages delivered	Number, (Integer)	Response	y_p	The average number of packages delivered per hour by a worker
The total cost of distribution *	TL	Response	y_c	The cost of distribution of packages to the administration includes energy, rent, and personnel expenses.
Age	Year	Input	x_{age}	Age information of employees involved in the e-scooter package distribution project
Gender	Categorical	Input	x_{gender}	Gender information of employees engaged in the e-scooter package distribution project
Tenure in the profession	Year	Input	x_{tenure}	Working times of employees involved in the e-scooter package delivery project in the delivery job (before the e-scooter project)
Area	Km^2	Input	x_{area}	Area sizes for which the employees involved in the e-scooter package distribution project are responsible
CO_2 Emission	g/km	Input	x_{CO_2}	The amount of CO_2 emissions per package

* Maintenance, repair, and insurance costs belong to the contractor company.

The driver's age, gender, and experience (tenure) factors, which are among the decision variables of the study and affect the number of packages distributed daily and monthly, are only for drivers using e-scooters. In addition, the amount of CO_2 emission, an environmental factor that is thought to affect the amount of distribution, was also included in this study. The area for which each driver is responsible is taken into account in km^2. Descriptive statistics of the data used for the decision variables are discussed in Table 3. Descriptive statistics data such as sample size, mean, standard deviation, first and third quartiles, variance, kurtosis, and skewness were analyzed for the data set of this study.

Table 3. Descriptive statistics of the variables of the e-scooter distribution.

Variable	Decision Variable					Response Variables		
	x_{CO_2}	x_{age}	x_{tenure}	x_{area}	y_p	y_c Cost_e-S	Cost_m	Cost_c
Mean	33.51	7.326	0.468	0.054	3511.8	1791.0	10,535	73,748
SE Mean	0.761	0.595	0.032	0.002	91.500	46.700	275.0	1922
StDev	7.611	5.946	0.313	0.021	915.00	466.70	2745	19,216
Variance	57.92	35.36	0.098	0.001	83,728	21,778	7×10^6	3.69×10^8
CoefVar	22.71	81.17	66.99	39.04	26.060	26.060	26.06	26.06
Minimum	19.00	0.100	0.113	0.021	91,500	466.70	2745	19,215
Q1	28.00	2.200	0.271	0.045	3082.3	1571.9	9247	64,727
Median	33.00	7.450	0.353	0.050	3517	1793.7	10,551	73,857
Q3	38.75	11.05	0.565	0.057	3920	1999.2	11,760	82,320
Maximum	55.00	24.80	1.989	0.192	8454	4311.5	25,362	177,534
Range	36.00	24.70	1.876	0.171	7539	3844.9	22,617	158,319
IQR	10.75	8.850	0.294	0.012	837.8	427.30	2513	17,593
Mode (Male, Female)	31.00	8.300		0.051	(3497, 3638)	(1784, 1856)	(10,491, 10,914)	(73,437, 76,398)
N for Mode	8.00	8.00	0.00	3.000	2.00	2.00	2.00	2.00
Skewness	0.33	0.91	2.52	3.840	1.10	1.10	1.10	1.10
Kurtosis	−0.13	0.35	8.88	20.08	8.31	8.31	8.31	8.31

Variable abbreviations: Delivery cost by package or postal vehicles: Cost_e-S: e-Scooter cost, Cost_m: motorcycle cost, Cost_c: combivan cost. Statistical abbreviations: SE Mean, standard error mean; StDev, standard deviation; CoefVar, variance coefficient; Q1, the first quartile, Q3, the third quartile; IQR, interquartile range; N, number of samples.

Two methods, Poisson regression and response-optimization mathematical models, were used for the methodology of the study. Minitab-18 computer software, including statistical and optimization tools, was used to organize and analyze the raw data of the study [60]. There are theoretical explanations of the methods in the continuation of this section.

2.2. Statistical Analysis

The Poisson regression model, developed by Consul and Famoye (1992) and Famoye (1993), was used to model data for factors affected by a set of response variables [61]. The Poisson distribution regression model includes a series of statistical analyses for multiple-affected response variables and co-influencing variables in under- or over-dispersed count data. Generally, models are developed using maximum likelihood and moment methods in Poisson distribution regression analysis [62,63]. Poisson regression is one of the most preferred methods of analysis for modeling response variables with integer properties [64]. Poisson regression analysis was preferred because the data of the decision variables were integer in this study [65]. The vehicles (e-scooters) were used to make the distribution, and the number of packages and the drivers (human factor) who perform the distribution process represent the whole number. The Poisson regression model is formulated with the given by $f(\mu_i, \alpha, y_i)$ [61]:

$$f(\mu_i, \alpha, y_i) = \left(\frac{\mu_i}{1+\alpha*\mu_i}\right)^{y_i} * \frac{(1+\alpha*y_i)^{y_i-1}}{1+\alpha*\mu_i} * \exp\left[\frac{-\mu_i*(1+\alpha*y_i)}{1+\alpha*\mu_i}\right] \quad (1)$$

where y_i donates the response or dependent variable of the regression model with $\{i = 1, 2, \ldots, n\}$. Independent or decision variables are defined as x_i and the mean and variance of the Poisson distribution are the same as:

$$E(y_i) = Var(y_i) = \mu_i \tag{2}$$

where the expected mean and variance value is defined as $E(y_i)$ and $Var(y_i)$, respectively.

$$\mu_i = \mu_i(x_i) \tag{3}$$

then;

$$\mu_i(x_i) = \exp(\sum x_{ij}\beta_j),\ j = (1, 2, \ldots, k) \tag{4}$$

where β_j represents the coefficient of independent variables of the regression equation [66]. In order to calculate the maximum likelihood estimator in the Poisson regression model, the response variable y_i must be in the form of non-negative integers (or count data). In this study, since the response variables are integers, the maximum likelihood function is given as follows [67]:

$$(y_i) = \exp\left[\frac{-\mu_i * (\mu_i)^{y_i}}{y_i}\right] \tag{5}$$

s.t.

$$\mu_i > 0 \tag{6}$$

where the likelihood function ($l(\beta_j)$) of the Poisson regression model is created as [67]:

$$l(\beta_j) = \prod_{i=1}^{n} \frac{\exp(-\mu_i * (\mu_i)^{y_i}}{y_i!} \tag{7}$$

then;

$$l(\beta_j) = \frac{\prod_{i=1}^{n}(\mu_i)^{y_i} \exp(-\sum_{i=1}^{n}\mu_i)}{\prod_{i=1}^{n} y_i!} \tag{8}$$

Approximate tests are considered for testing the adequacy of a Poisson distribution regression model. We adopted e-scooter delivery data to evaluate and analyze the performance of the response variables and other decision variables (independent factors) proposed in this study. In addition, as a result of Poisson regression statistical analysis, the optimum values of the response functions and the decision variables were calculated using the restrictive data belonging to the decision variables.

2.3. Optimization Models

Optimization (mathematical) modeling is generally defined as expressing real-life problems with equations. Optimization models consist of four different steps: determination of decision variables, the definition of objective functions, creation of limits of decision variables, and regulation of sign directions of decision variables. Independent factors (or decision variables) are based on Poisson distribution regression analysis and optimization models. The objective function equation of an optimization model given the decision variable as x_{ij} is formed as follows [68]:

$$\text{objective}_{\text{o}} f = \sum_{i=1}^{n}\sum_{j=1}^{m} c_i(x_{ij}) \tag{9}$$

where c_i represents the coefficient of the decision variables with $\{i = 1, 2, \ldots, n\}$. There are two versions of x, maximum and minimum. This version is preferred according to the purpose of the problem. Generally, the minimum preference is for the cost or time, while the maximum preference is for high-value purposes such as annual income or production amount [69]. Each optimization model has a limit of decision variables. These limits

are defined as constraints in optimization models. In an optimization model, constraint equations are usually created as follows [70]:

$$\sum_{i=1}^{n}\sum_{j=1}^{m} a_i(x_{ij}) \begin{cases} \geq \\ = v_l, \\ \leq \end{cases} \quad l = \{1, 2, \ldots, L\} \tag{10}$$

where a_i signifies the coefficient of the decision variables in the equations of the constraints. The values of the constraints' limit are denoted by v_l. The mixed-integer optimization model is created because some of the decision variables in the optimization models of this study are integers and others are natural numbers. The mixed-integer optimization model is constituted as [71]:

$$\text{objective}_{\text{o}} \quad f = x^t Q x + q^t x \tag{11}$$

s.t.

$$\begin{gathered} Ax = v \text{ (linear contsraints)} \\ l \leq x \leq u \text{ (bound contsraints)} \\ x^t Q_i x + {q_i}^t x \leq b_i \text{ (quadratic contsraints)} \\ \text{Some (or all) of } x \text{ values must be integer} \end{gathered} \tag{12}$$

The objective function of the optimization model of this study constitutes the equation obtained from the Poisson distribution regression model. Decision variables were defined as independent variables affecting the response factor. The mixed integer optimization model then turns out to be as follows [72]:

$$\text{objective}_{\text{maximize}} \{\text{Equation (11)}\} \tag{13}$$

s.t.

$$\begin{gathered} l \leq x_i \text{ (lower bound contsraints)} \\ x_i \leq u \text{ (upper bound contsraints)} \\ 0 \leq x_i, \text{ and integer} \end{gathered} \tag{14}$$

where, $x_i = \left\{ x_{age}, x_{gender}, x_{tenure}, x_{area}, x_{CO_2} \right\}$. The MILP problem presented in this article is essentially an optimization problem, where the aim is to maximize the number of distributed packages by taking into account the effect of independent variables and which provides a set of feasible solutions belonging to the solution set within the limits of the decision variables of the system to be optimized. The desirability functions measure the degree of importance of the feasible values of the optimization model. For all feasible output values of the objective functions determined by the desirability equations, we ensure that the values suitable for the design factors are found simultaneously so that the optimization model reaches an optimal solution [73]. Desirability values (d_i) are calculated according to the following formulation [74]:

for maximization problems:

$$d_i(y_i(x)) = \begin{cases} 0 & \text{if } y_i(x) < l_i \\ \left(\frac{y_i(x)-l_i}{u_i-l_i}\right)^{r_1} & \text{if } l_i \leq y_i(x) \leq u_i \\ 1 & \text{if } y_i(x) \geq u_i \end{cases} \tag{15}$$

for minimization problems:

$$d_i(y_i(x)) = \begin{cases} 1 & \text{if } y_i(x) < l_i \\ \left(\frac{u_i-y_i(x)}{u_i-l_i}\right)^{r_2} & \text{if } l_i \leq y_i(x) \leq u_i \\ 0 & \text{if } y_i(x) \geq u_i \end{cases} \tag{16}$$

for target values of the objective functions:

$$d_i(y_i(x)) = \begin{cases} 0 & \text{if } y_i(x) < l_i \\ \left(\frac{y_i(x)-l_i}{u_i-l_i}\right)^{r_1} & \text{if } l_i \leq y_i(x) \leq T_i \\ \left(\frac{u_i-y_i(x)}{u_i-l_i}\right)^{r_2} & \text{if } y_i(x) = T_i \\ & \text{if } T_i \leq y_i(x) \leq u_i \\ & \text{if } y_i(x) \geq u_i \end{cases} \quad (17)$$

where l_i and l_i are the upper and lower limit values of the desired response equation. The parameters of r_1 and r_1 express the importance of the response equations being close to the desired value [75]. We propose the limits of the independent variables for the plot regions, where the e-scooter application is planned with the Poisson distribution regression and optimization models we have developed.

3. Results

The numerical results of the study are discussed in this section. The statistical analyses and optimization results of the e-scooter data used for package and mail delivery were examined using the optimization Poisson regression distribution developed for the study. In addition, the numerical results were compared between the e-scooter vehicle and other distribution vehicles in terms of economic, environmental, and cost.

3.1. Statistical Results of Poisson Distribution Regression Analysis

Statistical data of the Poisson distribution regression analysis are given in Table 4. In the Poisson distribution regression analysis, data belonging to two dependent and five independent variables were used for statistical results. The regression analysis results for the dependent variable show that the independent factors have a significant effect with a p-value < 0.05. As a result of the statistical analysis, it has been determined that the amount of CO_2 emission from the five independent variables, the driver's experience in the profession (tenure), and the size of the area that the driver is responsible for distribution affect the number of packages distributed. The significance levels of x_{co2}, x_{tenure}, and x_{area} factors were calculated as 0.022, 0.001, and 0.001, respectively. The driver's experience in the profession (tenure) and the size of the area affect the cost of the packages distributed. The significance levels of x_{tenure}, and x_{area} factors were calculated as 0.0001, and 0.000, respectively. The effects of driver gender and age on dependent variables are limited based on the significance levels of the Poisson distribution.

Goodness-of-fit tests were used to determine whether the dataset used deviated in a way that the Poisson distribution did not predict. The model's data fit was assessed using the Pearson compatibility and Deviance tests. In these results, both goodness of fit tests had p values lower than the usual significance level of 0.05. Sufficient evidence has emerged to conclude that the number of predicted events does not deviate from the number of events observed. In addition, in terms of the accuracy and validity of the results of the Poisson distribution regression statistical analysis, the R-Squared (R-sq) and adjusted R-sq values for the packages delivered, which is a measure of goodness of fit for the model, were calculated as 90.24% and 90.21%, respectively. For the cost of the packages delivered, the value of the R-sq is computed as 90.24% and 90.19%, respectively.

Table 4. Poisson distribution regression analysis data of the e-scooter distribution.

	Term	Model	x_{CO_2}	x_{age}	x_{tenure}	x_{area}	x_{gender}	Deviance	Pearson
Packages/ Mails	SE Coef.	0.0123	0.0003	0.0004	0.0054	0.153	0.008		
	Z-Value	735.29	−2.29	−0.41	6.77	−113.41	−1.28		
	p-Value	0.0001	0.022	0.679	0.001	0.001	0.199	0.001	0.022
	VIF		1.67	1.69	1.04	1.06	1.01		
	R-Sq	0.9024							
	R-Sq(adj)	0.9021							
	DF	5.000	1.000	1.000	1.00	1.00	1.00	89.00	89.00
	Chi-Square	13,973.4	5.26	0.17	45.82	12,862	1.65	1954.8	2463
	Mean		33.51	7.326	0.468	0.054	33.51	21.964	27.67
	Estimate	9.0622	−0.0007	−0.0002	0.0364	−17.33	−0.01	1954.8	2463
Cost	SE Coef.	0.0173	0.00041	0.0005	0.0075	0.214	0.011		
	Z-Value	486.09	−1.64	−0.3	4.83	−80.99	−0.92		
	p-Value	0.0001	0.101	0.767	0.001	0.000	0.36	0.001	0.001
	VIF		1.670	1.69	1.04	1.06	1.01		
	R-Sq	0.9024							
	R-Sq(adj)	0.9019							
	DF	5.0000	1.00	1.000	1.00	1.00	1.00	89.00	89.000
	Chi-Square	7126.4	2.68	0.09	23.37	6559.7	0.84	996.9	1256.1
	Mean		33.51	7.326	0.468	0.0542	33.51	11.20	14.114
	Estimate	9.0500	−17.65	0.000	0.00	0.02	0.00	996.9	1256.1

SE Coef.: Coefficient of Standard Error, DF: Degree of Freedom, VIF: Variance Inflation Factor, R-Sq: R-squared, R-Sq (adj): Adjusted R-squared.

3.2. Comparison of the Economy, Energy, and Environmental Dimensions of the E-Scooter Model with Other Vehicles Used in the Package Distribution

In this section, we have analyzed the numerical results in terms of economic, energy, and environmental aspects so as to reveal the difference between the distribution provided by the e-scooter and the distribution operations performed with other vehicles. This section consists of three different subsections.

3.2.1. Cost Analyses

In package or mail distribution, main expenses such as personnel, insurance, energy, car rental, and packaging are included in the general costs. In this study, it is understood that many advantages are obtained regarding cost with the e-scooter application in package distribution. As a result of distribution made by e-scooters and other vehicles, there are some differences between energy and package distribution costs (for example, distribution of more packages with the same personnel wage) apart from the common expenses. Table 5 includes the costs depending on the number of packages distributed with e-scooters and other vehicles. The cost information in this table represents the total cost of a package to the administration.

Table 5. The vehicle types in terms of the economic dimension.

Vehicle Type	Number of Packets Distributed		Cost Per Package * (TL ***)	Total Cost of Packages Distributed (TL ***)		Savings (%)	
	Monthly	Daily		Monthly	Daily	Monthly	Daily
Combivan	1800	90	8.21	14,780.92	739.05	Base	Base
Motorcycle	1600	80	1.28	2049.46	102.47	86.13 *	86.13 *
E-scooter	1400	70	0.51	711.77	35.59	99.51 *, 96.49 **	95.18 *, 65.27 **

* Based on the Combivan, ** Based on the Motorcycle, *** TL: Turkish Lira.

We calculated that the delivery cost of a package with an e-scooter is 16 times more advantageous than a combivan and three times more than a motorcycle. Considering the daily distribution amounts, it was determined that the cost of distribution with the e-scooter decreased by 96.49% compared to the motorcycle and 99.51% compared to the combivan. Similarly, it was calculated that the cost of package distribution with a motorcycle decreased by 86.13% compared to a combivan. The hourly distribution amounts determined that the cost of distribution with the e-scooter decreased by 65.27% compared to the motorcycle and 95.18% compared to the combivan. Similarly, it was calculated that the cost of package distribution with a motorcycle decreased by 86.13% compared to a combivan. Depending on the package distribution quantity, the distribution costs of the package distribution vehicles are shown in Figure 4. The e-scooter's total distribution cost is minimal compared to other vehicles.

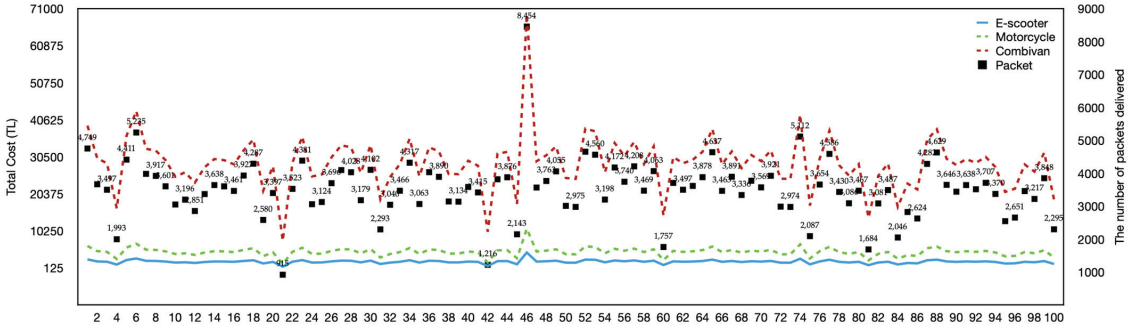

Figure 4. The total cost for a package delivered.

3.2.2. Energy Analyses

The type of energy required for the e-scooter is electrical energy. The fuel type meets the energy supply of other vehicles. For daily use, e-scooter batteries are made ready before working hours. An extra full battery is allocated to drivers in case of an unexpected situation during working hours. The difference between the amount of energy consumption of the e-scooter and other distribution vehicles is shown in Table 6.

Table 6. The vehicle types in terms of energy dimension.

Vehicle Type	Energy Type	Energy Cost (TL)			Savings (%)
		Monthly	Daily	Per Package	
Combivan	Fuel	3120	155.7	1.73	−95.95% * and −64.74 **
Motorcycle	Fuel	982.8	48.8	0.61	−88.52 * and +64.74 ***
E-scooter	Electric	99.3	4.9	0.07	Base

* Based on the E-Scooter, ** Based on the Motorcycle, *** Based on the Combivan.

Regarding energy, the advantage of using e-scooters in mail or package delivery is very high compared to other vehicles. While the use of a motorcycle is 64.74% advantageous compared to the combivan vehicle, it has an 88.52% disadvantage compared to the e-scooter. Similarly, it has been calculated that the use of combivan has a 64.74% disadvantage compared to the motorcycle vehicle and 95.95% compared to the e-scooter. The amount of energy consumption required for the e-scooter is less than other vehicles. For the use of e-scoter, energy consumption is ten times less than the amount of energy required for a motorcycle and almost 30 times less than the amount of energy required for a combivan. According to the number of packages distributed in a month, the amount of energy required varies according to the vehicles. The energy change rates based on the number of packages delivered are shown in Figure 5.

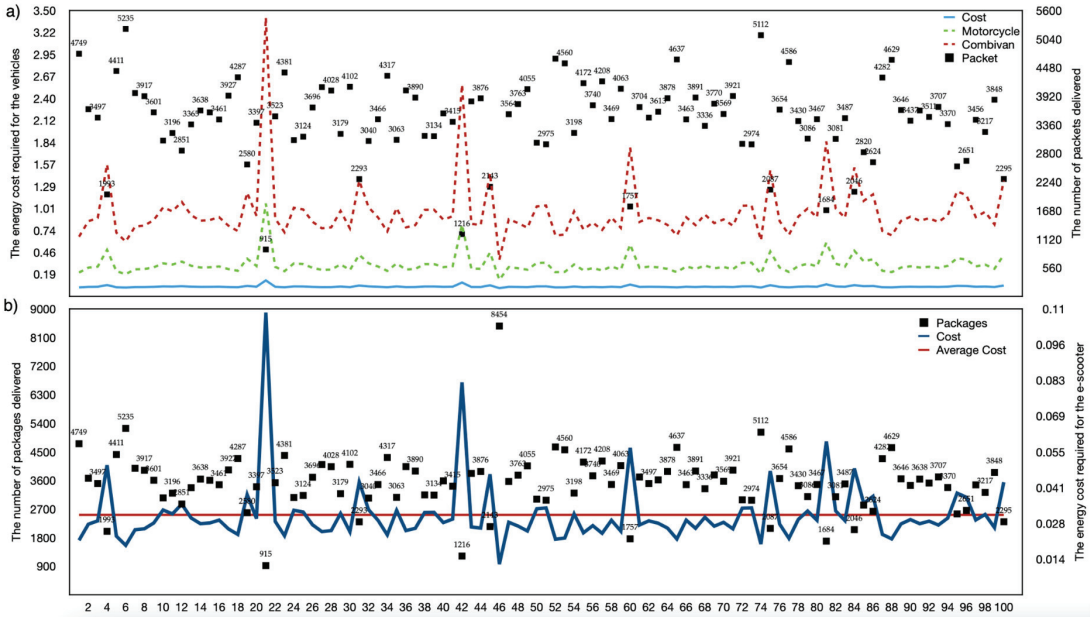

Figure 5. (**a**) The cost of energy required for a package delivered, (**b**) The number of packages or mails distributed with the e-scooter micro-mobility.

3.2.3. Environmental Analyses

The amount of CO_2 emissions, which is one of the environmental factors that affects the amount of package distribution, varies considerably between distribution vehicles. The operation of e-scooter vehicles with electrical energy is environmentally friendly and the amount of CO_2 emissions is very low. E-scooter use does not cause direct CO_2 emission. However, this study did not consider CO_2 emissions indirectly caused by e-scooter vehicles (e.g., battery charging, during the manufacturing process, transportation of e-scooter vehicles to users, etc.). The use of motorcycles and combivan vehicles in package distribution activities for many years has led to negative results in terms of environmental health.

The CO_2 emission amounts of the motorcycle and combivan distribution vehicles are compared to the e-scooter distribution vehicle since the emission amount of the e-scooter distribution vehicle is low (Parameters that indirectly cause CO_2 emissions from using the e-scooter vehicle were not considered, so the value of 0 was used in this study to reference the values of other vehicles). In the case of distribution by motorcycle, it has been calculated that the amount of CO_2 emission has a 190% disadvantage compared to the e-scooter delivery vehicle and an advantage of 13.15% compared to the combivan vehicle. We have determined that Combivan preference for distribution activities is 200% and 15.15% disadvantageous compared to e-scooter and motorcycle distribution vehicles, respectively. Figure 6 includes the CO_2 emission amounts of the motorcycle and combivan distribution vehicles, excluding the e-scooter distribution vehicle, according to the number of packages distributed.

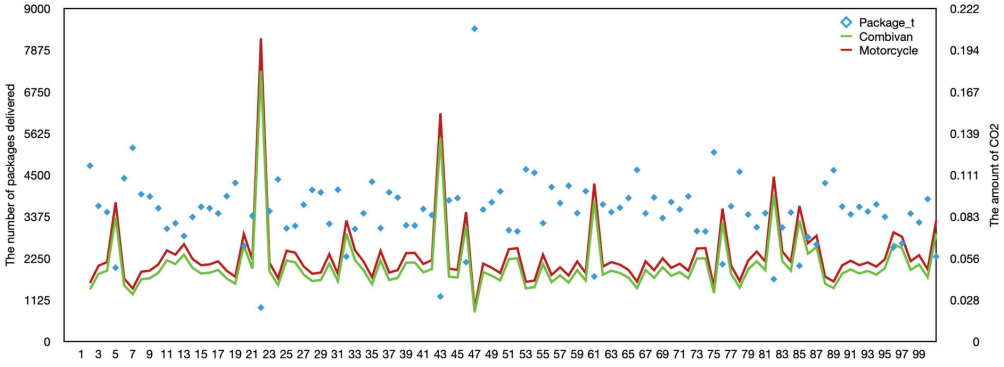

Figure 6. CO_2 emission values of motorcycle and combivan distribution vehicles depending on the package density distributed.

3.3. Results of the Optimization Models

Using mixed integer optimization models developed for this study, optimum values were obtained for objective functions and decision variables. Although these optimization models have the same constraints and decision variables, they have turned into a multi-objective optimization model type because they contain more than one objective function. Therefore, the optimum values obtained were also considered feasible values, as multi-objective optimization models also work like nonlinear optimization models. Generally, the results obtained in nonlinear optimization models are not optimum but feasible values.

Keeping the independent variables influencing the dependent variable at optimized values estimated by the desirability function approach allows one tfurther explore the effect of independent variables on individual output responses and overall desirability. In this study, Equations (14) and (15) were revised, and the following equation was used to obtain the desirability data obtained since two different objective functions were solved with the constraints consisting of five common independent variables:

$$2 * \text{Equation (14)},\ 2 * \text{Equation (15)} \tag{18}$$

With the e-scooter tool, the best 14 results (the feasible results after 14 iterations are the same) were obtained by running non-linear and mixed integer optimization models for the transportation of large numbers of packages in the package distribution service with minimum cost. These results are included in the solution set of the optimization model. The feasible results of the optimization models are depicted in Figure 7.

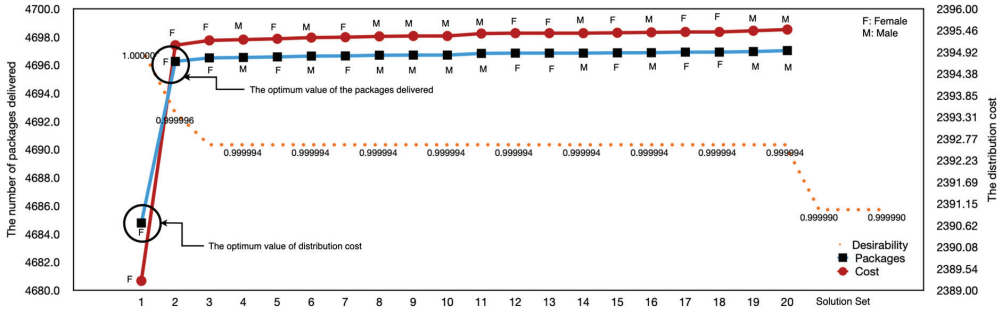

Figure 7. Optimum values of the number of packages distributed and distribution cost depending on the desirability values.

The optimum levels for a driver to deliver in a maximum time in a month, age, gender, experience in the profession, and area of responsibility were calculated as 22.63, F, 24.8 (maximum), and 0.113 km^2 (113,000 m^2), respectively. Depending on the decision variables and objective functions, the optimum values of the age, gender, experience, and area size of a driver performing the distribution process in terms of the average values of the best 20 feasible results were calculated as 38.98, M/F, 14.91 years, and 0.953 km^2, respectively. In the best 20 results of the optimization models, there were equal numbers of male and female drivers. The optimum values of the average number of packages distributed monthly and the monthly distribution cost, which are the objective functions, were calculated as 4685 and 2389 TL, respectively. The cost of distribution of a package to the administration was calculated as 0.509 TL based on the optimum results. We have determined that the effect of driver gender in the distribution process is low (unless physical characteristics are taken into account), and it is not essential in terms of distribution amount and cost.

4. Discussion

The Poisson distribution regression and optimization technique discussed in this paper is only applied to analyze the economic, energy, and environmental aspects of an e-scooter package delivery application in Turkey. The concept of micro-mobility has revealed that 40% of vehicle journeys worldwide are made at distances below 5 km, and only 5–10% of the fuel consumed in these vehicles is used to transport passengers. Micro-mobility has become an ideal system for journeys with vehicles traveling at a maximum speed of 20–25 km/h for distances up to 5–10 km. Considering that 70% of the world's population will live in cities and the use of individual vehicles will increase in 2050, the importance of micro-mobility will gradually increase in solving the problems caused by the number and density of vehicles.

The period in which the amount of distribution made by e-scooters is discussed and the amount of distribution made with other vehicles (including pedestrian distribution personnel) in the same period of the previous year are discussed. Data for both distribution types (e-scooter and other vehicles) are shown in Figure 8. In the same period, a total of 286,953 distributions were made with other vehicles and pedestrians. In comparison, a total of 351,180 distributions were made after using e-scooters, increasing the delivery performance by 22%. It should not be forgotten that with the pilot application started in Istanbul, the e-scooter not only increased the speed and distance traveled (~2x) during the day but also increased the comfort it provided to the pedestrian distribution personnel, who took thousands of steps.

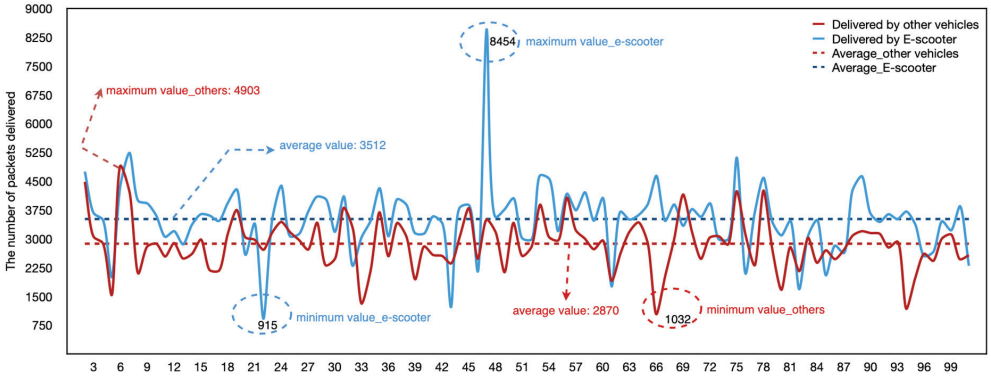

Figure 8. The number of packages distributed with e-scooters and other vehicle delivery personnel.

Therefore, as PTT, we can say that we see e-scooter as an important alternative not only for pedestrian distribution but also for motorcycle and vehicle distribution. As a matter of fact, PTT plans to increase the number of e-scooters, which was 100 in July 2021, to 500 as

of July 2022, upon high demand from the personnel. Among the results of this study, it is clearly seen that the e-scooter, which is an environmentally friendly vehicle with zero carbon emissions, is three times more efficient than motorcycle distribution and 16 times more efficient than vehicle distribution in terms of unit cost. In addition to the economic, energy, and environmental advantages of package and mail distribution, the e-scooter also provides the benefit of timely and fast distribution of packages or mail. We observed the advantage in the time factor by comparing two different years of a one-month period in which the data were taken into account. The average delivery time of a package or mail was established based on the following formulation:

$$p = 1/\frac{\sum_{i=1}^{n} n_i / \sum_{m=1}^{m} t_m}{\sum_{d=1}^{d} t_d} \tag{19}$$

where the number of packages is symbolized by p and $p = 1$ is considered in this research. n_i represents the number of packages delivered in a day. t_m signifies the days of working in a month. t_d denotes the daily working hours of an employee performing the distribution process. Average delivery times of a packet or mail in terms of data for two periods are shown in Figure 9.

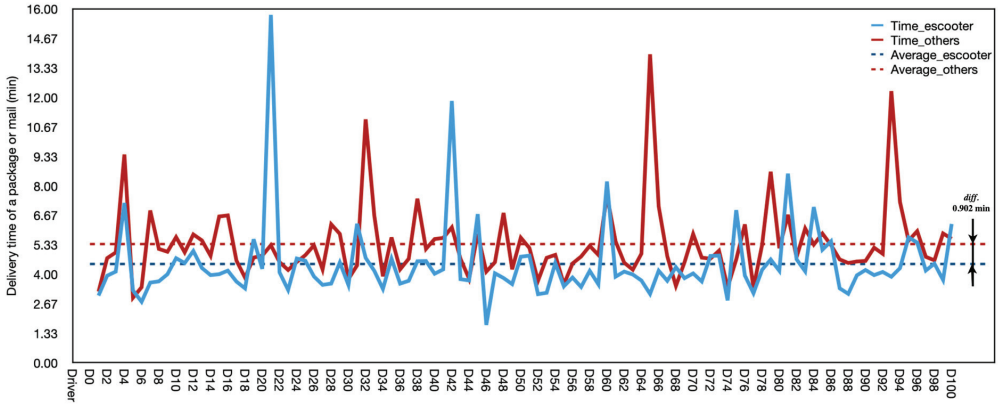

Figure 9. The delivery time of a package or mail on behalf of delivery vehicles.

Package or mail delivery times vary according to the distribution personnel due to factors such as gender, age, professional experience, and the extent of the responsible area. However, as a result of comparing the processing times of the same driver with different vehicles, it is understood that the e-scooter performs the distribution process in a faster time. While the average delivery time of a package or mail delivery is 4.462 min with the e-scooter of the driver who performs face distribution, the average delivery time is 5.364 min with the same driver with other vehicles. The delivery time of a package or mail is calculated to be shortened by approximately 0.902 min in terms of the means used for distribution. This period provides many benefits to the administration in terms of time, cost, and energy, as it is calculated for the distribution of numerous packages or mail. The use of other vehicles (especially combivan) in package or mail distribution, the physical structures of distribution locations such as road conditions, and parking problems are among the factors. However, considering that such problems are minimal with the e-scooter, the e-scooter makes a significant contribution to the delivery time of the package. Distance measures according to the type of vehicle used for a package are calculated as 0.61, 0.56, and 0.16 km for e-scooter, motorcycle, and combivan, respectively. We conclude that the most advantageous distribution vehicle is the e-scooter, as these vehicles differ in distance according to traffic, road, and building configurations.

This study has some limitations. While considering only the amount of CO_2 emissions that cause air pollution, some factors such as temperature, humidity, pressure, and wind speed are not considered. Another gap in the research's scope is that the physical (negative consequences of factors such as weight and height in driving) and psychological factors of the drivers who carry out the distribution business were not taken into account. It is requested by the administration to carry out the distribution operations upon the instruction given to the drivers. The physical structures of the region, such as road conditions, building configuration types, and parking problems in the plot areas considered in the e-scooter application, are not included in the study.

5. Conclusions

The postal or package delivery process is seeking faster, safer, and less costly options. Traditional distribution tools are lacking in meeting the necessary needs in today's world. Today, in addition to conventional vehicles, the e-scooter preference, which is increasingly used in the postal service, provides significant advantages. Official institutions/organizations that prefer e-scooter vehicles for package and mail distribution support them, with the results of scientific studies showing that they have obtained many important benefits in terms of economy, environment, and energy. In particular, a significant reduction is achieved in CO_2 emissions. In a project funded by Intelligent Energy Europe (IEE), researchers concluded that using electric micro-mobility vehicles in urban transport has a positive effect on reducing CO_2 emissions and saving energy [36]. Ruesch et al. emphasized that using e-scooters is economically cheaper than other delivery vehicles to increase mail or mail delivery efficiency [76]. A report by the Swiss Federal Energy Office (SFOE) concluded that using e-scooters contributes to low energy consumption and CO_2 emissions [77]. In general, many positive benefits are obtained by choosing e-scooters for package or mail delivery, and e-scooter vehicles are evaluated in many ways compared to traditional delivery vehicles with actual data in this study.

The e-scooter application has been started in four important districts of Istanbul, Turkey's most cosmopolitan city. This study offers the opportunity to compare and analyze the data of the results of the e-scooter application with the data of traditional transportation vehicles. This study calculated optimum results by examining the factors affecting e-scooter transportation using the optimization Poisson regression model. In particular, the values or types of factors that are effective for the e-scooter driver to deliver the maximum number of packages or mail in the shortest time have been determined. The delivery time with the e-scooter was calculated to be 16.81% faster than the delivery time with conventional vehicles. In addition, the number of packages delivered on time, as the number of deliveries made with e-scooters increased by 58.53% compared to traditional vehicles.

This study includes three primary parameters: energy, cost, and environmental effects of e-scooter use, provided that it is a short distance for logistics purposes. Using these parameters, we concluded that e-scooters are more advantageous than other delivery vehicles in terms of time and product (number of packages). This study's findings show that the average journey distance and travel time using the e-scooter is in the range of 0.113–1.98 km and 3.06 min [78]. An exemplary study of global findings showed that the average journey distance and travel time using an e-scooter was between 1.56 km and 10 min. However, in many studies, it has been noted that e-bikes, which are among the micro-mobility vehicles, cover a distance of 3.5 km in approximately 17.5 min [79]. The method we have developed shows that e-scooter vehicles, especially in courier services such as mail or package delivery, offer significant advantages to administrators compared to other studies. Therefore, the benefits of using micro-mobility vehicles such as e-scooters instead of traditional vehicles used in short-distance transportation contain great potential. This research presents the advantages of using e-scooters in urban package or mail delivery operations and offers models for future applications, making a significant contribution to the literature.

Author Contributions: Conceptualization, A.A. and C.Ç.D.; methodology, A.A.; software, A.A.; validation, A.A., C.Ç.D. and H.İ.; formal analysis, A.A.; investigation, A.A. and C.Ç.D.; resources, A.A., Y.E.A. and C.Ç.D.; data curation, Y.E.A., H.İ., A.A. and C.Ç.D.; writing—original draft preparation, A.A.; writing—review and editing, A.A.; visualization, A.A.; supervision, Y.E.A., H.İ. and C.Ç.D.; project administration, Y.E.A., H.İ. and C.Ç.D.; funding acquisition, Y.E.A. and H.İ. All authors have read and agreed to the published version of the manuscript.

Funding: This research received no external funding.

Institutional Review Board Statement: Not applicable.

Informed Consent Statement: Not applicable.

Data Availability Statement: Not applicable.

Conflicts of Interest: The authors declare no conflict of interest.

Appendix A

Number of packages or mails distributed monthly for 100 e-scooter drivers employed at PTT are represented in Figure A1.

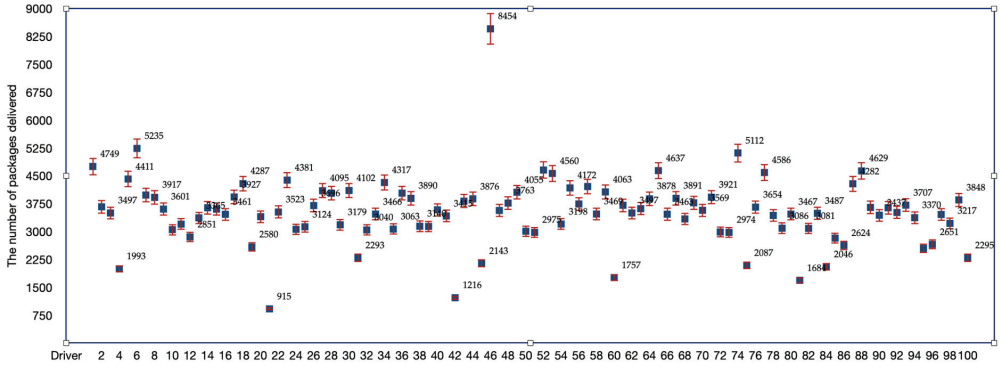

Figure A1. The number of packages delivered by the e-scooter.

References

1. Brown, A.; Klein, N.J.; Thigpen, C.; Williams, N. Impeding access: The frequency and characteristics of improper scooter, bike, and car parking. *Transp. Res. Interdiscip. Perspect.* **2020**, *4*, 100099. [CrossRef]
2. Agriesti, S.; Brevi, F.; Gandini, P.; Marchionni, G.; Parmar, R.; Ponti, M.; Studer, L. Impact of driverless vehicles on urban environment and future mobility. *Transp. Res. Procedia* **2020**, *49*, 44–59. [CrossRef]
3. Inac, H.; Oztemel, E. An Assessment Framework for the Transformation of Mobility 4.0 in Smart Cities. *Systems* **2021**, *10*, 1. [CrossRef]
4. Iwan, S.; Kijewska, K.; Lemke, J. Analysis of parcel lockers' efficiency as the last mile delivery solution—The results of the research in Poland. *Transp. Res. Procedia* **2016**, *12*, 644–655. [CrossRef]
5. Kiziltaş, M.Ç.; Ayözen, Y. A Review of Electrical Bicycle Sharing Systems as an Innovative Application. *Eur. J. Sci. Technol.* **2022**, *38*, 270–275. [CrossRef]
6. Sareen, S.; Remme, D.; Haarstad, H. E-scooter regulation: The micro-politics of market-making for micro-mobility in Bergen. *Environ. Innov. Soc. Transit.* **2021**, *40*, 461–473. [CrossRef]
7. Kjærup, M.; Skov, M.B.; van Berkel, N. E-Scooter Sustainability—A Clash of Needs, Perspectives, and Experiences. In Proceedings of the Human-Computer Interaction—INTERACT 2021, Bari, Italy, 30 August–3 September 2021; Ardito, C., Lanzilotti, R., Malizia, A., Petrie, H., Piccinno, A., Desolda, G., Inkpen, K., Eds.; Springer International Publishing: Cham, Switzerland, 2021; pp. 365–383.
8. Ebner, C.; Danzer, K.; Platz, C. Batteriepackage des E-Scooter-Konzepts von BMW Motorrad. *ATZ-Automob. Zeitschrift* **2012**, *114*, 248–253. [CrossRef]
9. Shaheen, S.A.; Cohen, A.P.; Broader, J.; Davis, R.; Brown, L.; Neelakantan, R.; Gopalakrishna, D. *Mobility on Demand Planning and Implementation: Current Practices, Innovations, and Emerging Mobility Futures*; Department of Transportation, Intelligent Transportation Systems Joint Program Office: Washington, DC, USA, 2020.

10. Castiglione, M.; Comi, A.; De Vincentis, R.; Dumitru, A.; Nigro, M. Delivering in Urban Areas: A Probabilistic-Behavioral Approach for Forecasting the Use of Electric Micromobility. *Sustainability* **2022**, *14*, 9075. [CrossRef]
11. Schoemaker, J.; Allen, J.; Huschebeck, M.; Monigl, J. *Quantification of Urban Freight Transport Effects I, Deliverable D5. 1*; BESTUFS Project: Zoetermeer, The Netherlands, 2005.
12. European Commission. *MDS Transmodal and CTL (2012). Study on Urban Freight Transport. Final Report for DGMOVE of the European Commission*; European Commission: Brussels, Belgium, 2022.
13. Bieliński, T.; Ważna, A. Electric Scooter Sharing and Bike Sharing User Behaviour and Characteristics. *Sustainability* **2020**, *12*, 9640. [CrossRef]
14. Aman, J.J.C.; Smith-Colin, J.; Zhang, W. Listen to E-scooter riders: Mining rider satisfaction factors from app store reviews. *Transp. Res. Part D Transp. Environ.* **2021**, *95*, 102856. [CrossRef]
15. Siddiqui, S.; Makrakis, D. Mpls-Based Micro-Mobility Architecture for 5g Vehicular Visible Light Communication Networks. In Proceedings of the 2020 International Symposium on Networks, Computers and Communications (ISNCC), Montreal, QC, Canada, 20–22 October 2020; IEEE: Manhattan, NY, USA, 2020; pp. 1–7.
16. Nocerino, R.; Colorni, A.; Lia, F.; Luè, A. E-bikes and E-scooters for Smart Logistics: Environmental and Economic Sustainability in Pro-E-bike Italian Pilots. *Transp. Res. Procedia* **2016**, *14*, 2362–2371. [CrossRef]
17. Heumann, M.; Kraschewski, T.; Brauner, T.; Tilch, L.; Breitner, M.H. A Spatiotemporal Study and Location-Specific Trip Pattern Categorization of Shared E-Scooter Usage. *Sustainability* **2021**, *13*, 12527. [CrossRef]
18. Jiao, J.; Bai, S. Understanding the Shared E-scooter Travels in Austin, TX. *ISPRS Int. J. Geo-Inf.* **2020**, *9*, 135. [CrossRef]
19. Jettanasen, C.; Songsukthawan, P.; Ngaopitakkul, A. Development of micro-mobility based on piezoelectric energy harvesting for smart city applications. *Sustainability* **2020**, *12*, 2933. [CrossRef]
20. Wu, H.; Dunn, S.C. Environmentally responsible logistics systems. *Int. J. Phys. Distrib. Logist. Manag.* **1995**, *25*, 20–38. [CrossRef]
21. Mekhilef, S.; Saidur, R.; Safari, A. Comparative study of different fuel cell technologies. *Renew. Sustain. Energy Rev.* **2012**, *16*, 981–989. [CrossRef]
22. Gebhardt, L.; Wolf, C.; Seiffert, R. "I'll Take the E-Scooter Instead of My Car"—The Potential of E-Scooters as a Substitute for Car Trips in Germany. *Sustainability* **2021**, *13*, 7361. [CrossRef]
23. Andreev, P.I.; Rupen Aprahamian, B.; Todorov, M.; Zhelev, G. Study of "MI Electric Scooter Pro" Capabilities. In Proceedings of the 2020 21st International Symposium on Electrical Apparatus & Technologies (SIELA), Bourgas, Bulgaria, 3–6 June 2020; IEEE: Manhattan, NY, USA, 2020; pp. 1–4.
24. Fu, Z.; Zhang, Y.; He, S.; Wang, H.; Jiang, X.; Wang, S. Multi-objective programming for economy–energy–environment system and policy mix with dual constraints of carbon emission and water consumption based on multi-scenario analysis. *Energy Rep.* **2022**, *8*, 7884–7891. [CrossRef]
25. Jia, Z.; Lin, B. CEEEA2.0 model: A dynamic CGE model for energy-environment-economy analysis with available data and code. *Energy Econ.* **2022**, *112*, 106117. [CrossRef]
26. Miao, Z.; Zhang, Y.; Liu, S.; Chen, X.; Baležentis, T. Heterogeneous strategy and performance decomposition: Energy-economy-environment nexus in the light of natural & managerial disposability. *Environ. Impact Assess. Rev.* **2022**, *95*, 106777. [CrossRef]
27. Wen, S.; Jia, Z. The energy, environment and economy impact of coal resource tax, renewable investment, and total factor productivity growth. *Resour. Policy* **2022**, *77*, 102742. [CrossRef]
28. Zhang, S.; Yu, Y.; Kharrazi, A.; Ren, H.; Ma, T. Quantifying the synergy and trade-offs among economy–energy–environment–social targets: A perspective of industrial restructuring. *J. Environ. Manag.* **2022**, *316*, 115285. [CrossRef] [PubMed]
29. Gebhardt, L.; Ehrenberger, S.; Wolf, C.; Cyganski, R. Can shared E-scooters reduce CO_2 emissions by substituting car trips in Germany? *Transp. Res. Part D Transp. Environ.* **2022**, *109*, 103328. [CrossRef]
30. Severengiz, S.; Finke, S.; Schelte, N.; Wendt, N. Life Cycle Assessment on the Mobility Service E-Scooter Sharing. In Proceedings of the 2020 IEEE European Technology and Engineering Management Summit (E-TEMS), Dortmund, Germany, 5–7 March 2020; IEEE: Manhattan, NY, USA, 2020; pp. 1–6.
31. Wanganoo, L.; Shukla, V.; Mohan, V. Intelligent Micro-Mobility E-Scooter: Revolutionizing Urban Transport. In *Trust-Based Communication Systems for Internet of Things Applications*; John Wiley & Sons, Ltd.: Hoboken, NJ, USA, 2022; pp. 267–290. ISBN 9781119896746.
32. Moreau, H.; de Jamblinne de Meux, L.; Zeller, V.; D'Ans, P.; Ruwet, C.; Achten, W.M.J. Dockless E-Scooter: A Green Solution for Mobility? Comparative Case Study between Dockless E-Scooters, Displaced Transport, and Personal E-Scooters. *Sustainability* **2020**, *12*, 1803. [CrossRef]
33. Hollingsworth, J.; Copeland, B.; Johnson, J.X. Are e-scooters polluters? The environmental impacts of shared dockless electric scooters. *Environ. Res. Lett.* **2019**, *14*, 084031. [CrossRef]
34. Quak, H.; Nesterova, N.; van Rooijen, T. Possibilities and barriers for using electric-powered vehicles in city logistics practice. *Transp. Res. Procedia* **2016**, *12*, 157–169. [CrossRef]
35. Riggs, W.; Kawashima, M.; Batstone, D. Exploring best practice for municipal e-scooter policy in the United States. *Transp. Res. Part A Policy Pract.* **2021**, *151*, 18–27. [CrossRef]
36. Lia, F.; Nocerino, R.; Bresciani, C.; Colorni Vitale, A.; Luè, A. Promotion of E-bikes for delivery of goods in European urban areas: An Italian case study. In Proceedings of the Transport Research Arena (TRA) 5th Conference: Transport Solutions from Research to Deployment, Paris, France, 14–17 April 2014; pp. 1–10.

37. Abduljabbar, R.L.; Liyanage, S.; Dia, H. The role of micro-mobility in shaping sustainable cities: A systematic literature review. *Transp. Res. Part D Transp. Environ.* **2021**, *92*, 102734. [CrossRef]
38. Zuniga-Garcia, N.; Tec, M.; Scott, J.G.; Machemehl, R.B. Evaluation of e-scooters as transit last-mile solution. *Transp. Res. Part C Emerg. Technol.* **2022**, *139*, 103660. [CrossRef]
39. Yilmaz, M.; Krein, P.T. Review of battery charger topologies, charging power levels, and infrastructure for plug-in electric and hybrid vehicles. *IEEE Trans. Power Electron.* **2013**, *28*, 2151–2169. [CrossRef]
40. Lee, H.; Baek, K.; Chung, J.-H.; Kim, J. Factors affecting heterogeneity in willingness to use e-scooter sharing services. *Transp. Res. Part D Transp. Environ.* **2021**, *92*, 102751. [CrossRef]
41. Lacoste, M.; Weiss-Lambrou, R.; Allard, M.; Dansereau, J. Powered tilt/recline systems: Why and how are they used? *Assist. Technol.* **2003**, *15*, 58–68. [PubMed]
42. Garber, S.L.; Bunzel, R.; Monga, T.N. Wheelchair utilization and satisfaction following cerebral vascular accident. *J. Rehabil. Res. Dev.* **2002**, *39*, 521–534. [PubMed]
43. Evans, S.; Frank, A.O.; Neophytou, C.; De Souza, L. Older adults' use of, and satisfaction with, electric powered indoor/outdoor wheelchairs. *Age Ageing* **2007**, *36*, 431–435. [CrossRef]
44. Jedeloo, S.; De Witte, L.P.; Linssen, B.A.J.; Schrijvers, A.J.P. Client satisfaction with service delivery of assistive technology for outdoor mobility. *Disabil. Rehabil.* **2002**, *24*, 550–557. [CrossRef]
45. Weinert, J.X. *The Rise of Electric Two-Wheelers in China: Factors for Their Success and Implications for the Future*; University of California: Davis, CA, USA, 2007; ISBN 0549494723.
46. Schellong, D.; Sadek, P.; Schaetzberger, C.; Barrack, T. The promise and pitfalls of e-scooter sharing. *Europe* **2019**, *12*, 15.
47. Tuncer, S.; Brown, B. E-scooters on the ground: Lessons for redesigning urban micro-mobility. In Proceedings of the 2020 CHI Conference on Human Factors in Computing Systems, Honolulu, HI, USA, 25–30 April 2020; pp. 1–14.
48. Hayat, M.J.; Higgins, M. Understanding poisson regression. *J. Nurs. Educ.* **2014**, *53*, 207–215.
49. Chesaniuk, M. Chapter 19: Logistic and Poisson Regression 2021. Available online: https://ademos.people.uic.edu/Chapter19.html (accessed on 21 September 2022).
50. Eccarius, T.; Lu, C.-C. Adoption intentions for micro-mobility—Insights from electric scooter sharing in Taiwan. *Transp. Res. Part D Transp. Environ.* **2020**, *84*, 102327. [CrossRef]
51. Reck, D.J.; Axhausen, K.W. Who uses shared micro-mobility services? Empirical evidence from Zurich, Switzerland. *Transp. Res. Part D Transp. Environ.* **2021**, *94*, 102803. [CrossRef]
52. Bozzi, A.D.; Aguilera, A. Shared E-Scooters: A Review of Uses, Health and Environmental Impacts, and Policy Implications of a New Micro-Mobility Service. *Sustainability* **2021**, *13*, 8676. [CrossRef]
53. Chiussi, F.A.; Khotimsky, D.A.; Krishnan, S. A network architecture for MPLS-based micro-mobility. In Proceedings of the 2002 IEEE Wireless Communications and Networking Conference Record. WCNC 2002 (Cat. No.02TH8609), Orlando, FL, USA, 17–21 March 2002; Volume 2, pp. 549–555.
54. Zhao, P.; Haitao, H.; Li, A.; Mansourian, A. Impact of data processing on deriving micro-mobility patterns from vehicle availability data. *Transp. Res. Part D Transp. Environ.* **2021**, *97*, 102913. [CrossRef]
55. Štefancová, V.; Kalašová, A.; Čulík, K.; Mazanec, J.; Vojtek, M.; Mašek, J. Research on the Impact of COVID-19 on Micromobility Using Statistical Methods. *Appl. Sci.* **2022**, *12*, 8128. [CrossRef]
56. Liu, L.; Miller, H.J. Measuring the impacts of dockless micro-mobility services on public transit accessibility. *Comput. Environ. Urban Syst.* **2022**, *98*, 101885. [CrossRef]
57. Sun, B.; Garikapati, V.; Wilson, A.; Duvall, A. Estimating energy bounds for adoption of shared micromobility. *Transp. Res. Part D Transp. Environ.* **2021**, *100*, 103012. [CrossRef]
58. Medina-Molina, C.; Pérez-Macías, N.; Gismera-Tierno, L. The multi-level perspective and micromobility services. *J. Innov. Knowl.* **2022**, *7*, 100183. [CrossRef]
59. PTT Turkish Post. Available online: https://www.ptt.gov.tr/ (accessed on 1 September 2022).
60. Atalan, A. A cost analysis with the discrete-event simulation application in nurse and doctor employment management. *J. Nurs. Manag.* **2022**, *30*, 733–741. [CrossRef]
61. Famoye, F.; Singh, K.P. Zero-inflated generalized Poisson regression model with an application to domestic violence data. *J. Data Sci.* **2006**, *4*, 117–130. [CrossRef]
62. Consul, P.C.; Famoye, F. Generalized poisson regression model. *Commun. Stat.-Theory Methods* **1992**, *21*, 89–109. [CrossRef]
63. Lu, Z.; Van Hui, Y.; Lee, A.H. Minimum Hellinger distance estimation for finite mixtures of Poisson regression models and its applications. *Biometrics* **2003**, *59*, 1016–1026. [CrossRef]
64. Koç, H.; Dünder, E.; Gümüştekin, S.; Koç, T.; Cengiz, M.A. Particle swarm optimization-based variable selection in Poisson regression analysis via information complexity-type criteria. *Commun. Stat.-Theory Methods* **2018**, *47*, 5298–5306. [CrossRef]
65. Gebski, V.; Ellingson, K.; Edwards, J.; Jernigan, J.; Kleinbaum, D. Modelling interrupted time series to evaluate prevention and control of infection in healthcare. *Epidemiol. Infect.* **2012**, *140*, 2131–2141. [CrossRef] [PubMed]
66. Atalan, A.; Şahin, H.; Atalan, Y.A. Integration of Machine Learning Algorithms and Discrete-Event Simulation for the Cost of Healthcare Resources. *Healthcare* **2022**, *10*, 1920. [CrossRef]
67. Lukman, A.F.; Adewuyi, E.; Månsson, K.; Kibria, B.M.G. A new estimator for the multicollinear Poisson regression model: Simulation and application. *Sci. Rep.* **2021**, *11*, 3732. [CrossRef] [PubMed]

68. Hamdy, T.A. *Operations Research: An Introduction*, 9th ed.; Pearson: Upper Saddle River, NJ, USA, 2010.
69. Atalan, A. Forecasting drinking milk price based on economic, social, and environmental factors using machine learning algorithms. *Agribusiness* **2022**, 1–28. [CrossRef]
70. Dönmez, N.F.K.; Atalan, A.; Dönmez, C.Ç. Desirability Optimization Models to Create the Global Healthcare Competitiveness Index. *Arab. J. Sci. Eng.* **2020**, *45*, 7065–7076. [CrossRef]
71. Mistry, M.; Letsios, D.; Krennrich, G.; Lee, R.M.; Misener, R. Mixed-Integer Convex Nonlinear Optimization with Gradient-Boosted Trees Embedded. *Optim. Control* **2018**, *33*, 1–40. [CrossRef]
72. Ayaz Atalan, Y.; Tayanç, M.; Erkan, K.; Atalan, A. Development of Nonlinear Optimization Models for Wind Power Plants Using Box-Behnken Design of Experiment: A Case Study for Turkey. *Sustainability* **2020**, *12*, 6017. [CrossRef]
73. Saleem, M.; Farooq, U.; Izhar, U.; Khan, U. Multi-Response Optimization of Electrothermal Micromirror Using Desirability Function-Based Response Surface Methodology. *Micromachines* **2017**, *8*, 107. [CrossRef]
74. Dönmez, C.Ç.; Atalan, A. Developing Statistical Optimization Models for Urban Competitiveness Index: Under the Boundaries of Econophysics Approach. *Complexity* **2019**, *2019*, 1–11. [CrossRef]
75. Atalan, A. Desirability Optimization Based on the Poisson Regression Model: Estimation of the Optimum Dental Workforce Planning. *Int. J. Health Manag. Tour.* **2022**, *7*, 200–216. [CrossRef]
76. Ruesch, M.; Schmid, T.; Bohne, S.; Haefeli, U.; Walker, D. Freight Transport with Vans: Developments and Measures. *Transp. Res. Procedia* **2016**, *12*, 79–92. [CrossRef]
77. Fuchs, A. *Energie-effizienter Leicht-Scooter im Gewichtsbereich eines Mofa*; Technical Report; Swiss Federal Office of Energy: Berne, Switzerland, 2005.
78. Şengül, B.; Mostofi, H. Impacts of E-Micromobility on the Sustainability of Urban Transportation—A Systematic Review. *Appl. Sci.* **2021**, *11*, 5851. [CrossRef]
79. Heineke, K.; Kloss, B.; Scurtu, D.; Weig, F. *Micromobility's 15,000-Mile Checkup*; McKinsey Company: Chicago, IL, USA, 2019; Volume 29.

energies

MDPI

Article

Analysis and Evaluation of Methods Used in Measuring the Intensity of Bicycle Traffic

Piotr Kędziorek [1], Zbigniew Kasprzyk [2], Mariusz Rychlicki [2] and Adam Rosiński [3,*]

[1] Heller Consult, Chałubińskiego 8, 00-613 Warsaw, Poland
[2] Division of Air Transport Engineering and Teleinformatics, Faculty of Transport, Warsaw University of Technology, 75 Koszykowa St., 00-662 Warsaw, Poland
[3] Division of Electronic Systems Exploitations, Institute of Electronic Systems, Faculty of Electronics, Military University of Technology, 2 Gen. S. Kaliski St., 00-908 Warsaw, Poland
* Correspondence: adam.rosinski@wat.edu.pl

Abstract: The work presents the methods of collecting and processing data with the use of devices used in individual measurement methods. Based on the collected video materials, the number of vehicles was determined, which at both measuring points actually exceeded each of the tested cross-sections of the bicycle path. More precise determination of the means of transport was divided into three categories: bicycles, electric scooters, and PT (personal transporters). The data collected with the use of each of the devices was properly processed and aggregated into a form that allows for their mutual comparison (they can be used to manage the energy of electric vehicles). Their greatest advantages and disadvantages were indicated, and external factors that had an impact on the size of the measurement error were identified. The cost of carrying out the traffic volume survey was also assessed, broken down into the measurement methods used. The purpose of this paper is to analyse and evaluate the methods used to measure bicycle traffic volume. Four different measurement methods were used to perform the practical part, which included such devices as a video recorder, microwave radar, perpendicular radar, and a meter connected to an induction loop embedded in the asphalt. The results made it possible to select a rational method for measuring the volume of bicycle traffic. The measurements carried out allow optimization of bicycle routes, especially for electric bicycles. The results indicate the method of physical counting of vehicles from video footage, thanks to which it is possible to achieve a level of measurement accuracy equal to 100%.

Keywords: bicycle traffic measurement; vehicle counter; induction loop; video recording; perpendicular radar; microwave radar; energy management

Citation: Kędziorek, P.; Kasprzyk, Z.; Rychlicki, M.; Rosiński, A. Analysis and Evaluation of Methods Used in Measuring the Intensity of Bicycle Traffic. *Energies* **2023**, *16*, 752. https://doi.org/10.3390/en16020752

Academic Editor: Katarzyna Turoń

Received: 12 December 2022
Revised: 2 January 2023
Accepted: 5 January 2023
Published: 9 January 2023

1. Introduction

The dynamic development of urban infrastructure, combined with pro-ecological trends, has made bicycles become increasingly popular means of transport. This phenomenon became ever more evident during the SARS-CoV-2 pandemic [1–4]. The more frequent selection of a bicycle as means of transport increasingly more often translates to limited air pollution emissions [5–7] and improved quality and level of life [8–12]. Dense populations in cities and the growing number of vehicles face engineers with a number of complex challenges [13–15]. Information on bicycle traffic volume is one of the inherent elements of designing new bicycle lane network sections. Regular traffic measurements have to be conducted in order to obtain such data.

Traffic measurements have been one of the issues taken into account in planning and designing road networks for many years [16–20]. The process applies not only to motor vehicles, but also to bicycles and even pedestrians. Decisions on expanding a road network or implementing solutions aimed at improving traffic safety are made based on traffic volume information collected during bicycle traffic measurements [21–27]. One example of recording such data is the bicycle traffic study in the capital city of Warsaw, conducted

in accordance with the guidelines of the Municipal Roads Authority in Warsaw. The first such measurement was conducted in 2007, and reports on bicycle traffic in the capital of Poland have been regularly developed based on acquired data since 2014 [28,29]. The annually collected traffic volume information enable conducting an effective analysis of forming trends and observed changes in the movement methods among the residents within the studied area [30–34]. This information can be used to manage the energy of electric vehicles [35–39].

2. Study Area

There are several methods applied in measuring bicycle traffic volume [40–44]. Devices automatically counting vehicles are gaining popularity with technical development [45–54]. Currently, the most frequently applied study methods include the observation and recording of the number of vehicles directly by an operator at the measurement point and counting objects in office conditions, based on acquired video footage from the measurement location. The second of these methods was used within the data collection method for the report "Pomiary Ruchu Rowerowego 2020" (Traffic volume measurements 2020), which involved a four-day measurement in 36 locations throughout Warsaw, in June and July of the given year. Vehicle volume was measured during morning and afternoon rush hours, i.e., 7–9 a.m. and 4–7 p.m., and the obtained data were aggregated into 15-minute intervals. The detailed categorization attributes involved traffic direction, sex, means of transport used, infrastructure type, wearing a helmet, and clothing type (sports/casual). Traffic volume information recorded using cameras [55,56] was expanded in the report with data from 35 automatic bicycle traffic measurement (ABTM) points, which counted vehicles passing through a given section via an induction loop embedded in the asphalt.

In order to discuss the whole issue of the analysis and evaluation of methods used in measuring bicycle traffic volume, the following organization of the article was adopted. First, an introduction is provided along with an analysis of the literature in the area under discussion. Then, the various methods used to record objects in selected locations are characterized. The next section presents the results of the measurements made, along with their analysis. The article concludes with conclusions, followed by a bibliography.

3. Materials and Methods

Determining the accuracy of measuring instruments required conducting a series of carefully planned activities [57]. Study implementation was divided into several stages. The first one involved determining bicycle lane sections, which were to be subject to the bicycle traffic volume study. Next, the radars and the camera were inspected in terms of damages and correct functioning. It was also checked whether batteries intended for powering the devices were charged, and the SIM card that was a component of one of the controllers used was topped up. The next stage involved setting up stations equipped with the measuring instruments at the selected locations. The task was completed a day prior to the planned start of the study. The correctness of data acquisition by the devices was checked several times in the course of the measurement. The next day, after the measurements were completed, both stations were disassembled, and the collected materials were copied to spare drives. The next stage involved converting the data collected by all the measuring instruments to a single, consistent format that ensured convenient implementation of subsequent analyses. This was followed by describing the methods used to record the objects at the selected locations.

3.1. Video Recording and Vehicle Classification

Bicycle traffic volume measurements resulted in a total of 96 h of video footage from two selected locations. The actual number of vehicles passing through the measurement section was manually determined based on this data. Furthermore, the authors adopted a categorization of the counted objects by means of transport, namely, a bicycle, electric scooter, and personal transporter. The measurement involved using a CCTV IP camera

that records the image in 1080 P (1920 × 1080 pixels) at 30 fps, which is characterized with viewing angles of almost 100° in the horizontal plane and 30° in the vertical plane. The aggregation level for recorded video materials was limited to video length below 15 min. The video recorder capability range was additionally expanded through the application of external devices. These involved a multifunctional microcomputer containing a set of inputs, outputs, and modules. It was connected to the camera via an RJ-45 network cable. The microcomputer was connected to a laptop via a LAN cable and entering a specific IP number in the web browser enabled video preview in real time. In addition, a topped-up SIM card and an RTSP port enabled remote video preview in real time.

3.2. Microwave Radar

A microwave radar (Figure 1) classifies vehicles into appropriate classes based on technical parameters defined during traffic volume measurement. Its recording and classification options can accumulate data on daily traffic. The applied FSK technology enables measuring vehicle length and speed. The FSK technology also allows the selection of locations that do not enable operation of certain radar groups due to, for example, protective barriers or other reflective structures. A detailed 8 + 1 vehicle class classification pursuant to TLS 2012 (technical conditions of delivery for road stations) is based on classification features regarding vehicle length, distance from counter, and acoustic detection. Technical parameters are determined according to the class of vehicles. Vehicle classification was done according to the A1 accuracy according to TLS (specification issued by BASt, the German Federal Highway Administration), in particular, based on vehicle length, distance from the meter, and acoustic detection. The device can be additionally integrated with a microphone, which enables determining, apart from traffic data, sound intensity at a given measuring point. Access to data was possible via cellular transmission and a manual data transfer through a Bluetooth connection with a laptop. Receiving and analysing data was possible owing to an installed application that enables obtaining not only information on the activity status of individual systems, but also receive warning messages, e.g., in the event of low battery level. Various variants for exporting files with traffic data were available. This enabled a simple assessment and visualization of the data using third-party engineering software.

Figure 1. Microwave radar installed next to a bicycle lane (own study).

3.3. Perpendicular Radar

A perpendicular radar (Figure 2) used in the study recorded traffic volume information using a radio frequency of 24.125 GHz (K-band). It is also capable of measuring traffic

volume, average speed, the individual speed of a vehicle, lane occupancy, and vehicle classification. The device sends two radio beams at different angles in the horizontal plane. As a result, each of the vehicles crosses both beams just once. The distance of a vehicle from the radar is determined based on the opening angle and the time between sending the beam, its reflection from the vehicle, and its return to the device. The distance, speed, and travel direction of recorded vehicles are determined based on the occupancy duration of each beam and the time between crossing both beams. The vertical range of the sent beam is an angle of 65°. The radar is capable of detecting vehicles within its field of view, regardless of the weather and lighting conditions. This is because the radar electromagnetic wavelength is significantly greater than that of light; therefore, a radar beam can penetrate rain, snow, and even fog. Heavy rain or snowfall may slightly affect microwave radar test results.

Figure 2. Perpendicular radar and CCTV IP camera (own study).

3.4. Induction Loop

Induction loops are used in many transport-related fields, one of which is the issue of measuring bicycle traffic volume. Induction loops can detect vehicles both on a bicycle lane and bicycle traffic sections of a road. A properly designed and constructed loop will not be impacted even by larger vehicles passing nearby [58]. Magnetic sensors are among the instruments used to detect two-track vehicles. Unfortunately, they do not correctly record all passing vehicles made of aluminium. In order to solve this issue, loop operation was based on exciting eddy currents in conductive bicycle parts, which leads to a decrease in loop inductance. The current flowing through the coils of an inductive loop sensor creates a sine-alternating magnetic field (primary field) around it. When this field encounters a metal object nearby, it induces eddy currents therein, which then generate a sine-variable magnetic field that weakens the primary field. As a consequence, the resultant field also has a reduced modulus and is phase-shifted [59].

Owing to the application of this technology, such factors as the electrical conductivity of the material that the vehicle is made of, the distance from the loop, and its surface are of major significance. In the event of connecting two separate induction loops to a counter, bicycle lane traffic volume can be measured in both directions [60].

4. Results

Traffic volume data were collected by two equally equipped measuring stations. The chapter below presents measurement results broken down by measuring stations.

4.1. Measurement of Traffic Volume at the Bicycle Lane at Stefana Banacha Street

The stations used to measure bicycle traffic as part of the practical section of the diploma thesis were located within the capital city of Warsaw. The first one was located in the Ochota district, at the intersection of Stefana Banacha and Żwirki i Wigury streets (52.210646 N, 20.987321 E) (Figure 3). It was characterized by the immediate vicinity of a public park, Pole Mokotowskie, and was located approximately 3 km from the city center. Such locations are often characterized by the highest bicycle traffic volume in the direction of the city center from 7 a.m. to 9 a.m. (morning rush hours) and from 3 p.m. to 6 p.m. (afternoon rush hours) [61]. Increased traffic during these periods is caused by residents commuting to work and returning to their places of residence. The studied section was located on the northwestern part of the intersection and covered a bicycle lane fragment perpendicular to Stefana Banacha street. The measurement section was 30 m away from the intersection center with traffic lights, and there was a bus stop in its proximity. There was a wide pavement made of concrete slabs next to the studied bicycle lane section, which was not structurally separated from it. Minor snowfall was recorded on the day preceding the measurements. The weather was cloudy with clear spells and patchy rain during the night two days prior to the study period. The pavement of the studied section was wet for most of the study, and the average temperature during the day was 5 °C.

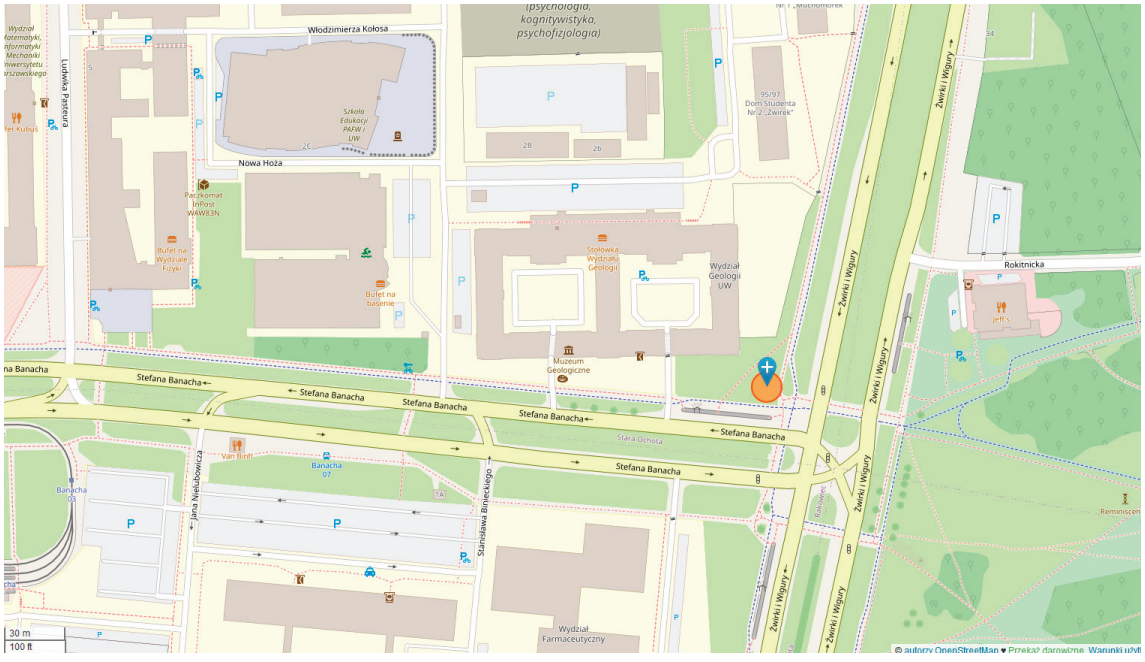

Figure 3. Location of the measuring station at Stefana Banacha street (own study, based on www.openstreetmap.org), accessed on 19 January 2022.

4.1.1. Video Recording

The source data from the perpendicular and microwave radars and the coded video footage data were appropriately aggregated and compared. The collected video footage was used in order to obtain the number of vehicles actually passing the measurement section. In the case of the station at Stefana Banacha street, the studied measurement section was passed by 1701 vehicles over the 48 h of measurements. According to the adopted classification, this included 1587 bicycles, 104 scooters, and 10 personal transporters. Over the two days, 881 vehicles (including 815 bicycles) were recorded travelling in direction

1, i.e., towards Grójecka street, and 820 vehicles (including 772 bicycles) in direction 2, i.e., towards Żwirki i Wigury street (Figure 3). On 15 December, the section was crossed by 823 vehicles (including 759 bicycles) and on 16 December by 878 vehicles (including 828 bicycles). Tables 1 and 2 contain information on the structure type of recorded vehicles, broken down by directions and measurement days.

Table 1. Vehicle structure type at the bicycle lane along Stefana Banacha street, broken down by directions (own study).

Category	Direction 1 (veh./Day)	Direction 1 (%)	Direction 2 (veh./Day)	Direction 2 (%)	Total (veh./Day)	Total (%)
Bicycles	815	92.5	772	94.1	1587	93.3
Scooters	60	6.8	44	5.4	104	6.1
Personal transporters	6	0.7	4	0.5	10	0.6
Total	881	100.0	820	100.0	1701	100.0

Table 2. Vehicle structure type at the bicycle lane along Stefana Banacha street, broken down by measurement days (own study).

Category	Day 1 (veh./Day)	Day 1 (%)	Day 2 (veh./Day)	Day 2 (%)	Total (veh./Day)	Total (%)
Bicycles	759	92.2	828	94.3	1587	93.3
Scooters	57	6.9	47	5.4	104	6.1
Personal transporters	7	0.9	3	0.3	10	0.6
Total	823	100.0	878	100.0	1701	100.0

4.1.2. Microwave Radar

During the 48 h of the measurement, the device recorded 1554 vehicles, which was 8.64% less than the number of vehicles that actually crossed the studied section. Based on the comparative analysis of data in the vehicle-by-vehicle structure with the video footage, it was concluded that the almost 9% difference resulted from the failure of the device to count a large number of scooters and personal transporters. Because the microwave radar does not classify such means of transport as a scooter or a personal transporter, all recorded vehicles were treated as bicycles in the course of further processing. The device also recorded the presence of three vehicles in the car category and nine in the motorcycle category. Due to the nature of the study, which involves only traffic along the bicycle lane, the aforementioned 12 records were classified as categorization errors and included in the comparative statement as bicycles. Under such an assumption, the device in question recorded 1554 bicycles, which compared to the actual number of bicycles of 1587 constituted a basis to adopt the estimated device measurement accuracy at almost 97.9%. It should also be emphasized that there were cases where scooters were recorded and classified by the microwave radar as bicycles, and where bicycles were not recorded at all. The analyses of the video recording indicate that such situations could have occurred for 30 to 40 vehicles, which amounts to approximately 2% of the entire research population. After taking these cases into account, the estimated measurement accuracy of the microwave radar in the bicycle category was determined at 96.0%. The measurement accuracies for direction 1 (Grójecka street) and direction 2 (Żwirki i Wigury street) compared to coded vehicles amounted to 99.0% and 93.4%, respectively. The device beam was directed not only on the bicycle lane, but also the pavement. Owing to the advancement of the used software, the device did not register pedestrians crossing the studied section in the output data. The graphs (Figures 4 and 5) below show the traffic volume measured at particular hours over the two measurement days. The first one shows a comparison of the number of

vehicles recorded by the microwave radar and the actual number of bicycles. The second one illustrates a comparison of the number of vehicles measured with the microwave radar and the number of vehicles crossing the measurement section.

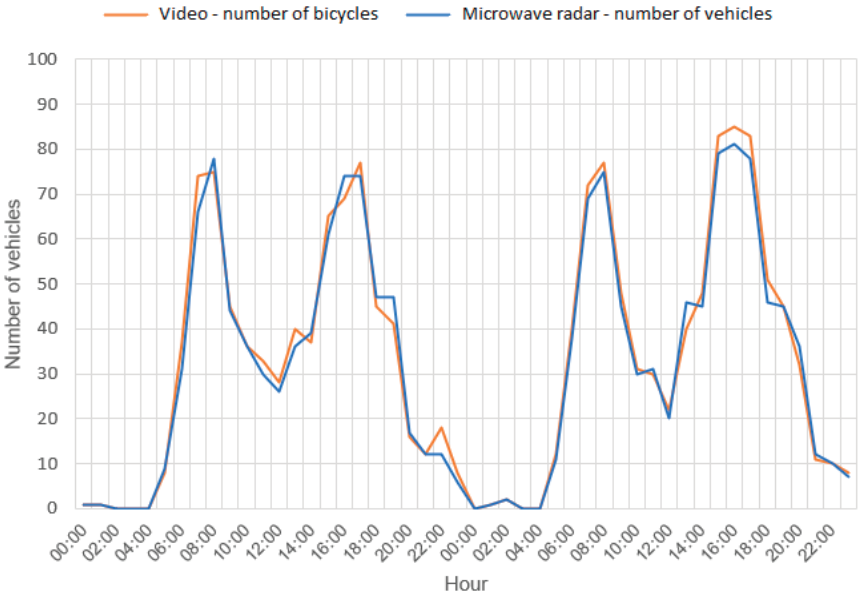

Figure 4. Comparison of the number of vehicles recorded by the microwave radar with the actual number of bicycles (own study).

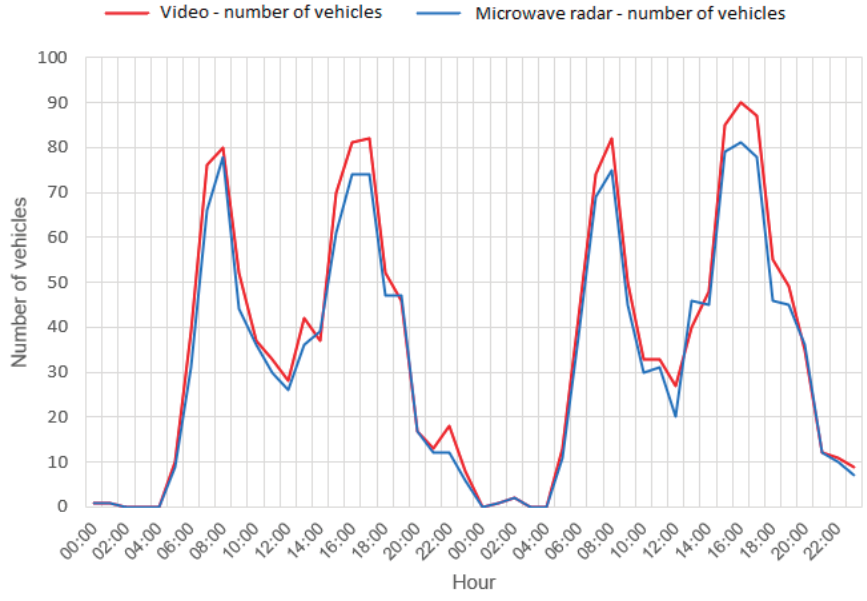

Figure 5. Comparison of the number of vehicles recorded by the microwave radar with the actual number of vehicles crossing the measurement section (own study).

Besides measuring the number of vehicles, the radar also measured their speed; in the case of the station at Stefana Banach street, the average value was 15.22 km/h. Factors that could have impacted this result include the vicinity of an intersection with traffic lights, which was located approximately 30 m from the measurement section. In addition, the studied bicycle lane section passed a pedestrian crossing. People moving with the use of vehicles should exercise particular caution due to the proximity of a bus stop and the resulting increased pedestrian traffic. The graph (Figure 6) below shows the distribution of vehicle speed recorded by the microwave radar.

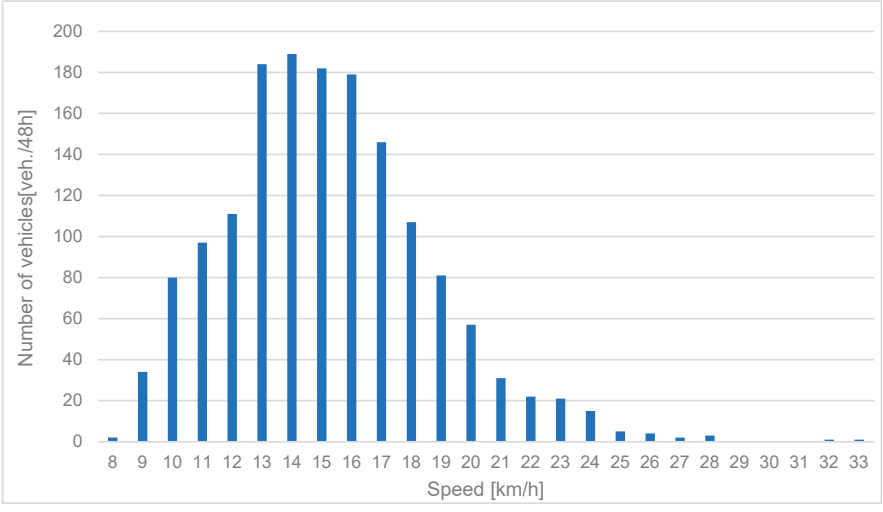

Figure 6. Distribution of vehicle speed at the bicycle lane along Stefana Banacha street (own study).

4.1.3. Perpendicular Radar

Over the two measurement days, the device registered 2187 records, which was 28.6% more than the actual number of vehicles and 37.8% more than the actual number of bicycles (Figure 7). After analysing video footage, it was concluded that the main reason behind the said differences was the counter recording pedestrians moving along the pavement adjacent to the bicycle lane. This happened despite setting out the detection area in the device calibration software. It should be noted that some people also moved directly on the bicycle lane. The device recorded the speed and length of objects crossing the measurement section, and thus, it was possible to discard records that did not fall within the expected value ranges. However, due to the nature of the conducted study, it was decided not to apply this step since the adopted analysis objective was to compare the data not modified in any way. The relative errors caused by the excessive number of recorded vehicles was 31.7% for direction 1 (Grójecka street) and 44.2% for direction 2 (Żwirki i Wigury street), relative to the actual number of bicycles.

4.1.4. Induction Loop

The last vehicle recording method applied as part of the bicycle traffic volume study was an induction loop embedded in asphalt combined with a counter. A camera, which was one of the elements of the measuring station, was installed in such a way so that its recorded image displayed the total daily and annual numbers of cyclists on the pylon screen. Due to the contrast between the display (an integral part of the pylon) and the surroundings, the number of cyclists was visible on video footage only between 9.30 a.m. and 2.30 p.m. The cameras recorded the image through the entire 15 and 16 December and until 11 a.m. on 17 December. As a result, based on the available traffic volume data, it

was possible to calculate the number of vehicles recorded by the induction loop on both measurement days. The first conducted step was to determine the total number of recorded bicycles for each of the three days and for the entire year 2021. The calculations adopted the number of cyclists for 10 a.m. on 15–17 December. Next, in order to obtain the number of cyclists at midnight between the analysed days, the daily recorded volume was subtracted from the displayed annual volume. The difference between the annual number of cyclists at midnight between successive days enabled calculating the total number of cyclists recorded in one day, both for 15 and 16 December. It should be emphasized that the conducted measurement did not involve a division into travel directions. The counter connected to the induction loop recorded 775 vehicles on 15 December and 855 on 16 December.

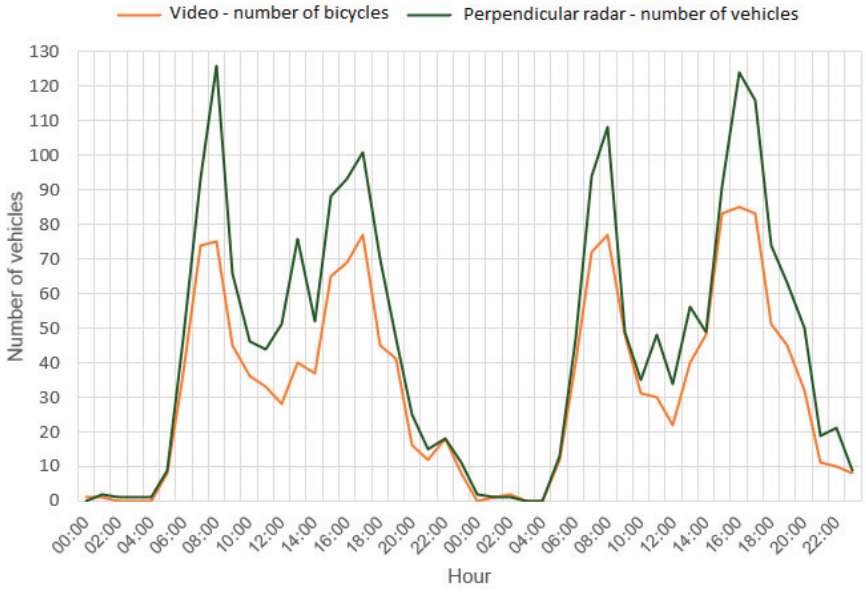

Figure 7. Comparison of the number of vehicles recorded by the perpendicular radar with the actual number of bicycles (own study).

Therefore, over the two measurement days, the counter connected with the induction loop recorded 1630 vehicles. This amounted to 95.5% of the actual number of vehicles that crossed the measurement section. Compared to the actual 1587 bicycles, the device recorded 43 extra vehicles, which means a relative error of 2.7%. Similar to the microwave radar, there were situations where the counter connected to the induction loop failed to record passing bicycles and situations where it recorded passing scooters and personal transporters. Based on video analysis, it was concluded that the counter recorded 96% of the actual number of bicycles passing the measurement section, as well as 93.9% of the scooters and personal transporters.

4.2. Measurement of Traffic Volume at the Bicycle Lane at Świętokrzyska Street

The second of the measurement locations was located in the Śródmieście district at 30 Świętokrzystka street, in the inner center of Warsaw (52.234959 N, 21.006358 E) (Figure 8). The studied section was located in the immediate vicinity of a pedestrian walkway, separated from the bicycle lane with a greenery belt in some places. An oblong residential building with several stores and eateries on the ground floor was located next to the section. Such locations are usually characterized by an above-average share of electric scooters in the vehicle type structure. Between the bicycle lane and the road, there was a paid car parking space dedicated for perpendicular parking. Due to the proximity of a

parking meter and a minor park, one could expect increased pedestrian traffic in the vicinity of the studied area. The nearest intersections were located 120 m from the measurement section towards the east (with Marszałkowska street) and approx. 140 m to the west (with Raoul Wallenberg street). As with the measurements at Stefana Banacha street, the asphalt bicycle lane pavement was wet during the measurement, with no rainfall on either day. The average air temperature during the day, both on 15 and 16 December, was approx. 6 °C. Despite the measurement being conducted in the winter season, no snowfall was recorded during its course. The Figures below illustrate the location of the measurement station and photos showing its equipment.

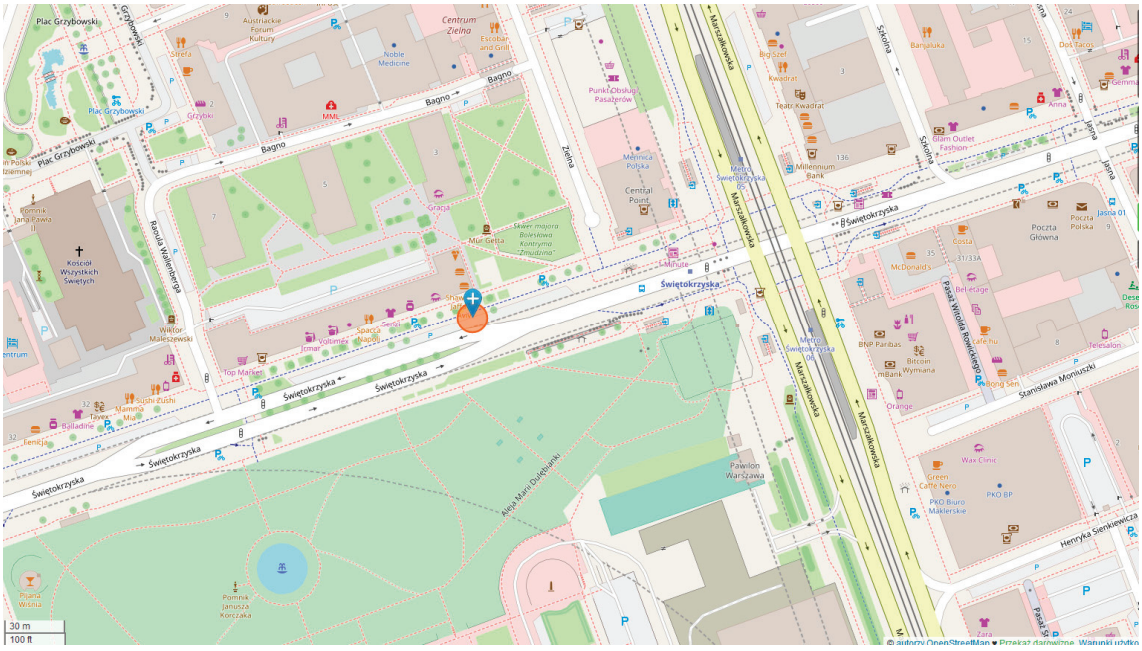

Figure 8. Location of the measuring station at Świętokrzyska street (own study, based on www.openstreetmap.org accessed on 12 December 2022).

4.2.1. Video Recording

According to the adopted assumption of conducting comparative analyses, the number of vehicles hand-coded from video footage fully represented the actual number of vehicles crossing the section located within the studied bicycle lane section. Over the two days of measurement covering the bicycle lane located by Świętokrzyska street, namely, the section between Marszałkowska street and Aleja Jana Pawła II, the authors recorded 1786 vehicles, including 1445 bicycles, 327 scooters, and 14 personal transporters. In direction 1, namely, Aleja Jana Pawła II, the studied section was crossed by 1158 vehicles (including 957 bicycles) and in direction 2 (Marszałkowska street), the equipment recorded 628 vehicles (including 488 bicycles). Tables 3 and 4 show the structure type of vehicles recorded in the bicycle lane at Świętokrzyska street, broken down by directions and measurement days.

Table 3. Vehicle structure type at the bicycle lane along Świętokrzyska street, broken down by directions (own study).

Category	Direction 1 (Veh./Day)	Direction 1 (%)	Direction 2 (Veh./Day)	Direction 2 (%)	Total (Veh./Day)	Total (%)
Bicycles	957	82.6	488	77.7	1445	80.9
Scooters	193	16.7	134	21.3	327	18.3
Personal transporters	8	0.7	6	1.0	14	0.8
Total	1158	100.0	628	100.0	1786	100.0

Table 4. Vehicle structure type at the bicycle lane along Świętokrzyska street, broken down by measurement days (own study).

Category	Direction 1 (Veh./Day)	Direction 1 (%)	Direction 2 (Veh./Day)	Direction 2 (%)	Total (Veh./Day)	Total (%)
Bicycles	708	80.9	737	80.9	1445	80.9
Scooters	161	18.4	166	18.2	327	18.3
Personal transporters	6	0.7	8	0.9	14	0.8
Total	875	100.0	911	100.0	1786	100.0

4.2.2. Microwave Radar

Over the 48 h of measurement (Figures 9 and 10), it recorded 1651 vehicles, including 1588 classified as bicycles, 57 at motorcycles, and 6 as cars on the dedicated bicycle path. Based on video footage analysis and according to the adopted procedure, 63 records involving motorcycles and cars were determined as categorization errors and included in further statements as bicycles. Under such an assumption, the counter recorded 1651 bicycles, which, compared to the 1445 bicycles that actually crossed the studied section, amounted to an absolute measurement error of the device of 14.3%. This was largely due to the fact that as many as 327 scooters as 14 personal transporters were recorded within the studied bicycle lane section, which translated to shares in the structure type of 18.3% and 0.8%, respectively. Similar to the measurement point at Stefana Banacha street, there were cases where electric scooters were classified by the counter as bicycles. The microwave radar placed on the bicycle lane at Świętokrzyska street recorded almost 79.2% of scooters and 95.6% of bicycles that crossed the measurement section.

Besides recording the very number of vehicles, the radar also measured their speed; in the case of the station at Świętokrzyska street, the average value was 20.14 km/h. This number was impacted by such factors as a good-quality asphalt pavement, distances from traffic flow intersections higher than 50 m in both directions, and a greenery belt separating the bicycle lane from the walkway. The graph (Figure 11) below illustrates the number of vehicles moving at particular speeds, rounded to whole numbers.

4.2.3. Perpendicular Radar

Over the two days, the device recorded 1833 vehicles. However, the measurement was conducted without categorization. The device relative error caused by an excessive number of records amounted to 2.6% for all vehicles and 26.9% for bicycles. The studied bicycle lane section was separated from the walkway by a greenery belt. After analysing the video footage, it was concluded that due to the proximity of the car park, the studied section could have been crossed by pedestrians several dozen times. It was still a number several-fold lower than in the case of the measurement at Stefana Banacha street, where the walkway was not separated from the bicycle lane in any manner and the measurement station was located near a bus stop. In the graph (Figure 12) illustrating traffic volume over the two measurement days, the greatest differences in the number of vehicles recorded

with the perpendicular radar and the actual number of vehicles can be seen between 2 and 3 a.m. on 15 December. After analysing the video footage, it was concluded that the measurement section was crossed by one bicycle, six electric scooters, and one pedestrian during that time. All other records were most likely recorded by the beam reflected from passing vehicles or other infrastructure elements located near the measuring device. The duration from 8 a.m. to 2 p.m. was where a significantly greater number of redundant objects recorded by the perpendicular radar was observed. Pedestrians constituted for the largest group during that time.

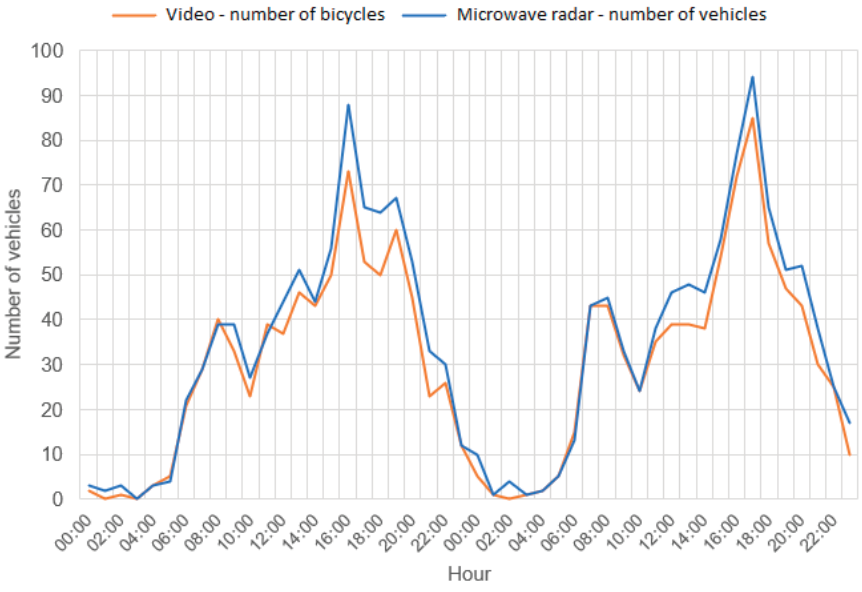

Figure 9. Comparison of the number of vehicles recorded by the microwave radar with the actual number of bicycles (the measuring station at Świętokrzyska street) (own study).

4.2.4. Induction Loop

The traffic volume measured using an induction loop within the studied bicycle lane section at Świętokrzyska street was calculated using similar conversions, as in the case of the point at Stefana Banacha street. This action was forced by a large contrast between the numbers displayed on the pylon and the surroundings at night, which prevented reading the day traffic volume based on available video footage.

The counter connected with the induction loop recorded 1901 vehicles during the traffic volume measurements. This number is 31.6% higher than the actual number of bicycles, equal to 1445, and 6.4% higher than the actual number of vehicles crossing the section, which amounted to 1786. Additional numerical juxtapositions were found based on traffic data for 10 a.m. on both measurement days. On 15 December, the total number of vehicles recorded from midnight until 10 a.m. was 172 by the induction loop, whereas 166 crossed the measurement section. This means the relative error of the device was equal to 3.6%. On 16 December, this number was equal to 180 for the induction loop counter and 206 for vehicles hand-coded from video footage. Based on this part of the data, the vehicle measurement accuracy was 87.3%. Due to the observed irregularity, further steps were taken aimed at precise observation of the number of vehicles displayed on the pylon. In the course of the analyses, the authors noticed that there were situations at night where one bicycle was counted as several dozen bikes by the counter. Due to the high contrast of the display, it was impossible to accurately determine the number. The situation in question may result from a software error. In light of these circumstances, it was assumed that the

data collected by the induction loop in the bicycle lane section at Świętokrzyska street were not a reliable reference point to assess this measurement method.

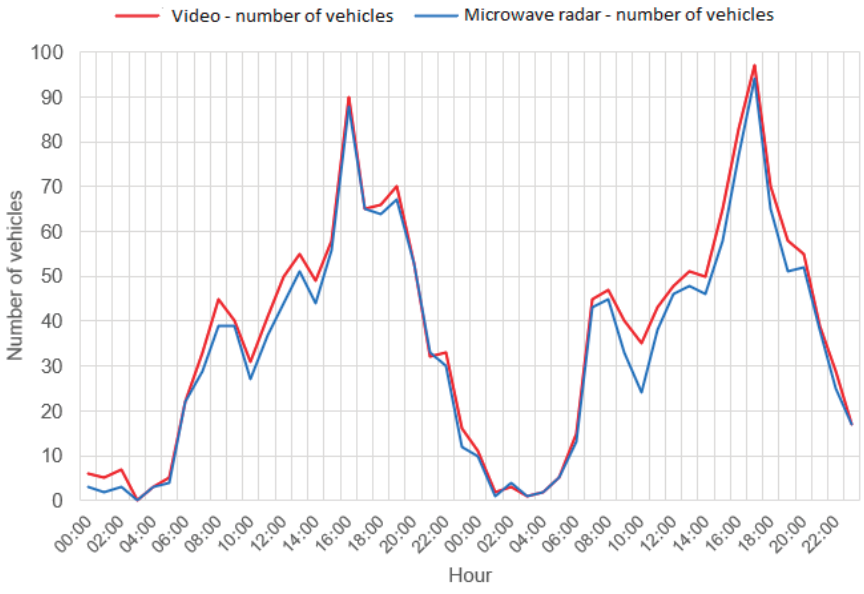

Figure 10. Comparison of the number of vehicles recorded by the microwave radar with the actual number of vehicles (the measuring station at Świętokrzyska street) (own study).

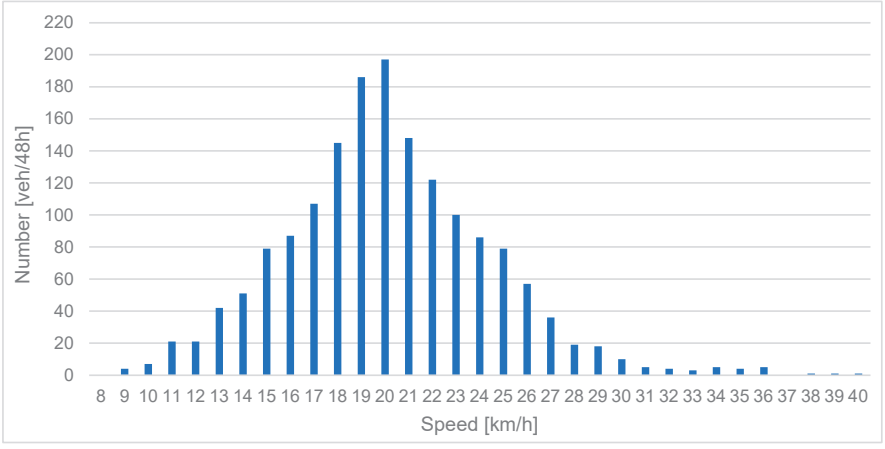

Figure 11. Distribution of vehicle speed in the bicycle lane along Świętokrzyska street (own study).

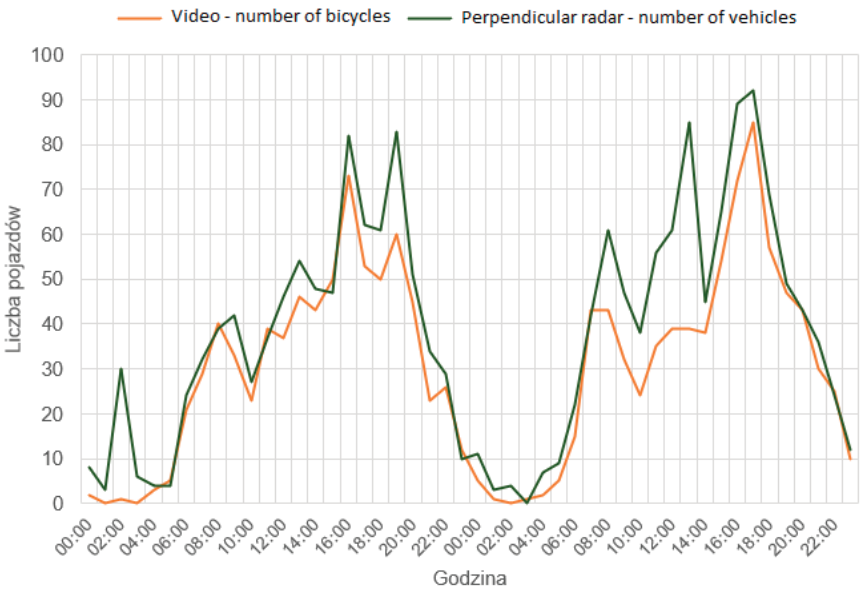

Figure 12. Comparison of the number of vehicles recorded by the perpendicular radar with the actual number of bicycles (the measuring station at Świętokrzyska street) (own study).

4.3. Summary

The practical part of the described experiment involved collecting, processing, and comparing traffic volume data for the selected bicycle lane sections. The authors also described the nature of traffic in both locations. Each of the four used measurement methods differed in terms of data collection technology and data recording accuracy. A situation where, for various reasons, measurement data might not fully reflect the actual traffic volume was possible in the case of each method. Such cases include measuring equipment theft, physical device failure, interruption or absence of an active instrumentation power supply source, and the covering of the measurement section by a different object, e.g., a delivery truck. Traffic data covered by this study were collected under favorable weather conditions; however, due to the data collection method by the counters, these factors should not translate to lower or higher measurement accuracy. Tables 5 and 6 show processed and aggregated traffic volume data collected on 15 and 16 December by the measurement points located at Stefana Banacha and Świętokrzyska streets, broken down by measurement method.

Table 5. List of all vehicles recorded at the Stefana Banacha street point, broken down by applied measurement method (own study).

Measurement Day	Video Recording	Microwave Radar	Perpendicular Radar	Induction Loop
15.12	823	747	1083	775
16.12	878	807	1104	855
Total	1701	1554	2187	1630

Table 6. List of all vehicles recorded at the Stefana Banacha street point, broken down by applied measurement method (own study).

Measurement Day	Video Recording	Microwave Radar	Perpendicular Radar	Induction Loop
15.12	875	815	863	947
16.12	911	836	970	954
Total	1786	1651	1833	1901

5. Conclusions

The purpose of this study is to analyse and evaluate the methods used to measure bicycle traffic volume. Four different measurement methods were used in the study, which included devices such as a video recorder, microwave radar, perpendicular radar, and a meter connected to an induction loop embedded in the asphalt. Measurement through physical counting of vehicles based on video footage should be classified as a method that enables achieving a measurement accuracy of 100%. A properly trained operator is able to categorize passing cyclists according to numerous features, such as sex, bicycle type, helmet worn (or not), sports clothing, or movement direction. In addition, this measurement method enables applying significantly broader categorization options, e.g., vehicle type. This is of particular importance in the face of technological development and the increasing availability of such devices as electric scooters or other electric personal transporters. The obtained measurements can be used to manage the energy of electric vehicles. This measurement method enables studying traffic volume in many locations simultaneously.

The microwave radar was able to record over 95% of the bicycles crossing a measurement section. The applied technology does not lead to errors that involve identifying passing pedestrians as vehicles. The beam emission method enables determining the movement distance and direction of a passing vehicle, its speed, and its distance from the radar. This method is able to moderately record and identify electric scooters and personal transporters. A set of categories that can be assigned by the counter used in the study is limited only to bicycles in the case of a bicycle lane measurement. Furthermore, there may be situations where a person riding a scooter is classified as a cyclist. In light of the above, a microwave radar should achieve the greatest measurement accuracy in sections with the least number of vehicles other than bicycles. In the case of a more diverse type structure, vehicle identification accuracy of the device will decrease, and the error in determining the actual number of cyclists will increase.

The perpendicular radar device measured vehicle traffic volume with the lowest accuracy among the applied methods. The radar beam reflected off objects other than bicycles in many situations, which resulted in a large number of redundant records. Due to the design and data processing method based on beam parameters, the radar recorded almost all traffic, including pedestrians and cyclists, as well as cars passing at a distance of more than 4 m from the bicycle lane. Such situations happened despite setting out a measurement area in the radar-dedicated application. The device is not strictly intended for measuring bicycle traffic volume, which was reflected in practice. A relative measurement error between 25% and 40% is, in the case of many types of possible studies, a factor that disqualifies this measurement method in terms of recording bicycles.

The induction loop embedded in asphalt recorded over 95% of the bicycles crossing the measurement section. There were situations in the course of the study where bicycle presence was not counted, as well as cases where a bicycle was double-counted. Due to the work effort required to install a measurement station, the described measurement method is suitable for continuous, long-term measurement. Owing to a constant power supply and a design resistant to weather conditions, it satisfies fundamental requirements in a manner consistent with the assumptions. Apart from the bicycles themselves, the counter also recorded more than 90% of electric scooters and personal transporters. This means that, just like with a microwave radar, a higher share of non-bicycle vehicles may

hinder determining the actual bicycle number. Given the vast measurement period while applying this method, studies aimed at controlling vehicle counting correctness should also be considered. A detailed observation of data displayed in one of the pylons participating in the study enables the conclusion that despite a relatively correct bicycle lane traffic recording, an incorrectly developed software may lead to displaying data encumbered with a significant error.

The measurements conducted made it possible to determine the advantages and disadvantages of the various methods of measuring bicycle traffic volumes. This can be used in the selection of a bicycle traffic volume measurement method for a specific bicycle route. The results of the bicycle traffic volume measurement allow the design and optimization of bicycle routes, including, in particular, for electric bicycles. This allows, on the one hand, for the rational placement of stations for the provision of electric bicycles, and on the other hand, for the optimization of the energy management system used for charging electric bicycles. The perpendicular radar measurement method showed the lowest accuracy in measuring the volume of bicycle vehicles among other methods in the same field. The measurement method of physically counting vehicles from video footage achieved a measurement accuracy level of 100%.

Author Contributions: Conceptualization, P.K. and Z.K.; methodology, P.K., Z.K. and M.R.; software, P.K. and Z.K.; validation, P.K., Z.K. and A.R.; formal analysis, P.K., Z.K. and M.R.; investigation, P.K., Z.K., M.R. and A.R.; resources, P.K. and Z.K.; data curation, P.K. and Z.K.; writing original draft preparation, P.K, Z.K. and M.R.; writing review and editing, P.K., Z.K., M.R. and A.R.; visualization, P.K. and Z.K.; supervision, P.K. and Z.K.; project administration, P.K., Z.K. and A.R; funding acquisition, A.R. All authors have read and agreed to the published version of the manuscript.

Funding: This work was co-financed by Military University of Technology under research project UGB 737.

Institutional Review Board Statement: Not applicable.

Informed Consent Statement: Not applicable.

Data Availability Statement: The data presented in this study are available on request from the corresponding author.

Conflicts of Interest: The authors declare no conflict of interest.

References

1. Buehler, R.; Pucher, J. Cycling through the COVID-19 Pandemic to a More Sustainable Transport Future: Evidence from Case Studies of 14 Large Bicycle-Friendly Cities in Europe and North America. *Sustainability* **2022**, *14*, 7293. [CrossRef]
2. Turoń, K.; Kubik, A. Business Innovations in the New Mobility Market during the COVID-19 with the Possibility of Open Business Model Innovation. *J. Open Innov. Technol. Mark. Complex.* **2021**, *7*, 195. [CrossRef]
3. Turoń, K.; Kubik, A.; Chen, F. Electric Shared Mobility Services during the Pandemic: Modeling Aspects of Transportation. *Energies* **2021**, *14*, 2622. [CrossRef]
4. Chen, J.; Zhou, D.; Zhao, Y.; Wu, B.; Wu, T. Life cycle carbon dioxide emissions of bicycle-sharing in China: Production, operation, and recycling. *Resour. Conserv. Recycl.* **2020**, *162*, 105011. [CrossRef]
5. Niu, Z.; Chai, L. Carbon Emission Reduction by Bicycle-Sharing in China. *Energies* **2022**, *15*, 5136. [CrossRef]
6. Bieliński, T.; Dopierała, Ł.; Tarkowski, M.; Ważna, A. Lessons from Implementing a Metropolitan Electric Bike Sharing System. *Energies* **2020**, *13*, 6240. [CrossRef]
7. Baptista, P.; Pina, A.; Duarte, G.; Rolim, C.; Pereira, G.; Silva, C.; Farias, T. From on-road trial evaluation of electric and conventional bicycles to comparison with other urban transport modes: Case study in the city of Lisbon, Portugal. *Energy Convers. Manag.* **2015**, *92*, 10–18. [CrossRef]
8. Lin, H.-H.; Shen, C.-C.; Hsu, I.-C.; Wu, P.-Y. Can Electric Bicycles Enhance Leisure and Tourism Activities and City Happiness? *Energies* **2021**, *14*, 8144. [CrossRef]
9. Vasiutina, H.; Szarata, A.; Rybicki, S. Evaluating the Environmental Impact of Using Cargo Bikes in Cities: A Comprehensive Review of Existing Approaches. *Energies* **2021**, *14*, 6462. [CrossRef]
10. Kwiatkowski, M.A.; Grzelak-Kostulska, E.; Biegańska, J. Could It Be a Bike for Everyone? The Electric Bicycle in Poland. *Energies* **2021**, *14*, 4878. [CrossRef]
11. Turoń, K.; Kubik, A.; Ševčovič, M.; Tóth, J.; Lakatos, A. Visual Communication in Shared Mobility Systems as an Opportunity for Recognition and Competitiveness in Smart Cities. *Smart Cities* **2022**, *5*, 802–818. [CrossRef]

12. Bęczkowska, S.A.; Grabarek, I.; Zysk, Z.; Gosek-Ferenc, K. Physical Activity and Ecological Means of Transport—Functional Assessment Methodology. *Int. J. Environ. Res. Public Health* **2022**, *19*, 9211. [CrossRef] [PubMed]
13. Kosai, S.; Yuasa, M.; Yamasue, E. Chronological Transition of Relationship between Intracity Lifecycle Transport Energy Efficiency and Population Density. *Energies* **2020**, *13*, 2094. [CrossRef]
14. Plazier, P.A.; Weitkamp, G.; van den Berg, A.E. "Cycling was never so easy!" An analysis of e-bike commuters' motives, travel behaviour and experiences using GPS-tracking and interviews. *J. Transp. Geogr.* **2017**, *65*, 25–34. [CrossRef]
15. Cieśla, M.; Sobota, A.; Jacyna, M. Multi-Criteria decision making process in metropolitan transport means selection based on the sharing mobility idea. *Sustainability* **2020**, *12*, 7231. [CrossRef]
16. Oskarbski, J.; Birr, K.; Żarski, K. Bicycle Traffic Model for Sustainable Urban Mobility Planning. *Energies* **2021**, *14*, 5970. [CrossRef]
17. Grigoropoulos, G.; Hosseini, S.A.; Keler, A.; Kaths, H.; Spangler, M.; Busch, F.; Bogenberger, K. Traffic Simulation Analysis of Bicycle Highways in Urban Areas. *Sustainability* **2021**, *13*, 1016. [CrossRef]
18. Luo, H.; Kou, Z.; Zhao, F.; Cai, H. Comparative life cycle assessment of station-based and dock-less bike sharing systems. Resour. *Conserv. Recycl.* **2019**, *146*, 180–189. [CrossRef]
19. Van Marsbergen, A.; Ton, D.; Nijënstein, S.; Annema, J.A.; van Oort, N. Exploring the role of bicycle-sharing programs in relation to urban transit. *Case Stud. Transp. Policy* **2022**, *10*, 529–538. [CrossRef]
20. Sheth, M.; Butrina, P.; Goodchild, A.; McCormack, E. Measuring delivery route cost trade-offs between electric-assist cargo bicycles and delivery trucks in dense urban areas. *Eur. Transp. Res. Rev.* **2019**, *11*, 11. [CrossRef]
21. Skoczyński, P. Analysis of Solutions Improving Safety of Cyclists in the Road Traffic. *Appl. Sci.* **2021**, *11*, 3771. [CrossRef]
22. Ma, C.; Yang, D.; Zhou, J.; Feng, Z.; Yuan, Q. Risk Riding Behaviors of Urban E-Bikes: A Literature Review. *Int. J. Environ. Res. Public Health* **2019**, *16*, 2308. [CrossRef] [PubMed]
23. Włodarek, P.; Olszewski, P. Traffic safety on cycle track crossings–traffic conflict technique. *J. Transp. Saf. Secur.* **2020**, *12*, 194–209. [CrossRef]
24. Anysz, H.J.; Włodarek, P.; Olszewski, P.; Cafiso, S. Identifying factors and conditions contributing to cyclists' serious accidents with the use of association analysis. *Arch. Civil Eng.* **2021**, *67*, 197–211. [CrossRef]
25. Murawski, J.; Szczepański, E.; Jacyna-Gołda, I.; Izdebski, M.; Jankowska-Karpa, D. Intelligent mobility: A model for assessing the safety of children traveling to school on a school bus with the use of intelligent bus stops. *Eksploat. i Niezawodn.* **2022**, *24*, 695–706. [CrossRef]
26. Kaziyeva, D.; Loidl, M.; Wallentin, G. Simulating Spatio-Temporal Patterns of Bicycle Flows with an Agent-Based Model. *ISPRS Int. J. Geo-Inf.* **2021**, *10*, 88. [CrossRef]
27. Kucharski, R.; Drabicki, A.; Żyłka, K.; Szarata, A. Multichannel queueing behaviour in urban bicycle traffic. *Eur. J. Transp. Infrastruct. Res.* **2019**, *19*, 116–141. [CrossRef]
28. Dudek, D.; Ostaszewski, P. *Pomiary Ruchu Rowerowego*; Simrun: Warsaw, Poland, 2000; pp. 4–7.
29. Krukowicz, T.; Firląg, K.; Sobota, A.; Kołodziej, T.; Novačko, L. The relationship between bicycle traffic and the development of bicycle infrastructure on the example of Warsaw. *Arch. Transp.* **2021**, *60*, 187–203. [CrossRef]
30. Kopta, T. Ruch rowerowy w Polsce na tle innych krajów UE. Stowarzyszenie Inżynierów i Techników Komunikacji Rzeczpospolitej Polskiej, Kraków. *Transp. Miej. I Reg* **2020**, *3*, 32–36.
31. Van Cauwenberg, J.; De Bourdeaudhuij, I.; Clarys, P.; de Geus, B.; Deforche, B. E-bikes among older adults: Benefits, disadvantages, usage and crash characteristics. *Transportation* **2019**, *46*, 2151–2172. [CrossRef]
32. Cherry, C.; Cervero, R. Use Characteristics and Mode Choice Behavior of Electric Bike Users in China, Transport Policy. Pergamon. 2007. Available online: https://www.sciencedirect.com/science/article/abs/pii/S0967070X07000169?via%3Dihub (accessed on 1 January 2023).
33. Kwiatkowski, M.A.; Szymanska, D. Cycling policy in strategic documents of Polish cities. *Environ. Dev. Sustain.* **2021**, *23*, 10357–10377. [CrossRef]
34. Ziółkowski, J.G.; Legas, A. Problem of Modelling Road Transport. *J. KONBiN* **2019**, *49*, 159–193. [CrossRef]
35. Czech, P.; Turoń, K.; Urbanczyk, R. Bike-Sharing as an Element of Integrated Urban Transport System. In *Advanced Solutions of Transport Systems for Growing Mobility Book Series Advances in Intelligent Systems and Computing*; Sierpinski, G., Ed.; Springer International Publishing: Berlin, Germany, 2018; Volume 631, pp. 103–111. [CrossRef]
36. Theurel, J.; Theurel, A.; Lepers, R. Physiological and cognitive responses when riding an electrically assisted bicycle versus a classical bicycle. *Ergonomics* **2012**, *55*, 773–781. [CrossRef] [PubMed]
37. Chen, Z.; Hu, Y.; Li, J.; Wu, X. Optimal deployment of electric bicycle sharing stations: Model formulation and solution technique. Networks and Spatial Economics. *Netw. Spat. Econ.* **2019**, *20*, 99–136. [CrossRef]
38. Corno, M.; Duz, A.; Savaresi, S.M. Design of a Charge-Sustaining Energy Management System for a Free-Floating Electric Shared Bicycle. *IEEE Trans. Control Syst. Technol.* **2021**, *24*, 1–13. [CrossRef]
39. Lee, K.; Chae, J.; Kim, J. A Courier Service with Electric Bicycles in an Urban Area: The Case in Seoul. *Sustainability* **2019**, *11*, 1255. [CrossRef]
40. Matyja, T.; Kubik, A.; Stanik, Z. Possibility to Use Professional Bicycle Computers for the Scientific Evaluation of Electric Bikes: Velocity, Cadence and Power Data. *Energies* **2022**, *15*, 1127. [CrossRef]
41. Borucka, A.; Kozłowski, E.; Oleszczuk, P.; Swiderski, A. Predictive Analysis of the Impact of the Time of Day on Road Accidents in Poland. *Open Eng.* **2020**, *11*, 142–150. [CrossRef]

42. Sun, Q.; Feng, T.; Kemperman, A.; Spahn, A. Modal shift implications of e-bike use in the Netherlands: Moving towards sustainability? Transp. *Res. Part D Transp. Environ.* **2020**, *78*, 102202. [CrossRef]
43. Pogodzinska, S.; Kiec, M.; D'Agostino, C. Bicycle Traffic Volume Estimation Based on GPS Data. *Transp. Res. Procedia* **2020**, *45*, 874–881. [CrossRef]
44. Rupi, F.; Poliziani, C.; Schweizer, J. Analysing the dynamic performances of a bicycle network with a temporal analysis of GPS traces. *Case Stud. Transp. Policy* **2020**, *8*, 770–777. [CrossRef]
45. Bíl, M.; Andrášik, R.; Kubeˇcek, J. How comfortable are your cycling tracks? A new method for objective bicycle vibration measurement. *Transp. Res. Part C Emerg. Technol.* **2015**, *56*, 415–425. [CrossRef]
46. Zhou, Y.; Dey, K.C.; Chowdhury, M.; Wang, K.C. Process for evaluating the data transfer performance of wireless traffic sensors for real-time intelligent transportation systems applications. *IET Intell. Transp. Syst.* **2017**, *11*, 18–27. [CrossRef]
47. Joo, S.; Oh, C.; Jeong, E.; Lee, G. Categorizing bicycling environments using GPS-based public bicycle speed data. *Transp. Res. Part C Emerg. Technol.* **2015**, *56*, 239–250. [CrossRef]
48. Scott, D.M.; Lu, W.; Brown, M.J. Route choice of bike share users: Leveraging GPS data to derive choice sets. *J. Transp. Geogr.* **2021**, *90*, 102903. [CrossRef]
49. Stawowy, M.; Duer, S.; Paś, J.; Wawrzyński, W. Determining Information Quality in ICT Systems. *Energies* **2021**, *14*, 5549. [CrossRef]
50. Jacyna, M.; Szczepański, E.; Izdebski, M.; Jasiński, S.; Maciejewski, M. Characteristics of event recorders in Automatic Train Control systems. *Arch. Transp.* **2018**, *46*, 61–70. [CrossRef]
51. Krzykowska-Piotrowska, K.; Dudek, E.; Wielgosz, P.; Milanowska, B.; Batalla, J.M. On the Correlation of Solar Activity and Troposphere on the GNSS/EGNOS Integrity. Fuzzy Logic Approach. *Energies* **2021**, *14*, 4534. [CrossRef]
52. Krzykowska-Piotrowska, K.; Dudek, E.; Siergiejczyk, M.; Rosiński, A.; Wawrzyński, W. Is Secure Communication in the R2I (Robot-to-Infrastructure) Model Possible? Identification of Threats. *Energies* **2021**, *14*, 4702. [CrossRef]
53. Krzykowska-Piotrowska, K.; Siergiejczyk, M. On the Navigation, Positioning and Wireless Communication of the Companion Robot in Outdoor Conditions. *Energies* **2022**, *15*, 4936. [CrossRef]
54. Opara, K.; Brzeziński, K.; Bukowicki, M.; Kaczmarek-Majer, K. Road roughness estimation through smartphone-measured acceleration. *IEEE Intell. Transp. Syst. Mag.* **2022**, *14*, 1–12. [CrossRef]
55. Paś, J.; Rosiński, A.; Wetoszka, P.; Białek, K.; Klimczak, T.; Siergiejczyk, M. Assessment of the Impact of Emitted Radiated Interference Generated by a Selected Rail Traction Unit on the Operating Process of Trackside Video Monitoring Systems. *Electronics* **2022**, *11*, 2554. [CrossRef]
56. Siergiejczyk, M.; Kasprzyk, Z.; Rychlicki, M.; Szmigiel, P. Analysis and Assessment of Railway CCTV System Operating Reliability. *Energies* **2022**, *15*, 1701. [CrossRef]
57. Matyja, T.; Kubik, A.; Stanik, Z. Possibility to Use Professional Bicycle Computers for the Scientific Evaluation of Electric Bikes: Trajectory, Distance, and Slope Data. *Energies* **2022**, *15*, 758. [CrossRef]
58. Bugdol, M.; Segiet, Z.; Kręcichwost, M.; Kasperek, P. Vehicle detection system using magnetic sensors. *Logistyka* **2014**, *3*, 858–867.
59. Malinowski, D.; Labuch, J. Poprawa Przepustowości Skrzyżowań w Sieci Miejskiej Poprzez Efektywniejsze Zarządzanie Przepływem Strumienia Pojazdów. 2019. Available online: www.ssmizpolska.pl (accessed on 19 January 2022).
60. Markevicius, V. *Dynamic Vehicle Detection via the Use of Magnetic Field Sensors*; Department of Electronics Engineering: Kaunas, Lithuania, 2016.
61. Knorr, F.; Schreckenberg, M. Influence of inter-vehicle communication on peak hour traffic flow. *Phys. A Stat. Mech. Appl.* **2012**, *391*, 2225–2231. [CrossRef]

energies

MDPI

Article

Possibility to Use Professional Bicycle Computers for the Scientific Evaluation of Electric Bikes: Velocity, Cadence and Power Data

Tomasz Matyja *, Andrzej Kubik * and Zbigniew Stanik

Department of Road Transport, Faculty of Transport and Aviation Engineering, Silesian University of Technology, 8 Krasinskiego Street, 40-019 Katowice, Poland; zbigniew.stanik@polsl.pl

* Correspondence: tomasz.matyja@polsl.pl (T.M.); andrzej.kubik@polsl.pl (A.K.)

Abstract: The aim of this study was to check whether the data recorded by a bicycle computer paired with typical measurement sensors can be useful for a scientific evaluation of the cyclist–bicycle anthropotechnical system, including electric bicycles. The problem arose when the authors searched for methods to assess the energy efficiency of electric bicycles and intelligent power management systems provided by the assistance system, in accordance with the current needs of the bicycle user. This can be of great importance in the efficient use of electric bicycles and their batteries, in the event that they are rented in public access systems. This article focuses primarily on data on bicycle speed, calculated by the GPS module or obtained from speed sensors, as well as data from the cadence sensor, power measurement, pedaling technique and heart rate. An attempt was made to evaluate the correctness and consistency of the data recorded by the computer through various types of comparatives analyses. The conducted research used data recorded when traveling the same route with various bikes, including electric ones, with and without assistance. This is the second part of the research. The first part focusing on data obtained by a computer from a GPS system and a barometric altimeter was published in an earlier article. In both parts, the authors presented some advantages and disadvantages of using bicycle computers as tools for measuring and acquiring data. In general, it seems that the existing technology used by bicycle computers and the measurement sensors that cooperate with it can be used in the development of a system that optimizes energy consumption.

Keywords: power; velocity; cadence; electric bike; bicycle computer

Citation: Matyja, T.; Kubik, A.; Stanik, Z. Possibility to Use Professional Bicycle Computers for the Scientific Evaluation of Electric Bikes: Velocity, Cadence and Power Data. *Energies* **2022**, *15*, 1127. https://doi.org/10.3390/en15031127

Academic Editor: Vítor Monteiro

Received: 5 January 2022
Accepted: 2 February 2022
Published: 3 February 2022

1. Introduction

The rapidly growing developing market of shared urban mobility brings with it newer and newer technical solutions. Initially, classic bicycles were one of the main means of transport used in shared mobility systems. In recent years, the shared mobility market has been increasingly filled with electric scooters [1]. Classic bikes used in shared mobility systems have been dominated by scooters, which can be found on every street in larger cities. An alternative to scooters has become bicycles with electric assistance. Electric bikes are becoming more popular and accessible [2–4]. In 2019, the market for electric bicycles in shared mobility systems was estimated to be 28%, and in 2020, it was already 44%. It is expected that in the coming years, the share of electric bicycles in vehicle sharing systems will continue to grow [5]; therefore, electric bikes will undoubtedly replace traditional bicycles in public bicycle rental systems.

The safe use of an electric bike requires that the rider has some experience in choosing the right assistance mode. Dangerously fast assisted driving is often observed, according to the following principle: "I can do more with power assistance". Manufacturers of electric bicycles are introducing a number of safeguards, consisting mainly of disconnecting the electric drive when the pedals stop rotating or there is no noticeable pressure on the pedals. Sometimes, speed limits are also applied, which is very important when driving in the

city. An electric bike has a much higher weight than a traditional bike and requires more power to move. At the same time, it allows people with a poor physical condition and diseases that exclude excessive physical activity to move. An important research problem is the comparison of the energy efficiency of electric and traditional bicycles, as well as the difference in purchase and operating costs, in the context of the profitability of the rental company. Optimization of energy consumption and, thus, maintenance costs of vehicles used in shared mobility systems is very important. The increased costs generated by electric vehicles will ultimately result in an increase in the price of renting bicycles. It is therefore important to use the battery efficiently, which will translate into overcoming longer distances using electric motor support.

Customers of public bike rental schemes are people who vary greatly in their experience in driving electric bikes, as well as their physical condition and health. According to the authors, it is becoming expedient to look for an intelligent electric assistance control system that would provide only as much additional energy to the cyclist–bicycle system as is needed at a given moment to move at a fixed and safe speed. Such a system would have to continuously and online monitor the mechanical parameters of the bike (e.g., speed, cadence, power generated by the human on the pedals) and human performance (e.g., pulse, pressure, saturation). An additional advantage of using this type of system would be savings in electricity consumption, which are part of the postulate of sustainable development. The introduction of an intelligent assistance system would mean recognizing that an electric bike from a public rental system is to serve only the needs of transport customers and will not be used, for example, for recreational and sports purposes. However, before such a system is created, it is first necessary to develop tools for assessing the energy efficiency of electric bicycles and mathematical models of control and simulation of bicycle dynamics. Second, a system to measure and acquire data needed to control the assistance should be chosen. For obvious reasons, the data measurement and acquisition system must be low budget. The authors asked themselves whether the technologies used in bicycle computers could be used for this purpose. Bicycle computers have become a typical and popular tool for recording the basic parameters of the route and the condition of the cyclist, used by both professional cyclists and amateurs using bicycles for recreational purposes [6]. As is standard, the computer records data from the built-in GPS module and from the barometric altimeter and thermometer. After installing additional measuring devices, it is possible to record, among others: speed converted from wheel rotation, cadence, power, pedaling asymmetry, pedaling effectiveness, pedaling smoothness and the cyclist's heart rate.

The bicycle computer and bikes used for the research, the test route and additional measurement sensors mounted on the bikes were discussed in the first part of this article. The first part of this article [7] proposed methods for processing and filtering data from the GPS module and the barometric altimeter. Data defining the trajectory of the bicycle's movement were analyzed, and an average route was determined on their basis. The height of the averaged route above sea level and its slope were also determined. The second part focuses on data obtained from external sensors. The aim of the research was to evaluate the recorded data in terms of their suitability for the scientific evaluation of the anthropotechnical cyclist–bicycle system. Among other things, this type of data could be used to compare the energy efficiency of electric bicycles with conventional bicycles, to design systems that optimize the cyclist's effort and to prepare cycling simulators.

It is obvious that a bicycle computer cannot be treated as a professional measuring apparatus. However, it has a number of advantages that make it a tool for measuring and recording data. The advantages include: easy installation on bikes, low weight, aerodynamic shapes, a large number of recorded parameters, easy attachment of additional transducers and low energy consumption of dedicated transducers. In addition, the low purchase cost (at the smartphone level) makes it possible to use multiple meters at the same time (simultaneous testing), and it is also possible to obtain data from the cycling community (many people have such equipment). The bicycle computer practically does not

disturb the experiment compared to the professional equipment that should be mounted on the bicycle.

2. Materials and Methods

The studies used four bicycles: two electric-assisted bicycles and two conventional bicycles. All rides were carried out by the same cyclist on the same route with a length of approximately 2.7 km and a difference in elevation of approximately 25 m. Since the main purpose of the study was the evaluation of electric bicycle energy, many more measurements were carried out and many more parameters were measured than were later used to evaluate the bicycle computer as a tool for measurement and data acquisition. A measurement kit was used to record the data, which included the bicycle computer ELEMNT ROAM, Wahoo CADENCE, Wahoo SPEED, TICKR and a dual pedal system with a built-in power sensor, Look Exact. More details on the bikes used, the measuring sensors and the test route can be found in the first part of the article [7], in which the quality of the trajectory, distance and slope data was evaluated. This part of the article focuses on velocity, cadence and power data. Electric bike rides were performed in four available assistance modes (Eco, Tour, Sport, Turbo) and without assistance. Conventional bikes were used for comparison with electric bikes in terms of power demand during the test route.

The cycling computer records data at a frequency of 1 Hz. Methods used in signal processing and time series analysis can be used to analyze them. It can be noted that these are nonperiodic and nonstationary signals. In the analysis of data on speed and distance traveled, elementary methods of numerical differentiation (of various orders) and signal integration were used. However, they introduce additional noise, and the results require the use of smoothing filters. The speed measured with an additional sensor (from the wheel) may differ from the speed calculated from GPS coordinates due to the slope of the route. In the case of a test route with a slight slope, these differences were negligibly small. One of the important elements of cycling technique is the choice of the right gear ratio. A method to detect the gear ratio used at a given moment of riding was proposed on the basis of cadence and speed data, as well as available bicycle gear ratios. Due to the freewheel, it should be taken into account that, in certain circumstances, it is not possible to clearly determine the gear ratio. An analysis of the recorded power signals generated by the roverist in various assistance modes was carried out. The aim was to show that a person would not be able to use the support on their own in an optimal way. To evaluate the asymmetry of power distribution to the pedals, the k-mean clustering method was used. To assess the condition of the cyclist, methods were used to study the correlation of pulse and power signals and cadence. The following analyses of the data recorded by the bicycle computer used information on the height above sea level of the test route, which was determined in the first part of the article based on data from the digital terrain model (DTM) [7].

3. Evaluation of Velocity Data

As is standard, the bicycle computer calculates the speed from the change in GPS coordinates over time. Due to the noise of the GPS data, this method is subject to a significant error. Currently, a method of calculating speed based on the delay of satellite signals, due to the Doppler effect, is being developed. Research shows that this method of determining speed is much more accurate [8]. Perhaps soon this method will also be implemented in bicycle computers.

The computer can also alternately record speed data from a speed sensor, if such a sensor is additionally installed on the bike and paired with the computer. Such data should be much more accurate. However, they depend on entering the correct value of the outer diameter of the wheel into the measurement system. The error thus caused will be a systematic error and can be easily corrected by comparison with the GPS data.

In the vast majority of cases, speed transducers work on the principle of magnetic sensors and require a magnet to be mounted on the wheel. One of the traditional bikes

used for the tests was equipped with such a speed measurement system. More modern speed converters do not need a magnet to detect wheel revolutions. Instead, a three-axis accelerometer is used to determine the rotation of the hub and thus the speed. Such a transducer was mounted on one of the electric bikes used for the tests.

Figure 1 shows exemplary speed charts recorded by a bicycle computer and calculated numerically from GPS coordinates (using three numerical differentiation methods: forward and central difference, five-point scheme) and also from the recorded distance traveled. At the very beginning of the movement, it is visible that the non-zero signal of the speed recorded by the computer appears with a certain delay. It is most likely the effect of using an averaging filter. This is also evidenced by the fact that the speed calculated from the recorded GPS coordinates is greater than zero at that time. The recorded speed signal is much smoother than the signals calculated from GPS data post factum. At the same time, the choice of the method of determining the speed by numerical differentiation is of no great importance, as can be seen in the enlarged fragment of the diagram (Figure 2). The averaging of the speed signal by the bicycle computer is also evidenced by small differences between the recorded distance and the distance calculated directly from the speed by integration using the trapezoidal method (Figure 3).

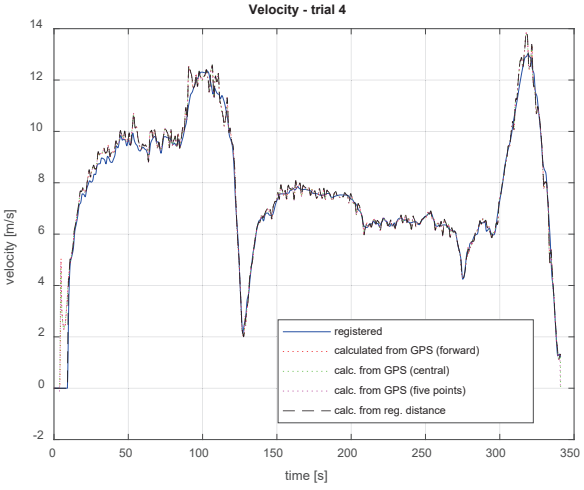

Figure 1. Example of velocity data.

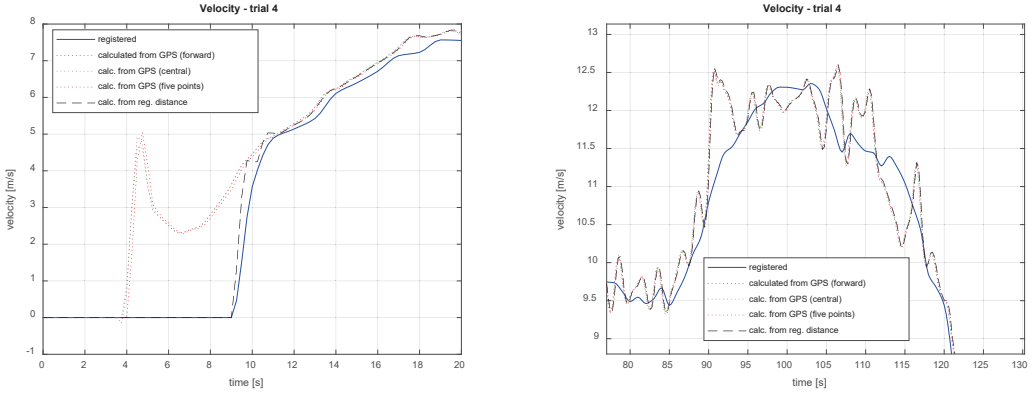

Figure 2. Enlarged parts of the speed chart.

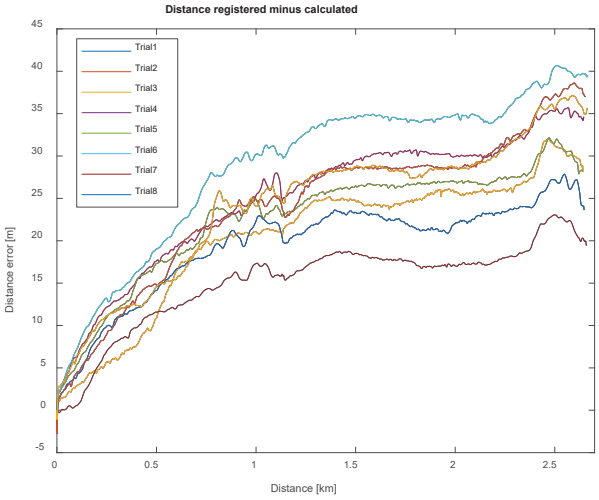

Figure 3. The difference between the recorded distance and the distance calculated from the speed signal.

Figure 4 compares exemplary graphs of the speeds recorded on the basis of the speed sensor data and those calculated numerically. In this case, there is no difference in the beginning of the movement. It is not known if the cycling computer also smoothed the signal received from the speed sensor. As stated before, numerically calculated speed signals are characterized by significant oscillations in relation to the recorded signal.

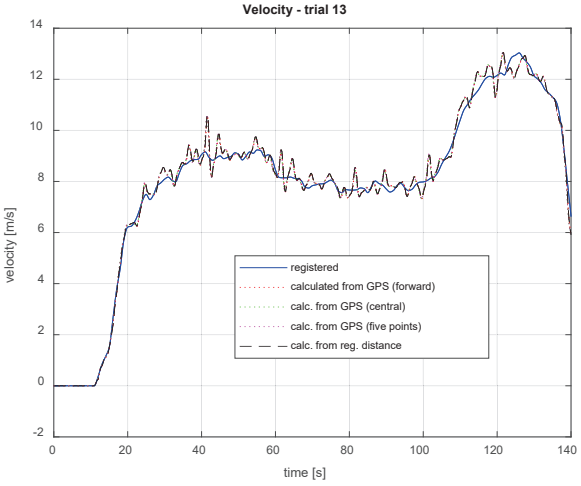

Figure 4. An example of the speed chart recorded on the basis of the speed sensor readings.

4. Cadence

Further analysis was limited to the data recorded for one of the electric bicycles. A wireless cadence sensor that does not require a magnet mounted on a crank was used. Figure 5 shows the recorded cadence and speed signals of this bike for four different assist modes and without assist. It can be seen that in all assist modes, the rider kept the cadence at a similar level, but the assisted speeds were higher. This means that with power assistance, the rider used higher gears.

Based on the speed and cadence signals, the current gear ratio of the bike can be determined while driving. An exception is made when the freewheel engages, for example,

when going downhill. Then, the cadence is not directly related to the driving speed, and the value of the gear ratio is undefined. Since both the speed and cadence signals are highly noisy, the calculated gear ratio does not correspond exactly to the value that would result from dividing the number of teeth in the rear cassette by the number of teeth in the front (Figure 6). In the case of calculations based on the speed recorded by the bicycle computer, a jump in the value is observed at the very beginning of the test, which results from the fact that the speed value is too low, probably due to the averaging filter used.

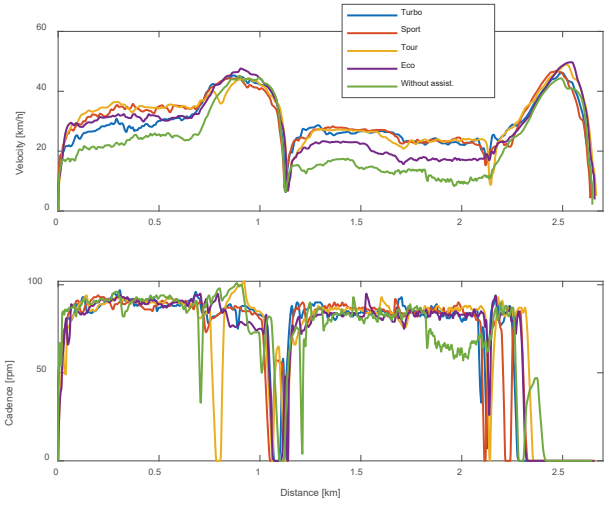

Figure 5. Examples of recorded cadence and speed signals in various assist modes.

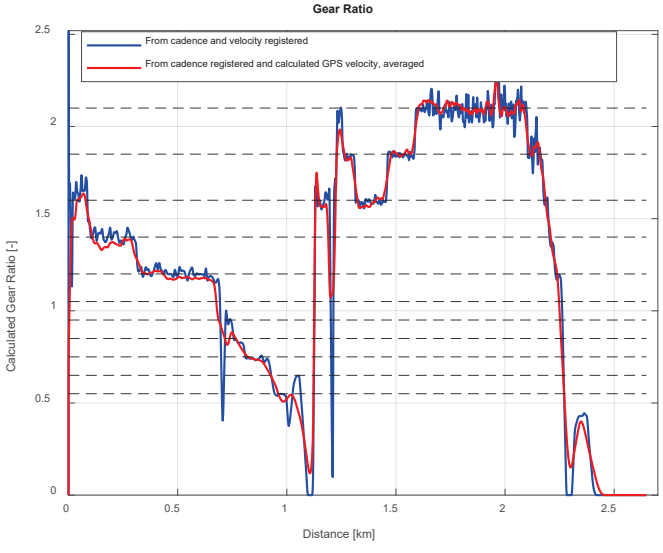

Figure 6. Gear ratios calculated from cadence and speed signals.

The used bicycle has wheels with the following numbers of teeth in the rear cassette: 11, 13, 15, 17, 19, 21, 24, 28, 32, 37, 42. The front sprocket only has 20 teeth, but due to the power steering system, it moves 2.5 times faster than the pedal crank (which is also the case in non-assist mode). The gear ratio, resulting directly from the number of teeth, is shown

in Figure 6 (dotted line). On the graph, some of the available gear ratios can be recognized, but the signal is noisy. The gear ratios were calculated from formula (1):

$$G_r = \frac{\omega_s}{\omega_r} = \frac{z_r}{z_s} = \frac{[11 \ldots 42]}{20} \quad (1)$$

where ω_s and ω_r are the angular velocity of the crankshaft (cadence 2.5) and the angular velocity of the rear wheel (calculated from the linear velocity), respectively.

If the gear ratios of the bicycle are known, a simple classifying function can be built, automatically assigning the actual allowable values to the noisy signal of the calculated gear ratio, except when the freewheel is engaged (Figure 7). The gear ratio data can be used to evaluate the driving technique [9].

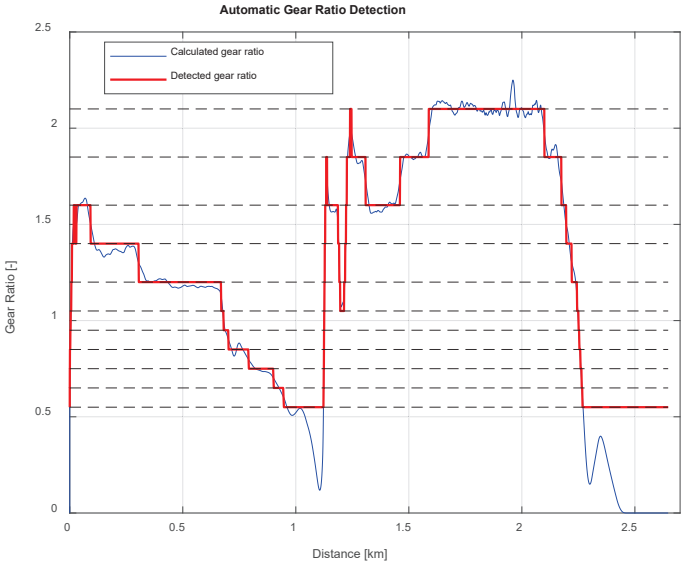

Figure 7. The results of the current gear ratio automatic detection.

5. Power, Power Balance and Torque Effectiveness Data

As in the case of the cadence, the analysis was limited to the data recorded for one of the electric bicycles. Power metering pedals were used that measure power and cadence simultaneously and analyze power balance, pedaling (torque) effectiveness and smoothness. There are systems that measure power using the measurement of the forces on the crank [10]. In laboratory conditions, optical systems for image analysis are also used [11].

Figure 8 shows the human-generated power in different assist modes depending on the position along the route. In addition, it is shown how the altitude of the route changed, meaning that the generated power can be compared with the slope of the route. The recorded power signal shows a very high variability. The power values in the subsequent sampling times differ significantly. This is shown in Figure 9, which shows the calculated forward difference of power signals in the turbo and unassisted modes. Over one second, the cyclist made, on average, less than two turns of the crank, and theoretically, during this time, he could rapidly change the force on the pedals. However, it is more likely to smoothly adapt the power to the increasing demand for it, for example, when climbing a hill. Unfortunately, with the sampling rate of 1 s, it is impossible to determine what is the cause of such large jumps in the power value. This means that, as with other data (e.g., GPS), the frequency of recording power every second is insufficient.

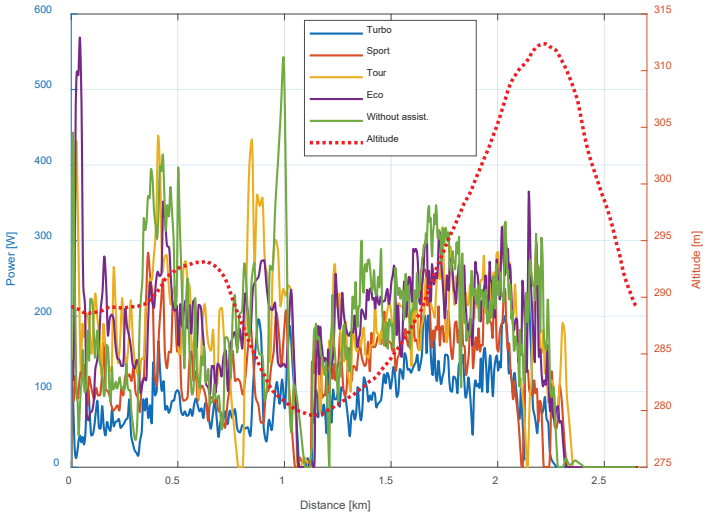

Figure 8. The power generated by the rider in a variety of assist modes.

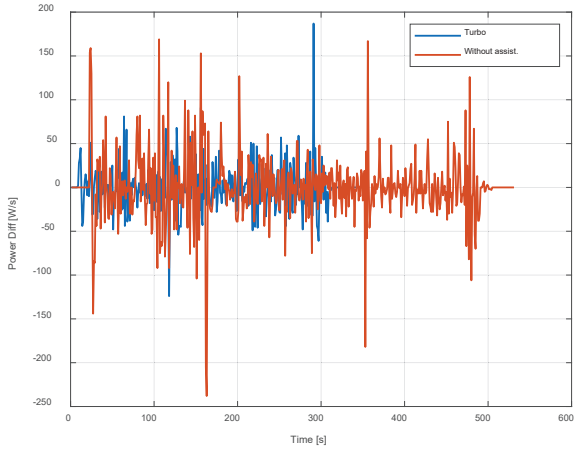

Figure 9. Change in the power value in subsequent moments of the sampling time.

In practice, two methods are used to calculate the average power [12]. The first of them, average angular velocity power (AAV), determines the average power per crank revolution on the basis of relationship (2):

$$P_{AAV} = F_{\tau M} \cdot l_c \cdot \omega_M F_{\tau M} = \frac{1}{N} \sum_{k=1}^{N} F_\tau(k),\ \omega_M = \frac{2\pi}{T} \tag{2}$$

where l_c—crank length; ω_M—angular speed of the crank averaged per revolution (T—period of one revolution); F_M—averaged force on pedals (N—number of samples per revolution).

The second more precise method, instantaneous angular velocity power (IAV), calculates power based on dependence (3):

$$P_{IAV} = \frac{l_c}{N} \sum_{k=1}^{N} F_\tau(k)\omega(k) \tag{3}$$

and requires sampling of instantaneous force and rotational speed. Unfortunately, the manufacturer of the power measurement pedals used in this research does not specify which calculation method it uses (probably AAV) [12].

The average human power generated in the turbo mode was 100 W less than the power needed to drive in the unassisted mode (Figure 10). At the same time, the average speed of the test route covered was significantly higher in the assisted modes. This means that the cyclist did not behave rationally and did not try to optimize their effort. Unfortunately, it is a human factor that will be difficult to eliminate during the trials.

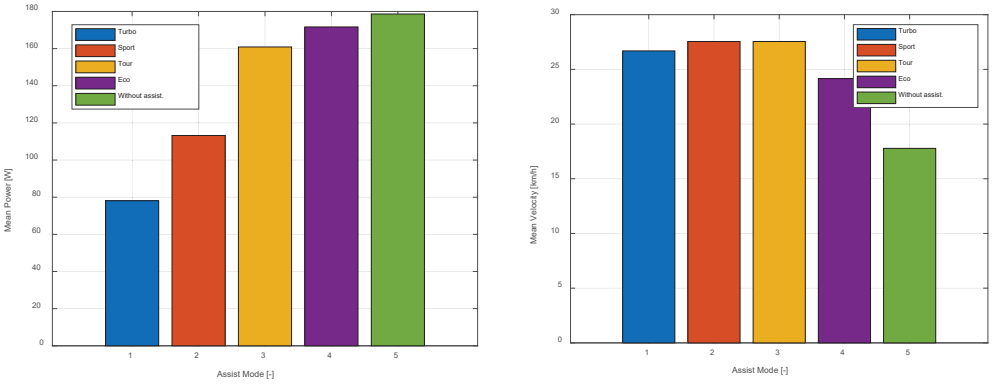

Figure 10. Comparison of average power and speed in different assist modes.

The bicycle computer determines and stores a series of information which allows for diagnosing pedaling asymmetries, which depend on the individual, and the biomechanical characteristics of each cyclist [13,14]. Professionals try to eliminate asymmetry through proper training. Even a preliminary analysis of the recorded data as a function of the distance traveled (Figure 11) shows that the asymmetry of pedaling depends on the assist mode. It is greater in turbo and sport modes, which is when the power delivered by the rider is lower. In general, the advantage of the right side over the left side is visible. The ideal values would be close to 50%.

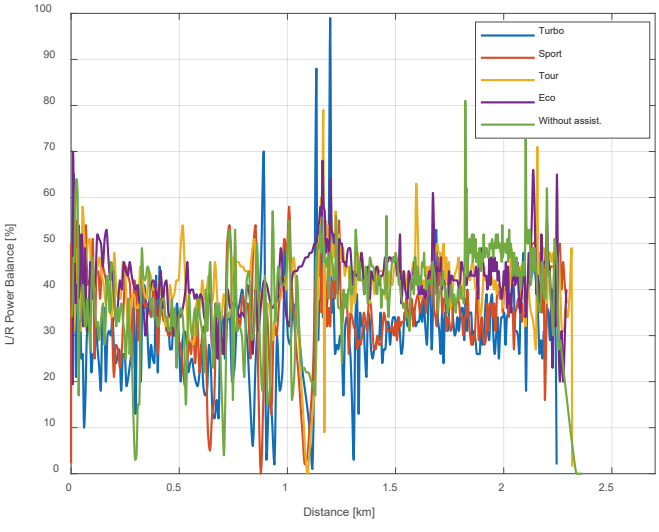

Figure 11. Left/right power balance.

The figure (Figure 12) shows the asymmetry of the power distribution to the pedals of the cyclist performing the tests, in the case of two extreme support modes: turbo and without. The L/R power balance is presented in this case as a function of human-generated power. The points on the graph are divided into five subsets using the k-mean clustering method. In turbo mode, where the power demand does not exceed 250 W, the asymmetry decreases with increasing power. A similar tendency occurs in the unassisted mode, except that after exceeding 250 W, the asymmetry increases again. Similar conclusions can also be reached by analyzing the graph (Figure 13), which collected the results from all five support modes.

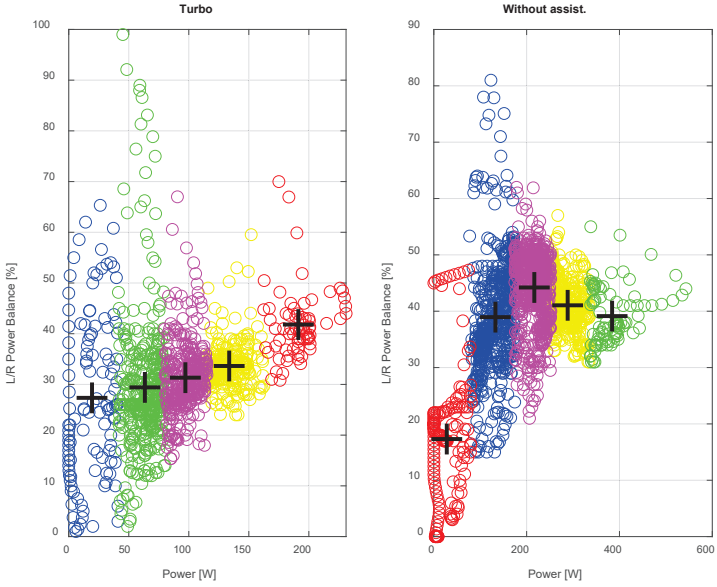

Figure 12. Left/right power balance as a function of power.

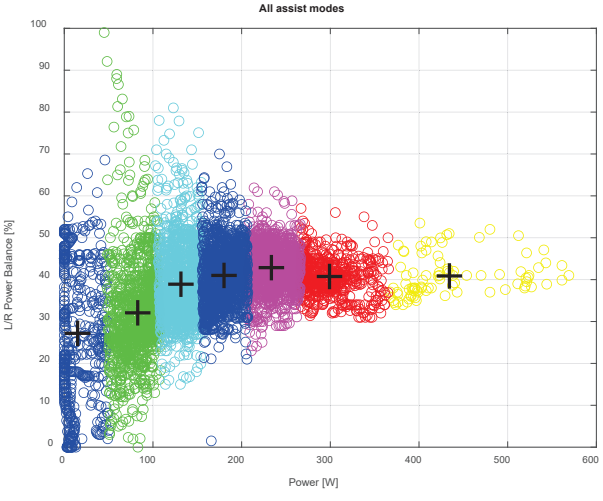

Figure 13. Left/right power balance as a function of power for all modes simultaneously.

The efficiency of the drive torque transmission to the pedals is calculated from Formula (4) [12]:

$$TE = \frac{P_+ + P_-}{P_+} \cdot 100\% \tag{4}$$

where P_+ and P_- are the highest and lowest peak power values per crank revolution, respectively.

The metering system provides information on pedaling efficiency for the left and right pedals separately. Pedaling efficiency is slightly inferior to the left side. Interestingly, the efficiency in the turbo mode is clearly lower than in the non-assist mode (Figure 14).

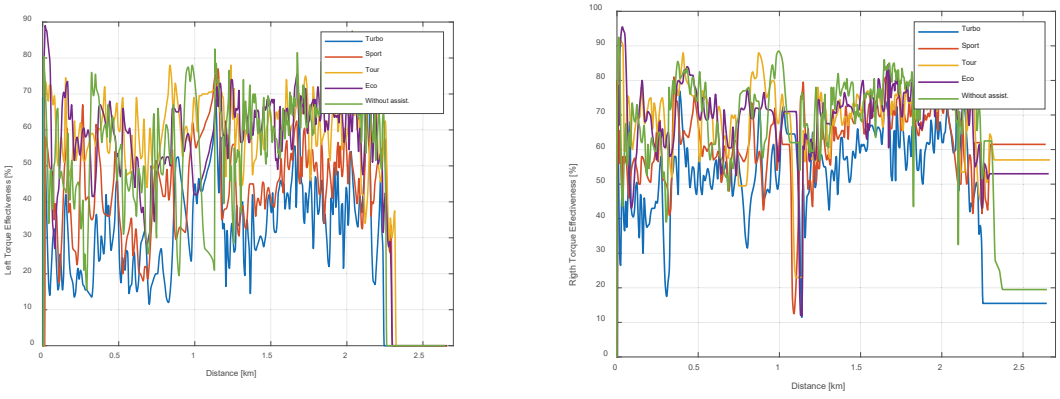

Figure 14. Left/right torque effectiveness.

Pedaling smoothness is obtained from formula (5) [6]:

$$PS = \frac{P_{avg}}{P_{max}} \cdot 100\% \tag{5}$$

where P_{avg} and P_{max} are the averaged and highest power values during one crank revolution, respectively.

As stated before, the smoothness of pedaling decreases in the assisted modes (Figure 15); this effect is most clearly visible in the turbo mode. Perhaps the reason could be found in some overdrive of the power steering system. When changing from a traditional to an electric bike, a cyclist has to adapt to new conditions.

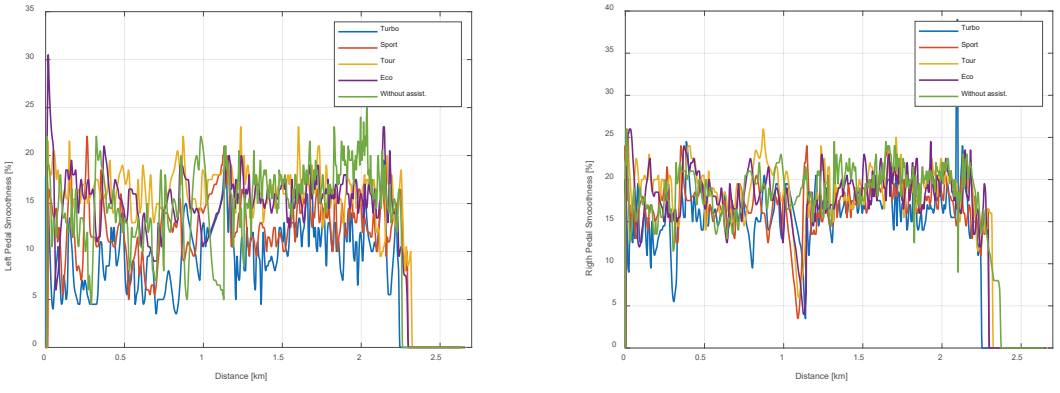

Figure 15. Left/right pedal smoothness.

The evaluation of the quality of data related to the torque and power transmitted by the cyclist would require additional tests with the use of specialized equipment for measuring crank speed and pedal force with a much higher sampling rate. This type of research was carried out for pedals with power measurement from another company [15].

6. Cyclist Health—Pulse Data

The cycling computer records the rider's current heart rate, which it receives from a sensor attached to the rider's wrist. A rider's heart rate is influenced by their effort while riding, which is dependent on the generated power and cadence. Figure 16 shows the recorded heart rate values while riding an e-bike in the different assist modes. Pulse values were related to the distance traveled, which allows showing the relationship of the pulse with the inclination of the route and the effort of the cyclist while riding. Obviously, the heart rate increases the least in maximum assist mode and is highest in non-assist mode. We can also see changes in the heart rate associated with changes in the slope of the route. The nature of the charts is significantly influenced by the human factor. As shown in Figure 17, the rider moves much faster in the assisted modes, although they may have conserved energy.

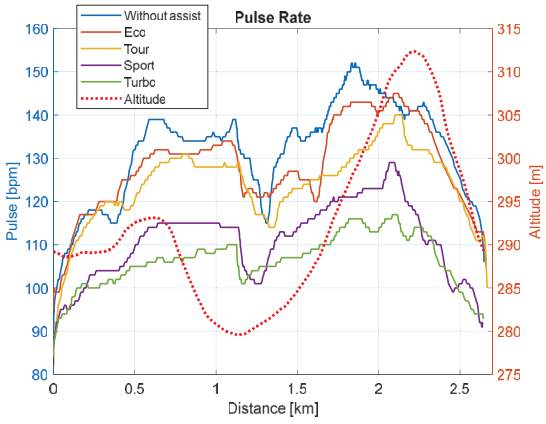

Figure 16. Graph of heart rate as a function of the distance traveled and the support mode.

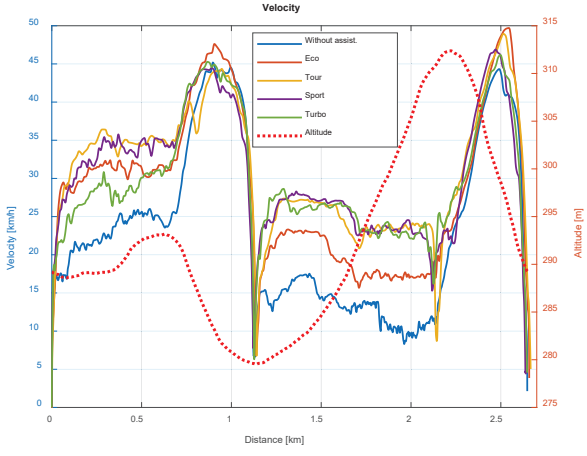

Figure 17. Distance travel speeds depending on the assist mode.

Physiologists observe two characteristic phenomena, namely, heart rate response lag and heart rate drift upward [9,16,17]. The first is a delayed response of the body to the increased (reduced) effort and is seen in the shift in time of the peaks in the heart rate graph and the persistence of elevated heart rate even after exercise has stopped (Figure 18). The second is a systematic increase in heart rate to a certain limit value despite the effort being kept at an almost constant level. This effect is also seen in Figure 18 in the range from 300 to 360 s.

Figure 18. Power generated in a run without assistance and heart rate changes.

The cross-correlation method can be used to investigate the delay between the signals. In order to assess the magnitude of the delay in the pulse signal, the correlation between the pulse and cadence signals as well as the pulse and power generated by the cyclist was investigated. Before that, all signals were normalized with their maximum values. The correlation between the cadence signal and the heart rate signal is slightly higher than the power generated by the rider and the heart rate. The graphs show the maximum values of the correlation in various electric bike riding modes and the determined mutual delays of the signals (Figure 19). In both cases, there is a time shift in the signals in the range from about 17 to 30 s. The delay is also influenced by the assisted or unassisted riding mode, i.e., the rider's effort level [18]. The lags are the smallest in turbo mode, which seems obvious as the least effort is spent in this mode.

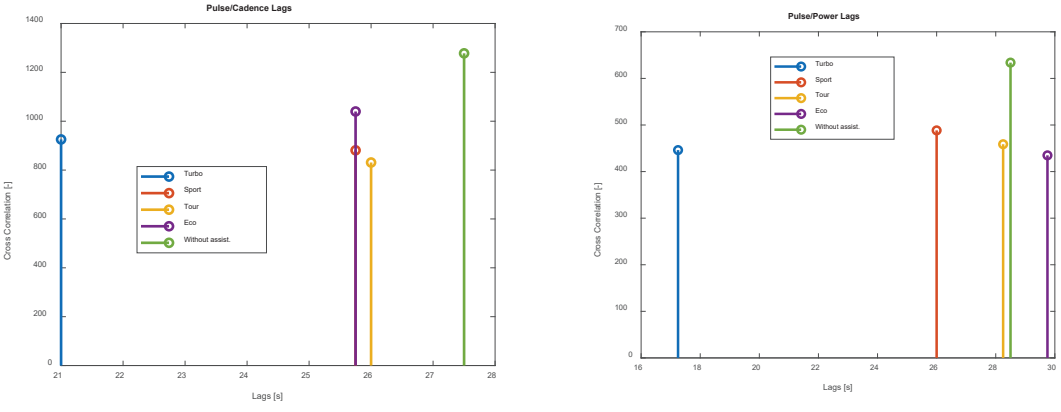

Figure 19. Delays in HR signals to cadence (**left**) and to power (**right**).

It should be emphasized that the presented results are unique and characteristic of the cyclist who conducted the tests. They can vary considerably depending on the individual characteristics of the organism and the level of training.

7. Discussion

According to the authors' knowledge, there are no examples of similar data-derived analyses obtained from bicycle computers in the literature; hence, it is not possible to compare the results. Only in [12] were algorithms for determining the average power per revolution used. The examples presented for the analysis of data related to the measurement of driving speed show that the best results are obtained if an additional speed sensor is mounted on the bike. Speed can also be determined numerically on the basis of GPS data. It has been shown that it is best to use the simplest method, i.e., the forward difference method. The numerical differential method generates noise, which can be eliminated by using averaging filters. The bicycle computer in the absence of a speed sensor also uses GPS data and averaging, but the algorithms selected by the computer manufacturer are not known. On the basis of the cadence and speed data, it is theoretically possible to determine what the gear ratio was. However, this task is made difficult by the humming cadence and speed data, the low sampling rate and the ability to ride on a freewheel. In the case of an intelligent e-bike assistance system, the decision to change gears should be made by an automaton, not a human. An alternative is to use existing automatic or continuously variable transmission solutions [19,20]. Data on average power per rotation provided by the rider along with speed and cadence will be key control variables in intelligent electric bike assist systems. The analyses carried out have shown that the quality of these data is sufficient. It would only be necessary to increase the sampling rate so that it is greater than the maximum frequency of the rotation of the crank (cadence). An important advantage of a bicycle computer is the ability to use cheap devices that monitor the efficiency of the cyclist. Pulse measurements, possibly pressure and saturation, will constitute the second group of variables controlling intelligent assistance systems. The sampling rate of 1 Hz is sufficient in this case.

8. Conclusions

Recording data with a frequency of 1 s is insufficient and reduces the usefulness of the recorded signal for later analyses. The same applies to the speed signal that the computer calculates from the GPS data. A much smoother speed signal can be obtained by using an additional specialized sensor for measuring speed connected to a computer using ANT+ technology. Of course, in this case, recording with a higher frequency would be very advantageous.

Cadence data can be obtained from the cycling computer from a dedicated sensor or from pedals with power measurement. The recorded cadence signal is quite smooth, and the sampling rate of 1 s seems acceptable. Based on the cadence and speed signals, the current gear ratio of the bicycle can be calculated, with the proviso that, in the case of freewheel operation, the result is ambiguous. The obtained gear values are strongly noisy. When the gear ratios of the bicycle resulting from the number of gear teeth are known, a simple classifying function can be built to identify the actual gear ratio on the route.

The power signal transmitted by the cyclist fluctuates significantly more than you might expect. There is no doubt that logging a power signal every 1 s is insufficient. In the case of the cyclist who performed the tests, the analysis showed asymmetry in pedaling. The power transmitted to the right pedal was greater than to the left pedal. Interestingly, this asymmetry was greater in the power-assisted modes. In general, the asymmetry was greater when the power delivered by the rider was lower. There was also an optimal power level with the lowest pedaling asymmetry. Similar comments can be made for the efficiency and smoothness of pedaling. In power assist modes, these indicators deteriorate. It seems that the control system providing the additional electrical power overdrives the dose of energy, and the rider has a hard time adjusting to it.

Recording a heart rate signal every 1 s seems acceptable. Based on heart rate and cadence or power output, the delays in the rider's physiological response to exercise can be detected. Electric assist significantly lowers the rider's pulse. Using the rider's heart rate information to control the dose of power in assist modes can be considered.

Summarizing the results of the analyses carried out in both parts of this article, it can be stated that the frequency of data recording by the bicycle computer is too low, which makes subsequent analyses difficult. It seems that it should be at least in the 4–5 Hz range. This is a postulate that the manufacturers of this type of device may consider in the future. Another problem is the lack of information about internal data processing algorithms, in particular the smoothing filters used.

Taking into account all the advantages and disadvantages of a bicycle computer presented above and in the first part of this article [7], it can be finally concluded that it is a tool that can be successfully used in the research of anthropotechnical cyclist–bicycle systems. According to the authors, the data recorded by the bicycle computer can be used successfully to assess the energy efficiency of electric bicycles and to develop simulation models of bicycle dynamics. This will be the subject of further research.

This is a necessary step to further develop the concept and algorithms of an intelligent assistance system on electric bicycles. Thanks to such a system, an electric bike rented in the public system would become even more accessible to a wide group of users with different physical predispositions. The system would also improve traffic safety. Currently, it is not possible to download data from a bicycle computer in online mode and transfer it to the power control system. In the case of building such a system, it seems more likely to use ANT+ technology to communicate with the necessary sensors. Another way is to cooperate with bicycle computer manufacturers.

Author Contributions: Conceptualization, A.K., T.M. and Z.S.; methodology, A.K., T.M. and Z.S.; software, A.K., T.M. and Z.S.; validation, A.K., T.M. and Z.S.; formal analysis, A.K., T.M. and Z.S.; investigation, A.K., T.M. and Z.S.; resources, A.K., T.M. and Z.S.; data curation, A.K., T.M. and Z.S.; writing—original draft preparation, A.K., T.M. and Z.S.; writing—review and editing, A.K., T.M. and Z.S.; visualization, A.K., T.M. and Z.S.; supervision, A.K., T.M. and Z.S.; project administration, A.K., T.M. and Z.S.; funding acquisition, A.K., T.M. and Z.S. All authors have read and agreed to the published version of the manuscript.

Funding: This research received no external funding.

Institutional Review Board Statement: Not applicable.

Informed Consent Statement: Not applicable.

Data Availability Statement: The data presented in this study are available on request from the authors.

Conflicts of Interest: The authors declare no conflict of interest.

References

1. UTO Poland Portal. The Market of e-Scooters. Available online: https://utopolska.pl/rynek-detaliczny-hulajnog-elektrycznych/. (accessed on 28 December 2021).
2. Czech, P.; Turon, K.; Urbanczyk, R. Bike-Sharing as an Element of Integrated Urban Transport System. In *Advanced Solutions of Transport Systems for Growing Mobility Book Series Advances in Intelligent Systems and Computing*; Sierpinski, G., Ed.; Springer International Publishing: Berlin, Germany, 2018; Volume 631, pp. 103–111.
3. Turoń, K.; Kubik, A.; Chen, F. When, What and How to Teach about Electric Mobility? An Innovative Teaching Concept for All Stages of Education: Lessons from Poland. *Energies* **2021**, *14*, 6440. [CrossRef]
4. Turoń, K.; Kubik, A.; Chen, F. Electric Shared Mobility Services during the Pandemic: Modeling Aspects of Transportation. *Energies* **2021**, *14*, 2622. [CrossRef]
5. Shared Micromobility State of the Industry Report. Available online: https://nabsa.net/wp-content/uploads/2020/10/NABSA-2020-State-of-the-Industry-Report.pdf. (accessed on 28 December 2021).
6. Okraszewska, R.; Grzelec, K.; Jamroz, K. Developing a cycling subsystem as part of a sustainable mobility strategy: The case of Gdansk. *Sci. J. Sil. Univ. Technol.* **2016**, *92*, 87–99. [CrossRef]
7. Matyja, T.; Kubik, A.; Stanik, Z. Possibility to Use Professional Bicycle Computers for the Scientific Evaluation of Electric Bikes: Trajectory, Distance, and Slope Data. *Energies* **2022**, *15*, 758. [CrossRef]

8. Sathyamorthy, D.; Shafii, S.; Fitry, M.; Amin, Z.; Jusoh, A.; Ali, S. Evaluation of the accuracy of global positioning system (GPS) speed measurement via GPS simulation. *Def. S T Tech. Bull.* **2015**, *8*, 51–62.
9. Cho, C.; Yun, M.; Yoon, C.; Lee, M. An ergonomic study on the optimal gear ratio for a multi-speed bicycle. *Int. J. Ind. Ergon.* **1999**, *23*, 95–100. [CrossRef]
10. Balbinot, A.; Milani, C.; Nascimento, J.D.S.B. A New Crank Arm-Based Load Cell for the 3D Analysis of the Force Applied by a Cyclist. *Sensors* **2014**, *14*, 22921–22939. [CrossRef] [PubMed]
11. Quintana-Duque, J.-C.; Dahmen, T.; Saupe, D. Estimation of Torque Variation from Pedal Motion in Cycling. *Int. J. Comput. Sci. Sport* **2015**, *14*, 1–17.
12. Favero Electronisc SRL. Influence of Angular Velocity of Pedaling on the Accuracy of the Measurement of Cyclist Power. Research Article. Available online: https://www.dcrainmaker.com/images/2018/05/Influence-of-Angular-Velocity-of-Pedaling-on-the-Accuracy-of-the-Measurement-of-Cyclist-Power.pdf (accessed on 28 December 2021).
13. Korff, T.; Romer, L.; Mayhew, I.; Martin, J. Effect of Pedaling Technique on Mechanical Effectiveness and Efficiency in Cyclists. *Med. Sci. Sports Exerc.* **2007**, *39*, 991–995. [CrossRef] [PubMed]
14. Yamashitaa, K.; Matsudaa, A.; Ishikuraa, K.; Takagia, H.; Otsukab, S. Visualization of pedaling technique using cleat-size biaxial load cells. *Procedia Eng.* **2013**, *60*, 415–421. [CrossRef]
15. Rodríguez-Rielves, V.; Lillo-Beviá, J.R.; Buendía-Romero, Á.; Martínez-Cava, A.; Hernández-Belmonte, A.; Courel-Ibáñez, J.; Pallarés, J.G. Are the Assioma Favero Power Meter Pedals a Reliable Tool for Monitoring Cycling Power Output? *Sensors* **2021**, *21*, 2789. [CrossRef] [PubMed]
16. Molkkari, M.; Angelotti, G.; Emig, T.; Räsänen, E. Dynamical heart beat correlations during running. *Sci. Rep.* **2020**, *10*, 13627. [CrossRef] [PubMed]
17. Nimmerichter, A.; Eston, R.; Bachl, N.; Williams, C. Longitudinal monitoring of power output and heart rate profiles in elite cyclists. *J. Sports Sci.* **2011**, *29*, 831–839. [CrossRef] [PubMed]
18. Theurel, J.; Theurel, A.; Lepers, R. Physiological and cognitive responses when riding an electrically assisted bicycle versus a classical bicycle. *Ergonomics* **2012**, *55*, 773–781. [CrossRef] [PubMed]
19. Automatic Transmission Is the Future of E-Bike Drivetrains. Available online: https://revonte.com/ (accessed on 28 December 2021).
20. Research Project on Smart e-Bikes. Smart e-Bike Monitoring System. 2018. Available online: http://www.smart-ebikes.com/smart-ebikes/smart-e-bikes-monitor-system-sems/ (accessed on 28 December 2021).

energies

MDPI

Article

What Car for Car-Sharing? Conventional, Electric, Hybrid or Hydrogen Fleet? Analysis of the Vehicle Selection Criteria for Car-Sharing Systems

Katarzyna Turoń [1,*], Andrzej Kubik [1,*] and Feng Chen [2]

[1] Department of Road Transport, Faculty of Transport and Aviation Engineering, Silesian University of Technology, 8 Krasińskiego Street, 40-019 Katowice, Poland
[2] Sino-US Global Logistics Institute, Shanghai Jiao Tong University, Shanghai 200240, China; fchen@sjtu.edu.cn
* Correspondence: katarzyna.turon@polsl.pl (K.T.); andrzej.kubik@polsl.pl (A.K.)

Abstract: Short-term car rental services called "car-sharing" or "carsharing" are systems that in recent years have been an alternative form of transport by individual car in an increasing number of cities around the world. With the growing popularity of services, new decision-making problems have arisen among system operators. Among the challenges faced by operators, due to the constantly growing environmental requirements, is the fleet of vehicles for car-sharing systems-appropriate selection. Noticing this research gap, this article was dedicated to determining the criteria that are important when choosing a fleet of vehicles for car-sharing and to indicate the best suited to the needs of car-sharing vehicles. Own research was proposed, considering desk research, expert research and analyses using the multi-criteria decision support method (ELECTRE III). This research was carried out for the Polish market of car-sharing services. Studying the Polish market is appropriate due to the occurrence of significant difficulties with the fleet incorrectly adjusted to the needs of urban conditions. This study covers vehicles with conventional, electric, hybrid and hydrogen propulsion. The analyses allowed for the determination of the vehicles best suited to the needs of car-sharing. The results show the dominance of hydrogen-powered vehicles over conventional, hybrid and electric vehicles. What is more, it was determined that the most important criteria are the purchase price of the vehicle and energy/fuel consumption per 100 km. The obtained results are a guide to proceeding when making decisions regarding the implementation or modernization of the fleet in car-sharing systems. The results also support achieving more sustainable urban mobility in the zero-emission trend through hydrogen mobility.

Keywords: car-sharing; carsharing; shared mobility; multi-criteria decision analysis; ELECTRE III; MCDA; decision making in transport; transportation engineering; hydrogen mobility; zero emission; green energy

Citation: Turoń, K.; Kubik, A.; Chen, F. What Car for Car-Sharing? Conventional, Electric, Hybrid or Hydrogen Fleet? Analysis of the Vehicle Selection Criteria for Car-Sharing Systems. *Energies* **2022**, *15*, 4344. https://doi.org/10.3390/en15124344

Academic Editor: Byoung Kuk Lee

Received: 19 May 2022
Accepted: 13 June 2022
Published: 14 June 2022

1. Introduction

Short-term car rental services called "car-sharing" or "carsharing" are systems that in recent years have been an alternative form of transport by individual car in an increasing number of cities around the world. The car-sharing market size surpassed USD 2 billion in 2020 [1], and it is expected to grow in 2022 with a Compound Annual Growth Rate (CAGR) of 17.4% [2]. Car-sharing systems have undergone many modifications along with their development. Over the years, system management, the location and relocation of vehicles, price lists and service packages, infrastructure and vehicles have changed [3–6]. These changes resulted from many different factors due to the gradual adaptation of society to new forms of transport [7], and thus changing demand [8,9], due to new legislation or municipal car-sharing regulations being implemented [10,11], changes in environmental requirements [12–14], etc.

Evaluating car-sharing systems has become an interesting topic for scientists. A frequently studied topic is the car-sharing fleet. However, there are several leading topics in the field of fleet research. The first of the leading themes is the size of the fleet in car-sharing systems. For example, fleet size considerations are among the main motives; Xu et al. dedicated their research to electric vehicle fleet size for car-sharing services considering on-demand charging strategy and battery degradation [15]. In comparison, Monteiro et al. optimized car-sharing fleet size to maximize the number of clients served [16]. In turn, Hu and Liu analyzed the joint design of parking capacities and fleet size for one-way station-based car-sharing systems with road congestion constraints [4]. The second leading topics regarding the car fleet are aspects of vehicle location and relocation. For example, the Chang et al. dealt with the subject of location design and relocation of a mixed car-sharing fleet with a CO_2 emission constraint [17]. Yoon et al. investigated car-sharing demand estimation and fleet simulation with electric vehicle adoption [18]. In turn, Fan et al. dealt with car-sharing dynamic decision-making obstacles for vehicle allocation [19]. There is, however, a literature gap in the research on the car-sharing fleet. The gap concerns analyses directly related to the type of vehicles used in the systems and their use. In our previous works, we dealt with the determination of the fleet which is most often used in car-sharing systems [20] and we analyzed the operational factors of vehicle use [21]. Receiving signals from operators of Polish car-sharing systems that they need to make changes to vehicle fleets, we have dedicated this article to the selection of vehicles for car-sharing systems.

From the point of view of common mobility services, the Polish market is a very interesting field. Although vehicle sharing services appeared relatively late to other European countries, e.g., bike-sharing in 2008 [22–26], car-sharing in 2016 [27], moped-sharing in 2017 [28], and scooter-sharing in 2018 [28], this market is characterized as dynamic and valuable [28]. A significant development of shared mobility services in Poland has been observed since 2017, when more and more car-sharing service operators appeared on the market [29]. At the peak of shared mobility systems development, there were 17 car-sharing operators available in 250 cities [29]. Revenues from car-sharing services in Poland in 2019 amounted to over 50 million PLN, and they achieved a double increase in 2021, reaching over 100 million PLN [30]. However, the market boom of new car-sharing operators has not lasted long. After the opening of many systems, the rapid disappearance of many systems from the market has occurred. The most spectacular closures included closure of the Vozilla electric car-sharing system with a fleet of 240 cars [31], closure of the InnogyGo system! with a fleet of 500 electric cars [32], and a few other operators who had pilot schemes have withdrawn from offering short-term car rental to long-term rental. It is worth mentioning that during the boom, the offered vehicle fleets and rental regulations were very chaotic and contradictory. For example, operators have implemented electric cars without having to consider the presence of infrastructure for electric vehicles in a given area [21]. Moreover, many system regulations prevented the efficient use of electric cars. For example, it was necessary to terminate the rental of a vehicle with an energy level in the car's battery that would allow another user to drive a further 30 km, where in practice there was no charging station in the area of the rental zone up to 30 km. What is more, many regulations forbid the user to connect cars to chargers by themselves, while others ordered the vehicle to be returned only under the charger. In practice, the idea of free-floating electric car-sharing did not take place at that time. The difficulties were not only with electric vehicles fleets. Conventionally fueled cars, on the other hand, were targeted at one car model, which discouraged some users from using the cars [20]. Despite the many challenges that Polish car-sharing has had to face in recent years, it is predicted that Polish car-sharing revenues will reach a value of over 265 million PLN in 2025 [30]. Currently, many Polish cities, striving to limit transport by individual cars [33–35], are implementing new transport policies, leading to a significant development of car-sharing service systems, which will result in the creation of new systems and modernization of existing systems

over several years; therefore, it is particularly important to determine the appropriate fleet to supply car-sharing systems to meet the expectations of stakeholders.

The aim of this study is to determine the criteria that are important when choosing a fleet of vehicles for car-sharing and to indicate the best suited to the needs of car-sharing vehicles. This research was carried out for the Polish market. This study covers vehicles with conventional, electric and hydrogen propulsion.

This article consists of four main sections. The first chapter presents a general description of the research problem and characterizes the Polish car-sharing market along with a historical outline. The second chapter presents information on the methods of multi-criteria decision support, as well as a detailed description of the ELECTRE III method used, together with a test plan. The third chapter shows a detailed analysis and the obtained results. The fourth chapter discusses the obtained results and confronts them with the research of other authors. This article is a guide when making decisions regarding the implementation or modernization of the fleet in car-sharing systems. The results also support achieving more sustainable urban mobility in the zero-emission trend through hydrogen mobility.

2. Materials and Methods

Deciding which vehicle fleet to choose is a problem that requires consideration of many different criteria. In this case, we use multi-criteria decision support methods. Multi-criteria decision making (MCDM), multi-criteria decision analysis (MCDA) or multi-criteria data analysis methods are a sub-discipline of operations research [36]. Their task is to provide a wide range of mathematical tools that can be used in the analytical process of decision making. MCDM means the process of determining the best feasible solution according to established criteria and problems that are common occurrences in everyday life [37]. Their specificity enables defining criteria, their weights and actors appearing in the decision-making process, i.e., stakeholders [38]. With their use, it is possible to obtain the final rankings of scenarios for the analyzed research questions [36–39]. MCDM is used to solve decision-making problems at the strategic, tactical, and operational levels [40].

MCDA is widely used to solve various transport problems, including for solving the problem of selecting projects to build the Paris metro [41], choosing the best transport connection between the city of Pittsburgh and international airport [42], or assessing transport solutions for the metropolitan area of Istanbul [43]. Moreover, these methods have also been applied to car-sharing systems. For example, they were used to determine the location of base stations of the EVCARD car-sharing system operator in the area of Shanghai [44], to analyze the selection of the location of car-sharing stations in Beijing [45] and to determine the location of car-sharing stations in the French city of La Rochelle [46]. Since MCDA is commonly used in decision-making aspects, one of the methods was included in the research process.

The research process considered secondary research on vehicles used in car-sharing systems, expert research among car-sharing service operators and the performance of mathematical analyses, considering the multi-criteria decision support method. The detailed procedure of the procedure is presented in Figure 1.

Figure 1. Research process.

Secondary research was carried out on a group of operators functioning in Poland in May 2022.They concerned the analysis of vehicle fleets in car-sharing systems in order to identify the most frequently used cars. Successively, the most popular and commercially available hydrogen-powered vehicles were added to conventional, electric and hybrid

vehicles. Secondary research allowed the building of a database of vehicles that were considered in the calculations.

The next step was to conduct expert research on a group of car-sharing operators present in Poland. The aim of the research was to indicate the importance of individual criteria considered when selecting a vehicle for car-sharing systems. In accordance with the MCDA methodology, the respondents made pairwise comparisons of individual criteria on a scale from 1 to 9, where 1—same meaning; 2—very weak advantage; 3—weak advantage; 4—more than weak advantage, less than strong; 5—strong advantage; 6—more than a strong advantage, less than very strong; 7—a very strong advantage; 8—more than a very strong advantage, less than an extreme; 9—extreme, total advantage. The weights obtained were included in the analyses using the MCDA method.

The last step was to perform analyses using one of the MCDA methods. Among the group of methods frequently used in transport problems is the set of ELECTRE [47]. ELECTRE is an acronym for *Elimination Et Choix Traduisant la Realitè* and represents a set of multi-criteria decision support methods (ELECTRE I, II, III, IV, IS, and TRI), which are based on partial preference aggregation by overrun [47–53]. Different types of ELECTRE methods have different approaches to decision-making problems. The first method produces elections, the others provide ranking [47–53]. The ELECTRE III method is the most popular of the ELECTRE family methods [39]. The ELECTRE III method is most often combined with expert research (e.g., Delphi method) [54]. The method introduces a two-level preference for a given criteria. This means that they may be strongly or slightly better than each other, which means situations when the decision variants differ very or little from each other [39].

The algorithm in the ELECTRE III method includes 3 stages [24]:

(1) Constructing the evaluation matrix and defining the preferences of decision makers,
(2) Building the surpassing relationship,
(3) Using the exceedance relationship to generate an ordered ranking of decision variants.

The first stage of the analysis begins with the definition of a set of criteria that will be used to evaluate the set of decision variants [47–53]. Each criterion from the set is assigned an appropriate weight. Subsequently, by comparing the two decision variants, the exceedance index is calculated [47–53].

In the second step, based on the exceedance index, the answer is whether the first variant is not worse than the second one due to a given criterion. Subsequently, a computation of the compliance rate is performed to be able to obtain a response with the advantage of one option over the other in terms of all criteria [47–53]. The compliance rate is the sum of the weights of the criteria for which the evaluation value of one variant is greater than or equal to the evaluation value of the other variant [47–53].

In the second stage, based on the exceedance index, the answer is whether the first option is not worse than the second one due to the given criterion. Subsequently, a computation of the compliance rate is performed to be able to obtain a response with the advantage of one option over the other in terms of all criteria [47–53]. The compliance rate is the sum of the weights of the criteria for which the evaluation value of one variant is greater than or equal to the evaluation value of the other variant [47–53].

The third stage is based on creating an altitude difference matrix. The scenarios should be ranked sequentially, which begins with their initial ordering by means of the classification procedures: ascend distillation and descend distillation [47–53]. Both distillations rank the best to worst scenarios [47–53].

Ascend distillation is a scheduling process that begins with selecting the best scenario and placing it at the top of the classification [47–53]. The best scenario is then selected again from among the remaining scenarios and placed in the next position in the classification. This procedure is repeated until the set of scenarios is exhausted [47–53].

For descend distillation, the scheduling process begins with the worst-case selection and placement at the end of the ranking. The sequence is the same as in the ascend distillation procedure, with the difference that in subsequent iterations of the remaining

scenarios to be considered, the worst scenario is always selected and placed on the next positions "from the bottom" [47–53].

Then, we create the final ranking based on the top-down and bottom-up ordering. The result is a final ranking of the scenarios. The results are presented in the next chapter.

3. Results

When determining which car-sharing vehicle to choose, in the first step, the most frequently used vehicle models on the Polish market, valid as of May 2022, were determined. The most frequently repeated cars are marked in green. The summary is presented in Table 1.

Table 1. Vehicles used in Polish car-sharing systems.

Engine Type		
Internal Combustion	**Electric Drive**	**Hybrid Drive**
Audi A3	BMW i3 (EV)	Toyota Yaris HSD
Audi Q2	BMW i3s (EV)	Toyota Corolla HSD
Citroen Jumper	Dacia Spring (EV)	Toyota CH-R HSD
Cupra Formentor	Nissan eNV 200 (EV)	
Dacia Dokker	Nissan Leaf (EV)	
Daewoo Lanos	Opel Ampera (EV)	
Ferrari F430	Renault Zoe (EV)	
Fiat 125p	Smart ForTwo EQ (EV)	
Fiat 126p	Tesla Model 3 (EV)	
Fiat 500	Tesla Model S (EV)	
Fiat Ducato	VW eGOLF (EV)	
Fiat Multipla		
FSO Polonez		
Mercedes GLA		
Mercedes W124		
Opel Astra		
Opel Corsa		
Opel Movano		
Porsche 911		
Renault Clio		
Renault Express		
Renault Master		
Seat Arona		
Skoda CityGo		
Skoda Fabia		
Skoda Kodiaq		
Skoda Octavia		
Toyota ProAce		
Trabant 1.1		
VW Crafter		
VW Golf II		
VW Scirocco II		

The most common vehicle models with conventional, electric and hybrid drive were selected successively. In line with global trends in reducing transport emissions, hydrogen-powered vehicles were also included. A total of 12 different vehicle models were included,

representing a diverse set of vehicle classes. A detailed list of vehicles considered in the analysis is presented in Table 2.

Table 2. Cars included in the analysis that can be used in car-sharing systems.

ID	Vehicle Model	Fuel Type
a_1	Toyota Mirai	Hydrogen
a_2	Hyundai Nexo	Hydrogen
a_3	Honda Clarity	Hydrogen
a_4	Opel Corsa	Petrol
a_5	Renault Clio	Petrol
a_6	Fiat 500	Petrol
a_7	Toyota Yaris	Hybrid
a_8	Toyota C-HR	Hybrid
a_9	Toyota Corolla	Hybrid
a_{10}	Renault Zoe	Electric
a_{11}	Smart Fortwo EQ	Electric
a_{12}	Dacia Spring	Electric

The criteria for selecting the vehicles that have been considered are successively defined. The list of critics is presented in Table 3.

Table 3. Criteria for selecting vehicles for the car-sharing fleet.

Factor ID	Definition of the Criterion
f_1	Vehicle price [€]
f_2	Motor power [kW]
f_3	Range on single battery charge/refueling [km]
f_4	Energy/fuel/hydrogen consumption [kWh/100 km]
f_5	Battery charging time/refueling time [min]
f_6	Luggage compartment capacity [L]
f_7	Number of seats in the vehicle [-]

The preferences of experts were directed towards vehicles with the highest possible comfort of movement, with relatively high engine power, luggage compartment capacity, and the lowest possible exhaust emissions due to possible restrictions on access to city centers in the future. The values of individual criteria have been presented in sequence for a selected fleet of vehicles that can be implemented in car-sharing systems. The results are presented in Table 4.

Table 4. Adopted values for particular criteria.

	Definition of the Criterion						
ID	Vehicle Price	Motor Power	Range on Single Battery Charge/ Refueling [km]	Energy/Fuel/ Hydrogen Consumption [kWh/100 km]	Battery Charging Time/Refueling Time [min]	Luggage Compartment Capacity [L]	Number of Seats in the Vehicle
	[€]	[kW]					[-]
a_1	64,400	134	650	33.1128	5	321	5
a_2	70,000	121	666	27.75168	4.5	461	5
a_3	56,852	131	700	39.42	6	439	5
a_4	15,024	55	650	50.02	2	309	5
a_5	14,590	48	1167	29.52	2	391	5
a_6	11,803	63	921	31.16	1.5	185	5
a_7	18,174	74	1029	28.7	1.5	286	5
a_8	21,242	90	1351	30.34	2.5	377	5
a_9	21,028	90	1389	29.52	2.5	361	5
a_{10}	33,231	80	395	13.164	68	338	5
a_{11}	20,783	60	160	15.2	270	260	2
a_{12}	19,711	33	230	13.9	90	300	5

Then, in accordance with the guidelines of the ELECTRE III method, the equivalence, preference, and veto thresholds were determined for each of the criteria, which are presented in Table 5.

Table 5. Values of the equivalence, preference, and veto thresholds in light of the considered criteria.

Factor ID	Maximum Difference of Criteria Values	Equivalence Threshold	Preference Threshold	Veto Threshold
	$\Delta = \max - \min$	$Q = 0.25 \times \Delta$	$p = 0.5 \times \Delta$	$V = \Delta$
f_1	58,197	14,549.25	29,098.5	58,197
f_2	101	25.25	50.5	101
f_3	1229	307.25	614.5	1229
f_4	36.856	9.214	18.428	36.856
f_5	268.5	67.125	134.25	268.5
f_6	276	69	138	276
f_7	3	0.75	1.5	3

In the next step, the values of the concordance matrix were determined, which are presented in Table 6.

Table 6. Concordance matrix C values.

Concordance Matrix:	a_1	a_2	a_3	a_4	a_5	a_6	a_7	a_8	a_9	a_{10}	a_{11}	a_{12}
a_1	0	0.95	0.9645	0.7494	0.931	1	0.9766	0.9	0.9	1	0.9	0.9734
a_2	1	0	0.92	0.7	0.9369	1	0.9819	0.9	0.9	1	0.9	0.9726
a_3	1	1	0	0.9549	0.948	1	0.9929	0.9	0.9	1	0.9	0.9749
a_4	0.6	0.55	0.5558	0	0.9223	1	0.9766	0.8614	0.8614	0.9246	0.9	0.9689
a_5	0.6	0.5993	0.5777	0.7	0	1	0.997	0.9337	0.9337	0.8889	0.9	0.9689
a_6	0.5514	0.55	0.55	0.6601	0.95	0	0.9768	0.9031	0.8908	0.8082	0.8957	0.9348
a_7	0.6	0.5639	0.501	0.7	0.9739	1	0	0.9793	0.9785	0.9895	0.9	0.9682
a_8	0.6257	0.6664	0.6376	0.7	1	1	1	0	1	1	0.9	0.9696
a_9	0.6257	0.6548	0.6088	0.7	1	1	1	1	0	1	0.9	0.9696
a_{10}	0.3	0.4236	0.3898	0.7	0.6675	0.6429	0.6942	0.6408	0.6675	0	0.9	1
a_{11}	0.2074	0.3267	0.1242	0.5905	0.6388	0.6304	0.7105	0.6035	0.6418	0.9435	0	0.95
a_{12}	0.2633	0.3572	0.197	0.6633	0.6755	0.6192	0.6557	0.5589	0.5914	0.9139	0.8931	0

The non-compliance indicators were successively determined for each of the seven considered criteria, which are presented in Tables A1–A7. Based on the non-compliance indicators, the values of reliability indicators were determined, which are presented in Table A8.

The next step was to perform the ascend and descend distillation. The results are presented in the form of a dominance matrix in Table 7.

Table 7. Dominance matrix L.

Dominance Matrix:	a_1	a_2	a_3	a_4	a_5	a_6	a_7	a_8	a_9	a_{10}	a_{11}	a_{12}
a_1	0	I	P−	P+	P+	P+	P+	P+	P+	P+	P+	P+
a_2	I	0	P−	P+	P+	P+	P+	P+	P+	P+	P+	P+
a_3	P+	P+	0	P+	P+	P+	P+	P+	P+	P+	P+	P+
a_4	P−	P−	P−	0	P+	P+	P+	P+	P+	P+	R	P+
a_5	P−	P−	P−	P−	0	P+	I	P−	P−	P+	R	P+
a_6	P−	P−	P−	P−	P−	0	P−	P−	P−	P+	R	P+

Table 7. *Cont.*

Dominance Matrix:	a_1	a_2	a_3	a_4	a_5	a_6	a_7	a_8	a_9	a_{10}	a_{11}	a_{12}
a_7	P−	P−	P−	P−	I	P+	0	P−	P−	P+	R	P+
a_8	P−	P−	P−	P−	P+	P+	P+	0	I	P+	R	P+
a_9	P−	P−	P−	P−	P+	P+	P+	I	0	P+	R	P+
a_{10}	P−	P−	P−	P−	P−	P−	P−	P−	P−	0	R	P+
a_{11}	P−	P−	P−	R	R	R	R	R	R	R	0	R
a_{12}	P−	P−	P−	P−	P−	P−	P−	P−	P−	P−	R	0

Where I—a pair of variants is equivalent; P+—the first option is better than the second option; P−—the first option is worse than the second option.

Based on the value of the exceedance relation matrix, the final ranking of decision values was created, depending on the type of distillation, which are presented in Table 8. The final ranking presented in Table 8 defines which of the considered scenarios is the most optimal in terms of the assumed criteria and the assessment of the preferences of experts.

Table 8. Final ranking.

Dominance Matrix:	Ascend Distillation	Descend Distillation	Average
a_1	1	2	1.5
a_2	1	2	1.5
a_3	1	1	1
a_4	3	3	3
a_5	5	4	4.5
a_6	5	5	5
a_7	5	4	4.5
a_8	4	4	4
a_9	4	4	4
a_{10}	6	5	5.5
a_{11}	2	7	4.5
a_{12}	7	6	6.5

Based on the value of the exceedance relation matrix, the final ranking of decision values was created, depending on the type of distillation, which are presented in Figure 2.

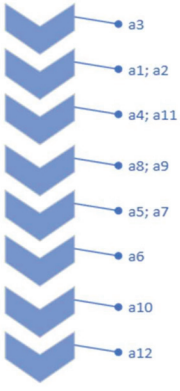

Figure 2. The final ranking of the best vehicles to implement in the car-sharing fleet.

4. Discussion and Conclusions

The research carried out with the use of the ELECTRE III multi-criteria decision support method was used to determine the best selection of vehicles for car-sharing systems based on the criteria established and assessed by experts. The obtained results indicate that

of the analyzed car models, Honda Clarity achieved the top ranking and is the optimal vehicle that meets the expectations of experts.

Moreover, the conducted research shows that hydrogen-powered vehicles are on the podium in the obtained ranking. When analyzing the obtained results in detail, it can be noticed that electric vehicles occupy the last places in the ranking. An interesting finding is that conventionally powered vehicles rank better than electric vehicles. This result is mainly caused by a large disproportion between the purchase prices of an electric vehicle and a vehicle with a conventional drive.

Based on the obtained results, it was found that the most important criteria are the purchase price of the vehicle, energy/fuel consumption per 100 km and the time of refueling/charging the vehicle's battery. The results, therefore, indicate that it is the economic and operational criteria that are of greatest importance for shared mobility cars.

It is worth mentioning that vehicles in car-sharing systems generate profits in terms of traffic. Unfortunately, all vehicles whose battery charging process requires a large amount of time have limited transport availability for users, reducing the often-insufficient vehicle fleet in car-sharing systems.

Therefore, despite the widespread interest in electric vehicles for car-sharing, if the fleet of vehicles is not so large that cars that are being charged cannot be replaced with ready-to-use vehicles, and the infrastructure will not allow the charging time to be reduced to the level of conventional or hydrogen vehicles, electric cars in a car-sharing model will not be the optimal choice.

When translating the obtained results into business practices of car-sharing systems, it is worth emphasizing that hydrogen-powered vehicles are not currently used in systems both in Poland and Europe, and the current trends are directed towards electric vehicles. Unfortunately, the analysis of the market activities of companies shows that most companies with a fleet of electric vehicles in Poland failed, and the systems were closed after several months of operation. This type of practice was also visible in the case of the Paris car-sharing system and the American system in San Diego. Currently, especially in the Polish market, infrastructure for servicing electric vehicles is still too little for individual cars, let alone for servicing car-sharing systems [55]. As Poland is looking for solutions for the development of low-emission transport, more and more hopes are placed on hydrogen. Currently, hydrogen refueling stations are already being created with plans to expand by 2025, when the number of stations will increase by 3200% [56]. Therefore, the dissemination of a hydrogen-powered car for Polish car-sharing is a future-proof scenario.

Due to the area character of the research and the results being limited to the Polish market, the authors plan to expand future research to a larger scale and conduct research considering other European countries. Due to the lack of scientific research on the selection of the vehicle fleet, no direct reference was made in the discussion to the results of other authors' research.

The obtained results support the operators of car-sharing systems in the decision-making process when selecting vehicles for the fleet of their systems.

Author Contributions: Conceptualization, K.T.; methodology, K.T. and A.K.; validation, F.C.; resources, K.T., A.K., and F.C.; data curation, K.T. and A.K.; writing—original draft preparation, K.T., and A.K.; writing—review and editing, K.T. and A.K.; supervision, F.C.; project administration, K.T.; funding acquisition, K.T. All authors have read and agreed to the published version of the manuscript.

Funding: This research received no external funding. Research conducted as part of the Silesian University of Technology subsidy for the maintenance and development of the research potential of early career researchers—BKM-692/RT1/2022, 12/010/BKM22/1058 and BKM-693/RT1/2022 12/010/BKM22/1059.

Institutional Review Board Statement: Not applicable.

Informed Consent Statement: Not applicable.

Data Availability Statement: The data presented in this study are available on request from the authors.

Conflicts of Interest: The authors declare no conflict of interest.

Appendix A

Table A1. Values of the non-compliance indicators according to the 1st criterion.

Discordance Matrix (f_1):	a_1	a_2	a_3	a_4	a_5	a_6	a_7	a_8	a_9	a_{10}	a_{11}	a_{12}
a_1	0	0	0	0	0	0	0	0	0	0	0	0
a_2	0	0	0	0	0	0	0	0	0	0	0	0
a_3	0	0	0	0	0	0	0	0	0	0	0	0
a_4	0.6969	0.8893	0.4375	0	0	0	0	0	0	0	0	0
a_5	0.7118	0.9042	0.4524	0	0	0	0	0	0	0	0	0
a_6	0.8076	1	0.5482	0	0	0	0	0	0	0	0	0
a_7	0.5886	0.7811	0.3292	0	0	0	0	0	0	0	0	0
a_8	0.4832	0.6756	0.2238	0	0	0	0	0	0	0	0	0
a_9	0.4905	0.683	0.2311	0	0	0	0	0	0	0	0	0
a_{10}	0.0712	0.2636	0	0	0	0	0	0	0	0	0	0
a_{11}	0.4989	0.6914	0.2395	0	0	0	0	0	0	0	0	0
a_{12}	0.5358	0.7282	0.2764	0	0	0	0	0	0	0	0	0

Table A2. Values of the non-compliance indicators according to the 2nd criterion.

Discordance Matrix (f_2):	a_1	a_2	a_3	a_4	a_5	a_6	a_7	a_8	a_9	a_{10}	a_{11}	a_{12}
a_1	0	0	0	0	0	0	0	0	0	0	0	0
a_2	0	0	0	0	0	0	0	0	0	0	0	0
a_3	0	0	0	0	0	0	0	0	0	0	0	0
a_4	0.5644	0.3069	0.505	0	0	0	0	0	0	0	0	0
a_5	0.703	0.4455	0.6436	0	0	0	0	0	0	0	0	0
a_6	0.4059	0.1485	0.3465	0	0	0	0	0	0	0	0	0
a_7	0.1881	0	0.1287	0	0	0	0	0	0	0	0	0
a_8	0	0	0	0	0	0	0	0	0	0	0	0
a_9	0	0	0	0	0	0	0	0	0	0	0	0
a_{10}	0.0693	0	0.0099	0	0	0	0	0	0	0	0	0
a_{11}	0.4653	0.2079	0.4059	0	0	0	0	0	0	0	0	0
a_{12}	1	0.7426	0.9406	0	0	0	0	0.1287	0.1287	0	0	0

Table A3. Values of the non-compliance indicators according to the 3rd criterion.

Discordance Matrix (f_3):	a_1	a_2	a_3	a_4	a_5	a_6	a_7	a_8	a_9	a_{10}	a_{11}	a_{12}
a_1	0	0	0	0	0	0	0	0.1408	0.2026	0	0	0
a_2	0	0	0	0	0	0	0	0.1147	0.1766	0	0	0
a_3	0	0	0	0	0	0	0	0.0594	0.1212	0	0	0
a_4	0	0	0	0	0	0	0	0.1408	0.2026	0	0	0
a_5	0	0	0	0	0	0	0	0	0	0	0	0
a_6	0	0	0	0	0	0	0	0	0	0	0	0
a_7	0	0	0	0	0	0	0	0	0	0	0	0
a_8	0	0	0	0	0	0	0	0	0	0	0	0
a_9	0	0	0	0	0	0	0	0	0	0	0	0
a_{10}	0	0	0	0	0.2563	0	0.0317	0.5557	0.6176	0	0	0
a_{11}	0	0	0	0	0.6387	0.2384	0.4142	0.9382	1	0	0	0
a_{12}	0	0	0	0	0.5248	0.1245	0.3002	0.8242	0.8861	0	0	0

Table A4. Values of the non-compliance indicators according to the 4th criterion.

Discordance Matrix (f_4):	**a_1**	**a_2**	**a_3**	**a_4**	**a_5**	**a_6**	**a_7**	**a_8**	**a_9**	**a_{10}**	**a_{11}**	**a_{12}**
a_1	0	0	0	0	0	0	0	0	0	0	0	0
a_2	0	0	0	0.2085	0	0	0	0	0	0	0	0
a_3	0	0	0	0	0	0	0	0	0	0	0	0
a_4	0	0	0	0	0	0	0	0	0	0	0	0
a_5	0	0	0	0.1124	0	0	0	0	0	0	0	0
a_6	0	0	0	0.0234	0	0	0	0	0	0	0	0
a_7	0	0	0	0.1569	0	0	0	0	0	0	0	0
a_8	0	0	0	0.0679	0	0	0	0	0	0	0	0
a_9	0	0	0	0.1124	0	0	0	0	0	0	0	0
a_{10}	0.0824	0	0.4248	1	0	0	0	0	0	0	0	0
a_{11}	0	0	0.3143	0.8895	0	0	0	0	0	0	0	0
a_{12}	0.0424	0	0.3848	0.9601	0	0	0	0	0	0	0	0

Table A5. Values of the non-compliance indicators according to the 5th criterion.

Discordance Matrix (f_5):	**a_1**	**a_2**	**a_3**	**a_4**	**a_5**	**a_6**	**a_7**	**a_8**	**a_9**	**a_{10}**	**a_{11}**	**a_{12}**
a_1	0	0	0	0	0	0	0	0	0	0	0.9739	0
a_2	0	0	0	0	0	0	0	0	0	0	0.9777	0
a_3	0	0	0	0	0	0	0	0	0	0	0.9665	0
a_4	0	0	0	0	0	0	0	0	0	0	0.9963	0
a_5	0	0	0	0	0	0	0	0	0	0	0.9963	0
a_6	0	0	0	0	0	0	0	0	0	0	1	0
a_7	0	0	0	0	0	0	0	0	0	0	1	0
a_8	0	0	0	0	0	0	0	0	0	0	0.9926	0
a_9	0	0	0	0	0	0	0	0	0	0	0.9926	0
a_{10}	0	0	0	0	0	0	0	0	0	0	0.5047	0
a_{11}	0	0	0	0	0	0	0	0	0	0	0	0
a_{12}	0	0	0	0	0	0	0	0	0	0	0.3408	0

Table A6. Values of the non-compliance indicators according to the 6th criterion.

Discordance Matrix (f_6):	**a_1**	**a_2**	**a_3**	**a_4**	**a_5**	**a_6**	**a_7**	**a_8**	**a_9**	**a_{10}**	**a_{11}**	**a_{12}**
a_1	0	0.0145	0	0	0	0	0	0	0	0	0	0
a_2	0	0	0	0	0	0	0	0	0	0	0	0
a_3	0	0	0	0	0	0	0	0	0	0	0	0
a_4	0	0.1014	0	0	0	0	0	0	0	0	0	0
a_5	0	0	0	0	0	0	0	0	0	0	0	0
a_6	0	1	0.8406	0	0.4928	0	0	0.3913	0.2754	0.1087	0	0
a_7	0	0.2681	0.1087	0	0	0	0	0	0	0	0	0
a_8	0	0	0	0	0	0	0	0	0	0	0	0
a_9	0	0	0	0	0	0	0	0	0	0	0	0
a_{10}	0	0	0	0	0	0	0	0	0	0	0	0
a_{11}	0	0.4565	0.2971	0	0	0	0	0	0	0	0	0
a_{12}	0	0.1667	0.0072	0	0	0	0	0	0	0	0	0

Table A7. Values of the non-compliance indicators according to the 7th criterion.

Discordance Matrix (f_7):	a_1	a_2	a_3	a_4	a_5	a_6	a_7	a_8	a_9	a_{10}	a_{11}	a_{12}
a_1	0	0	0	0	0	0	0	0	0	0	0	0
a_2	0	0	0	0	0	0	0	0	0	0	0	0
a_3	0	0	0	0	0	0	0	0	0	0	0	0
a_4	0	0	0	0	0	0	0	0	0	0	0	0
a_5	0	0	0	0	0	0	0	0	0	0	0	0
a_6	0	0	0	0	0	0	0	0	0	0	0	0
a_7	0	0	0	0	0	0	0	0	0	0	0	0
a_8	0	0	0	0	0	0	0	0	0	0	0	0
a_9	0	0	0	0	0	0	0	0	0	0	0	0
a_{10}	0	0	0	0	0	0	0	0	0	0	0	0
a_{11}	1	1	1	1	1	1	1	1	1	1	0	1
a_{12}	0	0	0	0	0	0	0	0	0	0	0	0

Table A8. Credibility matrix values D.

Credibility Matrix:	a_1	a_2	a_3	a_4	a_5	a_6	a_7	a_8	a_9	a_{10}	a_{11}	a_{12}
a_1	0	0.95	0.9645	0.7494	0.931	1	0.9766	0.9	0.9	1	0.2346	0.9734
a_2	1	0	0.92	0.7	0.9369	1	0.9819	0.9	0.9	1	0.2011	0.9726
a_3	1	1	0	0.9549	0.948	1	0.9929	0.9	0.9	1	0.3017	0.9749
a_4	0.4547	0.1353	0.5558	0	0.9223	1	0.9766	0.8614	0.8614	0.9246	0.0335	0.9689
a_5	0.321	0.1432	0.4875	0.7	0	1	0.997	0.9337	0.9337	0.8889	0.0335	0.9689
a_6	0.2366	0	0.1948	0.6601	0.95	0	0.9768	0.9031	0.8908	0.8082	0	0.9348
a_7	0.6	0.2831	0.501	0.7	0.9739	1	0	0.9793	0.9785	0.9895	0	0.9682
a_8	0.6257	0.6479	0.6376	0.7	1	1	1	0	1	1	0.067	0.9696
a_9	0.6257	0.6013	0.6088	0.7	1	1	1	1	0	1	0.067	0.9696
a_{10}	0.3	0.4236	0.3674	0	0.6675	0.6429	0.6942	0.6408	0.6675	0	0.9	1
a_{11}	0	0	0	0	0	0	0	0	0	0	0	0
a_{12}	0	0.0605	0.0101	0.0787	0.6755	0.6192	0.6557	0.2227	0.1649	0.9139	0.8931	0

References

1. Global Market Insights. Car Sharing Market Size by Model (P2P, Station-Based, Free-Floating), By Business Model (Round Trip, One Way), By Application (Business, Private), COVID-19 Impact Analysis, Regional Outlook, Application Potential, Price Trend, Competitive Market Share & Forecast, 2021–2027. Available online: https://www.gminsights.com/industry-analysis/carsharing-market (accessed on 16 May 2022).
2. 360 Research Reports. Global Carsharing Market Insights and Forecast to 2028. Available online: https://360researchreports.com/global-carsharing-market-19963041 (accessed on 16 May 2022).
3. Esfandabadi, Z.S.; Diana, M.; Zanetti, M.C. Carsharing services in sustainable urban transport: An inclusive science map of the field. *J. Clean. Prod.* **2022**, *357*, 131981. [CrossRef]
4. Hu, L.; Liu, Y. Joint design of parking capacities and fleet size for one-way station-based carsharing systems with road congestion constraints. *Transp. Res. Part B Methodol.* **2016**, *93*, 268–299. [CrossRef]
5. Zhang, S.; Zhao, X.; Li, X.; Yu, H. Heterogeneous fleet management for one-way electric carsharing system with optional orders, vehicle relocation and on-demand recharging. *Comput. Oper. Res.* **2022**, *145*, 105868. [CrossRef]
6. Wu, C.; Le Vine, S.; Philips, S.; Tang, W.; Polak, J. Free-floating carsharing users' willingness-to-pay/accept for logistics management mechanisms. *Travel Behav. Soc.* **2020**, *21*, 154–166. [CrossRef] [PubMed]
7. Aguilera-García, A.; Gomez, J.; Antoniou, C.; Vassallo, J.M. Behavioral factors impacting adoption and frequency of use of carsharing: A tale of two European cities. *Transp. Policy* **2022**, *123*, 55–72. [CrossRef]
8. Huang, W.; Huang, W.; Jian, S. One-way carsharing service design under demand uncertainty: A service reliability-based two-stage stochastic program approach. *Transp. Res. Part E Logist. Transp. Rev.* **2022**, *159*, 102624. [CrossRef]
9. Yao, Z.; Gendreau, M.; Li, M.; Ran, L.; Wang, Z. Service operations of electric vehicle carsharing systems from the perspectives of supply and demand: A literature review. *Transp. Res. Part C Emerg. Technol.* **2022**, *140*, 103702. [CrossRef]
10. Balac, M.; Ciari, F.; Axhausen, K.W. Modeling the impact of parking price policy on free-floating carsharing: Case study for Zurich, Switzerland. *Transp. Res. Part C Emerg. Technol.* **2017**, *77*, 207–225. [CrossRef]

11. Repoux, M.; Kaspi, M.; Boyacı, B.; Geroliminis, N. Dynamic prediction-based relocation policies in one-way station-based carsharing systems with complete journey reservations. *Transp. Res. Part B Methodol.* **2019**, *130*, 82–104. [CrossRef]
12. Shams Esfandabadi, Z.; Ravina, M.; Diana, M.; Zanetti, M.C. Conceptualizing environmental effects of carsharing services: A system thinking approach. *Sci. Total Environ.* **2020**, *745*, 141169. [CrossRef]
13. Meng, Z.; Li, E.Y.; Qiu, R. Environmental sustainability with free-floating carsharing services: An on-demand refueling recommendation system for Car2go in Seattle. *Technol. Forecast. Soc. Change* **2020**, *152*, 119893. [CrossRef]
14. Roblek, V.; Meško, M.; Podbregar, I. Impact of Car Sharing on Urban Sustainability. *Sustainability* **2021**, *13*, 905. [CrossRef]
15. Xu, M.; Wu, T.; Tan, Z. Electric vehicle fleet size for carsharing services considering on-demand charging strategy and battery degradation. *Transp. Res. Part C Emerg. Technol.* **2021**, *127*, 103146. [CrossRef]
16. Monteiro, C.M.; Soares Machado, C.A.; de Oliveira Lage, M.; Berssaneti, F.T.; Davis, C.A.; Quintanilha, J.A. Optimization of carsharing fleet size to maximize the number of clients served. Computers. *Environ. Urban Syst.* **2021**, *87*, 101623. [CrossRef]
17. Chang, J.; Yu, M.; Shen, S.; Xu, M. Location Design and Relocation of a Mixed Car-Sharing Fleet with a CO_2 Emission Constraint. *Serv. Sci.* **2017**, *9*, 205–218. [CrossRef]
18. Yoon, T.; Cherry, C.R.; Ryerson, M.S.; Bell, J.E. Carsharing demand estimation and fleet simulation with EV adoption. *J. Clean. Prod.* **2019**, *206*, 1051–1058. [CrossRef]
19. Fan, W.; Machemehl, R.B.; Lownes, N.E. Carsharing: Dynamic Decision-Making Problem for Vehicle Allocation. *Transp. Res. Rec.* **2008**, *2063*, 97–104. [CrossRef]
20. Turoń, K.; Kubik, A.; Łazarz, B.; Czech, P.; Stanik, Z. Car-sharing in the context of car operation. *IOP Conf. Ser. Mater. Sci. Eng.* **2018**, *421*, 032027. [CrossRef]
21. Turoń, K.; Kubik, A.; Chen, F. Operational Aspects of Electric Vehicles from Car-Sharing Systems. *Energies* **2019**, *12*, 4614. [CrossRef]
22. Kwiatkowski, M.A. Bike-sharing-boom—Development of new forms of sustainable transport in Poland on the example of a public bike. *Work. Comm. Geogr. Commun. PTG* **2018**, *21*, 60–69.
23. Matyja, T.; Kubik, A.; Stanik, Z. Possibility to Use Professional Bicycle Computers for the Scientific Evaluation of Electric Bikes: Trajectory, Distance, and Slope Data. *Energies* **2022**, *15*, 758. [CrossRef]
24. Czech, P.; Turoń, K.; Urbańczyk, R. Bike-sharing as an element of integrated Urban transport system. Advanced Solutions of Transport Systems for Growing Mobility. In *Proceedings of the Scientific and Technical Conference Transport Systems Theory and Practice, Katowice, Poland, 18–20 September 2017*; Sierpiński, G., Ed.; TSTP: Katowice, Poland, 2017.
25. Matyja, T.; Kubik, A.; Stanik, Z. Possibility to Use Professional Bicycle Computers for the Scientific Evaluation of Electric Bikes: Velocity, Cadence and Power Data. *Energies* **2022**, *15*, 1127. [CrossRef]
26. Turoń, K.; Sierpiński, G. Bike-sharing as a possibility to support Vision Zero. In Proceedings of the 12th International Road Safety Conference GAMBIT 2018—"Road Innovations for Safety—The National and Regional Perspective", GAMBIT 2018, Gdańsk, Poland, 12–13 April 2018.
27. Delloite. Shared Mobility in Poland. Overview. Available online: https://www.teraz-srodowisko.pl/media/pdf/aktualnosci/6982-mobility-in-poland-2019.pdf (accessed on 5 June 2022).
28. Puzio, E. The development of shared mobility in Poland using the example of a city bike system. *Res. Pap. Wrocław Univ. Econ.* **2020**, *64*, 162–170. [CrossRef]
29. Research and Market Portal. Shared Mobility Market Size, Share & Trends Analysis Report by Service Model (Ride Hailing, Bike Sharing, Ride Sharing), by Vehicle Type (Cars, Two-Wheelers), by Region (North America, Europe, APAC, Latin America), and Segment Forecasts, 2022–2030. Available online: https://www.researchandmarkets.com/reports/5595792/shared-mobility-market-size-share-and-trends?utm_source=BW&utm_medium=PressRelease&utm_code=qr3qtb&utm_campaign=1704132+-+World+Shared+Mobility+Market+Analysis+Report+2022-2030+Featuring+Car2Go%2c+Deutsche+Bahn+Connect%2c+Didi+Chuxing%2c+Drive+Now%2c+Evcard%2c+Flinkster%2c+Grab%2c+Greengo%2c+Lyft%2c+Uber%2c+%26+Zipcar&utm_exec=chdo54prd (accessed on 5 June 2022).
30. Statista. Forecast Revenues from Carsharing Services in Poland from 2019 to 2025. Available online: https://www.statista.com/statistics/1059362/poland-carsharing-revenues/ (accessed on 5 June 2022).
31. Bankier Portal. Vozilla Wyprzedaje "Elektryki". Do Kupienia Ponad Sto Aut. Available online: https://www.bankier.pl/moto/vozilla-wyprzedaje-elektryki-do-kupienia-ponad-sto-aut-6367/ (accessed on 28 May 2022).
32. Rzeczpospolita. Moto Raport. Available online: https://moto.rp.pl/tu-i-teraz/art17350741-innogy-go-konczy-z-elektrycznymi-autami-na-minuty (accessed on 28 May 2022).
33. Concept of the Strategic Action Program of the Metropolis GZM until 2022. Available online: https://bip.metropoliagzm.pl/artykul/34552/125421/program-dzialan-strategicznych-gornoslasko-zaglebiowskiej-metropolii-do-roku-2022 (accessed on 14 May 2022).
34. Plan of the Development of the Śląskie Voivodeship 2020+. Available online: https://planzagospodarowania.slaskie.pl/download/content/33 (accessed on 15 May 2022).
35. Environmental Protection Plan for the Silesian Voivodeship from 2019, including the Perspective until 2024. Available online: https://www.slaskie.pl/download/content/67075 (accessed on 15 May 2022).
36. Roy, B. *How Outranking Relation Halps Multiple Criteria Decision Making*; University of South Carolina Press: Columbia, SC, USA, 1973.

37. Jahan, A.; Edwards, K.L. Multi-criteria Decision-Making for Materials Selection. In *Multi-Criteria Decision Analysis for Supporting the Selection of Engineering Materials in Product Design*; Butterworth-Heinemann: Oxford, UK, 2013; pp. 31–41. [CrossRef]
38. Ishizaka, A.; Nemery, P. *Multi-Criteria Decision Analysis, Methods and Software*; Wiley and Sons Ltd.: Chichester, UK, 2013.
39. Nermend, K. *Methods of Multi-Criteria and Multi-Dimensional Analysis in Decision Suport. [Metody Analizy Wielokryterialnej i Wielowymiarowej we Wspomaganiu Decyzji]*; Wydawnictwo PWN: Warszawa, Polska, 2017.
40. Ziemba, P. Multi-Criteria Stochastic Selection of Electric Vehicles for the Sustainable Development of Local Government and State Administration Units in Poland. *Energies* **2020**, *13*, 6299. [CrossRef]
41. Dyer, J.S.; Fishburn, P.C.; Steuer, R.E.; Wallenius, J.; Zionts, S. Multiple Criteria Decision Making, Multiattribute Utility Theory: The Next Ten Years. *Manag. Sci.* **1992**, *38*, 645–654. [CrossRef]
42. Saaty, T. How to make decision: The analytic hierarchy process. *Eur. J. Oper. Res.* **1990**, *48*, 9–26. [CrossRef]
43. Istanbul Metropolitan Municipality & Japan International Cooperation Agency, The Study on Integrated Urban Transport Master Plan for Istanbul Metropolitan Area in the Republic of Turkey. Available online: https://openjicareport.jica.go.jp/pdf/11965720_01.pdf (accessed on 5 June 2022).
44. Li, W.; Li, Y.; Fan, J.; Deng, H. Siting of Carsharing Stations Based on Spatial Multi-Criteria Evaluation: A Case Study of Shanghai EVCARD. *Sustainability* **2017**, *9*, 152. [CrossRef]
45. Lin, M.; Huang, C.; Xu, Z. Multimoora Based Mcdm model for site selection of car sharing station under picture fuzzy environment. *Sustain. Cities Soc.* **2020**, *53*, 101873. [CrossRef]
46. Awasthi, A.; Breuil, D.; Singh Chauhan, S.; Parent, M.; Reveillere, T. A Multicriteria Decision Making Approach for Carsharing Stations Selection. *J. Decis. Syst.* **2007**, *16*, 57–78. [CrossRef]
47. Figueira, J.R.; Greco, S.; Roy, B.; Słowiński, R. ELECTRE methods: Main features and recent developments. In *Handbook of Multicriteria Analysis*; Springer: Berlin/Heidelberg, Germany, 2010; pp. 51–89.
48. La Scalia, G.; Micale, R.; Certa, A.; Enea, M. Ranking of shelf life models based on smart logistic unit using the ELECTRE III method. *Int. J. Appl. Eng. Res.* **2015**, *10*, 38009–38015.
49. Bottero, M.; Ferretti, V.; Figueira, J.R.; Greco, S.; Roy, B. Dealing with a multiple criteria environmental problem with interaction effects between criteria through an extension of the ELECTRE III method. *Eur. J. Oper. Res.* **2015**, *245*, 837–850. [CrossRef]
50. Norese, M.F. ELECTRE III as a support for participatory decision-making on the localisation of waste-treatment plants. *Land Use Policy* **2006**, *23*, 76–85. [CrossRef]
51. Certa, A.; Enea, M.; Lupo, T. ELECTRE III to dynamically support the decision maker about the periodic replacements configurations for a multi-component system. *Decis. Support Syst.* **2013**, *55*, 126–134. [CrossRef]
52. Buchanan, J.T.; Sheppard, P.J.; Vanderpooten, D. *Project Ranking Using ELECTRE III*; Department of Management Systems, University of Waikato: Hamilton, New Zealand, 1999.
53. Yu, X.; Zhang, S.; Liao, X.; Qi, X. ELECTRE methods in prioritized MCDM environment. *Inf. Sci.* **2018**, *424*, 301–316. [CrossRef]
54. Battisti, F. ELECTRE III for Strategic Environmental Assessment: A "Phantom" Approach. *Sustainability* **2022**, *14*, 6221. [CrossRef]
55. Electric Market Portal. Available online: https://www.rynekelektryczny.pl/infrastruktura-ladowania-pojazdow-elektrycznych/ (accessed on 5 June 2022).
56. Murator Portal. Available online: https://www.muratorplus.pl/technika/oze/stacje-wodoru-w-polsce-gdzie-powstana-ile-punktow-aa-iRpp-S1Ax-VNwG.html (accessed on 5 June 2022).

energies

MDPI

Article

Compromise Multi-Criteria Selection of E-Scooters for the Vehicle Sharing System in Poland

Paweł Ziemba [1,*] and Izabela Gago [2]

[1] Institute of Management, University of Szczecin, Aleja Papieża Jana Pawła II 22A, 70-453 Szczecin, Poland
[2] Technical Secondary School of Economics in Szczecin, 70-236 Szczecin, Poland; izabela.gago@te.edu.pl
* Correspondence: pawel.ziemba@usz.edu.pl

Abstract: In Poland, there is a high ratio of private transport and unfavorable patterns of daily commuting. These patterns can be changed by introducing comfortable and eco-friendly vehicles, such as e-scooters and e-bikes. At the same time, the development of the e-micromobility-based vehicle sharing services market is developing. The aim of the article is to analyze selected e-scooters available on the Polish market and to identify the most useful vehicles from two opposing perspectives, i.e., the potential customer and owner of the vehicle sharing system. The PROSA GDSS (PROMETHEE for Sustainability Assessment—Group Decision Support System) method and the graphical representation of GAIA (Geometrical Analysis for Interactive Assistance) were used to search for a compromise and balance between the needs of the indicated stakeholders. The results of the methods used were compared with the results of the PROMETHEE GDSS method, which does not take into account the balance between the stakeholders and allows for a strong compensation of the assessments of decision makers. The conducted research allowed indicating the optimal e-scooter to meet the needs of both decision makers, and it is the JEEP 2xe Urban Camou. Both the sensitivity analysis and the solution obtained with the use of the PROMETHEE GDSS method confirmed that it is the optimal alternative, the least sensitive to changes in criteria weights and changes in the decision makers' compensation coefficients.

Keywords: e-micromobility; e-scooters; electric vehicles; PROSA GDSS; multi-criteria decision aid; MCDA; MCDM; compromise solution

Citation: Ziemba, P.; Gago, I. Compromise Multi-Criteria Selection of E-Scooters for the Vehicle Sharing System in Poland. *Energies* **2022**, *15*, 5048. https://doi.org/10.3390/en15145048

Academic Editor: Katarzyna Turoń

Received: 5 June 2022
Accepted: 6 July 2022
Published: 11 July 2022

1. Introduction

The development of the automotive industry significantly affects not only the comfort of travel for motorists, but also has a significant impact on the Earth. The amount of exhaust fumes emitted into the environment is constantly increasing. This is a huge problem in the further progress of civilization, having a destructive influence on the air, soil, and atmosphere. The Organization of the Petroleum Exporting Countries [1] estimates that the number of passenger cars will increase from nearly 870 million in 2009 to 1.76 billion in 2035. These data show how important it is to popularize alternative means of transportation. In the case of Poland, it is most important in the case of larger cities such as Warsaw, Poznań, Gdańsk, Szczecin, Katowice, Kraków, or Wrocław. These cities are particularly vulnerable to vehicle exhaust fumes and the associated environmental pollution. Due to the structure of the Polish energy mix, in the winter season the pollution is additionally combined with the burning of coal in order to heat houses and generate energy in coal-fired power plants. All these factors create smog which is harmful to both human health and the environment.

The reduction of greenhouse gas (GHG) emissions resulting from the combustion of crude oil and coal is the first major step in meeting the requirements imposed by the European Union (EU) to combat climate change. Continuous automotive progress and the related greater demand for crude oil and gas, until a few years ago, accounted for approx. 60% of total energy consumption and GHG emissions in transport [2].

Passenger transport requires decisive steps to meet the requirements imposed by the EU. In the light of the European Green Deal, the key task is to make Europe the first climate neutral continent [3]. The decarbonization of the transport sector is expected to contribute to the achievement of an 80% reduction in GHG emissions by 2050 [4]. EU countries impose restrictions on the movement of older, substandard means of transport in designated zones, e.g., in cities such as Berlin or Paris. In Poland, these standards are also beginning to take shape and are described in the Act on electromobility and alternative fuels [5]. This is important due to the fact that Poland has the second largest percentage of cars over 10 years of age (approx. 73%) in the EU [6]. This impacts significantly the number of exhaust gases emitted into the environment [7]. Older cars, which do not have a Diesel Particulate Filter, emit much more soot, i.e., solid particles, and if they enter the circulatory or respiratory system, they can cause cancer.

Another important factor determining the need to use alternative means of transport is the difficult access to raw materials necessary in the transport process, such as crude oil, its derivatives, and gas. So far, Russia has been the main supplier of both gas and crude oil to Poland. Due to the war in Ukraine and the sanctions imposed on Russia as a result of the war, the prices of oil and gas have increased significantly. The lack of independence in obtaining such important raw materials has caused unstable fuel prices throughout Europe, including in Poland.

The context mentioned above indicates the need to change the structure of means of transport used in urban traffic. A potential direction for such a change is the development of electro-micromobility (e-micromobility) and the use of e-scooters and e-bikes, implementing the idea of green cities [8]. Interest in such vehicles on the part of individual users has been growing dynamically in recent years [9]. There are also more and more rental companies of this type of vehicles in larger cities [10]. The advantage of using e-bikes and e-scooters is the relief of the vehicle user compared to a traditional bicycle or scooter. Thanks to the use of electric means of microtransport, you can cover a longer distance without losing your strength and park these vehicles practically anywhere (which is not possible in the case of cars) [11]. The use of e-vehicles additionally allows you to travel from several to several dozen kilometers on a single battery charge. E-bikes and e-scooters are also an ideal choice for people with health problems who want to gradually start playing sports [9,12]. The hybrid ability to ride these vehicles allows you to switch to assist mode in order to regain strength. Manufacturers of vehicles such as e-bikes and e-scooters are releasing newer and newer functionalities on the market, e.g., the ability to synchronize with a smartphone and share the distances covered with others. Using e-bikes and e-scooters to travel to and from work, users do not waste time waiting in traffic jams. In large, crowded cities, this is a particularly important advantage. In addition, people using e-bikes and e-scooters to travel to work do not waste energy to cover the distance, which would be the case with a traditional bicycle or scooter. Although the environmental benefits of using e-micromobility are debatable, there is a consensus among researchers that switching from cars and motorcycles to e-micromobility would result in an overall reduction in GHG emissions [13]. A natural way of introducing e-micromobility in cities are, in turn, sharing stations, which make vehicles available to users quickly and cheaply, while also providing other benefits, such as creating jobs, stimulating economic growth, etc. [14]. In the case of such sharing systems, it is important to respect the points of view of all stakeholders, i.e., both investors and users [15]. Due to the wide availability on the Polish market and frequent use by sharing stations in Poland [16], this study considers e-scooters as the primary means of e-microtransport in cities.

The aim of the article is to analyze selected e-scooters available on the Polish market and to recommend the most useful vehicles of this type. The practical contribution of the article is to consider e-scooters both from the perspective of the individual user as well as the owner of the vehicle sharing system (VSS). Each of these stakeholders has different preferences when choosing a vehicle (fleet of vehicles). It is important to find a compromise between the owner and the VSS customer so that each is satisfied with the

vehicle they use. The multi-criteria decision aid (MCDA) method called PROMETHEE for Sustainability Assessment—Group Decision Support System (PROSA GDSS) was used to identify e-scooters taking into account the preferences of both stakeholders [17]. PROSA GDSS supports groups decisions by rewarding compromise solutions and punishing unbalanced solutions between stakeholders. The use of this method in the context of seeking a compromise between two contradictory perspectives (VSS customer and owner) is a methodological contribution of the article. The resulting compromise was visualized graphically using the PROSA Geometrical Analysis for Interactive Assistance (GAIA) plane. The article is divided into seven sections. Section 2 provides an overview of contemporary research related to micromobility and e-micromobility. Section 3 discusses the research procedure and the methods used. The research results are presented in Section 4 and the results are discussed in Section 5. Section 6 contains managerial and environmental implications, and the article's conclusions are presented in Section 7.

2. Literature Review

In recent years, the interest in research on micromobility and e-micromobility has grown significantly. This is confirmed by the dynamically growing number of research papers on this subject [18,19]. MCDA methods are also used more and more often in such studies, both in the case of classic micromobility and e-micromobility. Tian et al. [20] developed a decision support framework for bike-sharing programs. The framework is based on the fuzzy BWM and MDM methods, which were used to weigh the criteria, and the MULTIMOORA method, with which preferences were aggregated. Karolemeas et al. [21] prepared an index based on the AHP method for the planning of bicycle routes in the existing road network. In turn, in the studies by Kurniadhini and Roychansyah [22], Kabak et al. [23], Eren and Katanalp [24], and Guler and Yomralioglu [25], the potential locations of the bike-sharing system stations were considered and assessed. In the aforementioned studies, the aggregation of multi-criteria preferences was carried out using various MCDA methods, which were, respectively: SMCA, MULTIMOORA, VIKOR, and TOPSIS. In each of these studies, the AHP method was used to obtain the criteria weights, and in the publication by Guler and Yomralioglu [25], the criteria were additionally weighed using the BWM and fuzzy AHP methods. The above-mentioned articles dealt with decision-making problems related to conventional bikes, while the following papers mainly related to e-micromobility. Fazio et al. [26] used the SMCA method to study the adjustment of the road network to the needs of e-scooters. Kalakoni et al. [27] developed an environment matching index for different types of micromobility based on the AHP method. Using the developed index, they adjusted the appropriate micromobility and e-micromobility vehicles for individual areas. Torkayesh and Deveci [28] proposed a TRUST-based location assessment framework for battery swapping stations for e-scooters. Tang and Yang [29] used the interval-valued Pythagorean fuzzy preference relation to choose a supplier of e-bikes recycling. Deveci et al. [30] dealt with the issue of safety assessment of e-scooters using the fuzzy LAAW and qROFS Einstein WASPAS methods. Bajec et al. [15] using a set of DAHP and DEA methods selected the supplier of the e-bike-sharing system. Wankmüller et al. [31] used the BWM method to identify criteria relevant to the selection of e-micromobility vehicles for mountain rescue. Finally, Sałabun et al. [32] using the COMET method chose e-bikes for sustainable urban transport. More detailed applications of MCDA methods in research on micromobility and e-micromobility are presented in Table 1.

Table 1. Applications of MCDA methods in decision problems related to microtransport.

Aim of the Research	Subject of Research	Location	MCDA Methods	No of Criteria/Subcriteria	No of Alternatives	Comment	Ref.
Development of a smart performance evaluation framework BSPs	BSPs	Changsha, China	Fuzzy BWM (CW), Fuzzy MDM (CW), Fuzzy MULTIMOORA (PA)	18	5	4 experts	[20]
Development of an index assessing the possibility of using a bicycle in the existing road network	Roads (road network)	Zografou, Greece	AHP	3/10	Infinity		[21]
Identification of suitable locations for BSS stations	Potential locations of BSS stations in the GIS system	Yogyakarta, Indonesia	AHP (CW), SMCA (PA)	3/13	Infinity		[22]
Location suitability analysis for BSS stations	Potential locations of BSS stations in the GIS system	Karsiyaka, Izmir, Turkey	AHP (CW), MULTIMOORA (PA)	3/12	19		[23]
Determining the appropriate locations of BSS stations depending on the type of land development	Potential locations of BSS stations in the GIS system	Izmir, Turkey	AHP (CW), VIKOR (PA), Psychometric VIKOR (PA)	9/21	42 (transportation related), 28 (recreational)		[24]
Decision support in the selection of locations for BSS and BL stations	Potential locations of BSS and BL stations in the GIS system	Istanbul, Turkey	AHP (CW), Fuzzy AHP (CW), BWM (CW), TOPSIS (PA)	9	39 (BSS station), 6 (BL)	3 scenarios	[25]
Transport network suitability analysis for e-scooters	Roads (road network)	Catania, Italy	SMCA	7	Infinity		[26]
Development of an index to assess the fit of the neighborhood for specific types of micromobility and selection of the micromobility system for a given area	Micromobility systems (station-based, free floating, privately owned: bikes, e-bikes, e-scooters)	Paris, France	AHP	11/78 (index related), 8/12 (selection related)	0 (index related), 7 (selection related)		[27]
Development of a BSST location selection framework for e-scooters	Potential BSST locations	Istanbul, Turkey	TRUST	10	4		[28]
Choosing sustainable e-bike-sharing recycling supplier	Recycling service providers	-	IVPFIDM	8	4	3 experts	[29]
Development of a DSS to evaluate strategies leading to the safe use of e-scooters	Policies to develop e-scooters security	-	Fuzzy LAAW (CW), qROFS Einstein WASPAS (PA)	14	3	5 experts	[30]
Choosing an e-BSS provider	Real and fictional e-BSS providers	Slovenia	DAHP (CW), DEA (PA)	26	24		[15]
Selection of assessment attributes for e-micromobility transport solutions	E-microtransport evaluation criteria for mountain rescue	Austria / Italy	BWM (CW)	22	-		[31]
Analysis of e-bikes in the context of sustainable transport in order to select the best vehicle	E-bikes	-	COMET	8	64		[32]

BSP—Bike-Sharing Program, BSS—Bicycle/Bike-Sharing System, BL—Bicycle Lane, BSST—Battery Swapping Stations, DSS—Decision Support System, GIS—Geographic Information System, BWM- Best-Worst Method, MDM—Maximizing Deviation Method, MULTIMOORA—Multi-Objective Optimization by Ratio Analysis plus the Full Multiplicative Form, AHP—Analytic Hierarchy Process, SMCA—Spatial Multi-Criteria Analysis, VIKOR—Multicriteria Optimization and Compromise Solution (Visekriterijumska Optimizacija i Kompromisno Resenje), TOPSIS—Technique for Order of Preference by Similarity to Ideal Solution, TRUST—Multi-Normalization Multi-Distance Assessment, IVPFIDM—Interval-Valued Pythagorean Fuzzy Information Decision-Making Approach, DAHP—Distance-based AHP, DEA—Data Envelopment Analysis, LAAW—Logarithmic Additive Assessment of the Weight Coefficients, qROFS—q-Rung Orthopair Fuzzy Sets, WASPAS—Weighted Aggregated Sum Product Assessment, COMET—Characteristic Objects Method.

When analyzing Table 1, it is easy to notice that there are few publications in which vehicles belonging to the e-micromobility category were assessed in a multi-criteria evaluation. Such issues appear only in the work of Sałabun et al. [32], where e-bikes were considered. The works of Wankmüller et al. [31] and Bajec et al. [15] are also partially similar to this topic. The first of these articles analyzed the potential criteria for selecting various e-micromobility solutions. In the second article, in the context of choosing the e-bike-sharing system supplier, there were also criteria that directly refer to the vehicles offered by the suppliers. Therefore, a research gap is visible in the topic of selecting e-scooters for the needs of individual users or VSSs. The second research gap is that few studies take into account the different perspectives represented by individual stakeholders. Only in the articles by Tian et al. [20], Tang and Yang [29], and Deveci et al. [30] was a group assessment approach used. Nevertheless, in each of these articles, the decision was the result of the views of field experts (entrepreneurs, academic professors, officials), and to the best of our knowledge, in the context of e-micromobility, no study has been conducted so far taking into account the contrary views of VSSs customers and owners.

3. Materials and Methods

3.1. Research Approach

The research scheme was based on the PROSA GDSS method, consisting of three stages [17]:

1. generation of alternatives and criteria,
2. individual evaluation by each decision maker,
3. global evaluation by the group.

In the first stage, a set of decision alternatives $A = \{a_1, a_2, \ldots, a_m\}$ is defined, containing the acceptable alternatives (variants), from among which the alternative that best satisfies the decision makers is selected. This stage also specifies a set of criteria for evaluating alternatives $C = \{c_1, c_2, \ldots, c_n\}$. On the basis of the sets A and C, the performance table $E = C(A)$ is built, containing the performance of alternatives based on criteria. This matrix is the basis for the assessment for each of the K decision-makers (stakeholders, experts) belonging to the set $DM = \{dm_1, dm_2, \ldots, dm_K\}$.

The second stage is an individual assessment of the various alternatives by each of the decision makers. In this stage, you can use one of the methods belonging to the PROMETHEE / PROSA families. In the e-scooters study, the PROMETHEE II method was used due to the fact that it is computationally simple and, at the same time, sufficient to aggregate the criteria for the purposes of this study. The result of this stage are the values of $\varsigma^{dm_k}(a_i)$ obtained for each alternative, separately for individual decision makers.

In the third stage, the values $\varsigma^{dm_k}(a_i)$ are aggregated into a group assessment taking into account a compromise or balance between decision makers. An aggregation is made using the PROSA-C method, and the result are the $PSV_{net}(a_i)$ values obtained for each of the alternatives considered. Both in the second and third stage, numerical studies can be supported by graphical analyses using the PROMETHEE GAIA method in the second stage and PROSA GAIA in the third stage. The diagram of the research procedure is presented in Figure 1.

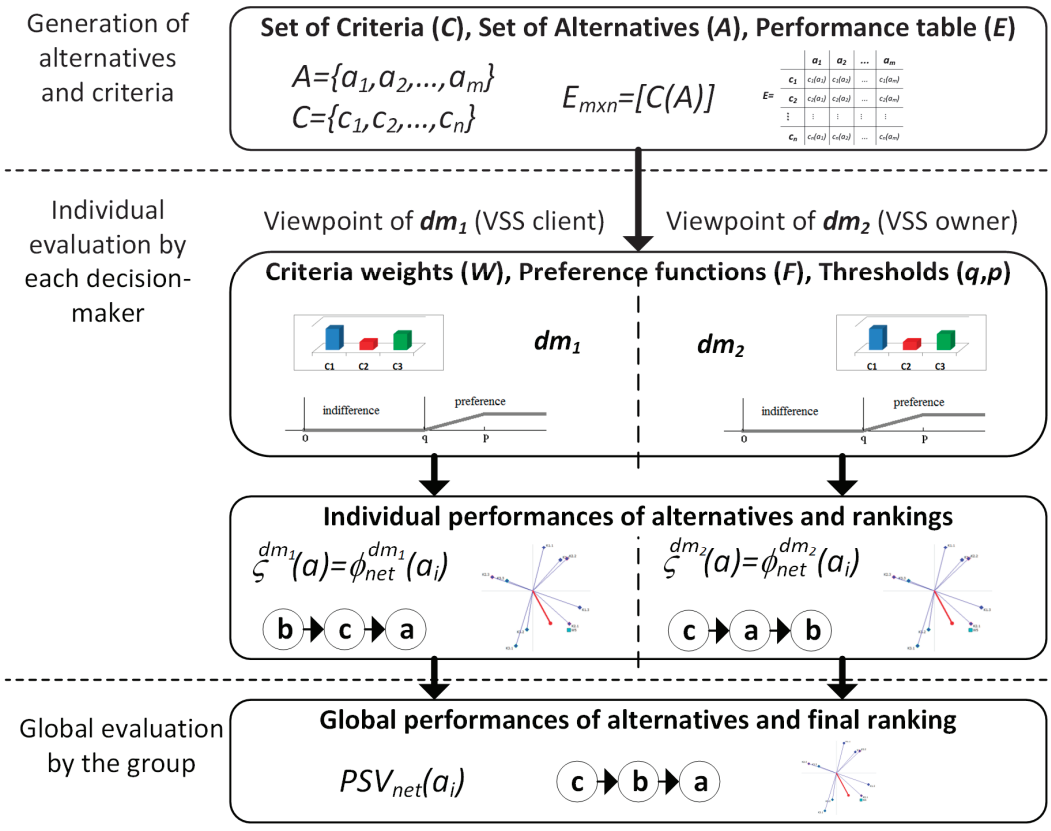

Figure 1. Diagram of the research procedure based on the PROSA GDSS method.

3.2. PROMETHEE II Method

The second stage of the proposed research approach is based on the PROMETHEE II method [33,34] in the variant using the single criterion net flow. Four steps are performed in this stage.

Step 1. Calculating the deviations based on pair-wise comparisons.

In this step, all alternatives from set A are compared in pairs in terms of successive criteria c_k and for each such comparison the deviation $d_k(a_i, a_j)$ is determined, according to Formula (1):

$$d_k(a_i, a_j) = c_k(a_i) - c_k(a_j), \quad \forall i, j = 1, \ldots, m, \quad \forall k = 1, \ldots, n \tag{1}$$

where $c_k(a_i)$ is the rating/performance of the alternative a_i in terms of the c_k criterion.

Step 2. Applying the preference functions.

For each k-th criterion, preference functions F_k are selected, allowing for the conversion of the deviation d_k to the normalized preference value $P_k \in [0, 1]$, according to Formula (2):

$$P_k(a_i, a_j) = F_k\left[d_k(a_i, a_j)\right], \forall i, j = 1, \ldots, m, \quad \forall k = 1, \ldots, n \tag{2}$$

Six different preference functions as shown in Figure 2 can be used in this step.

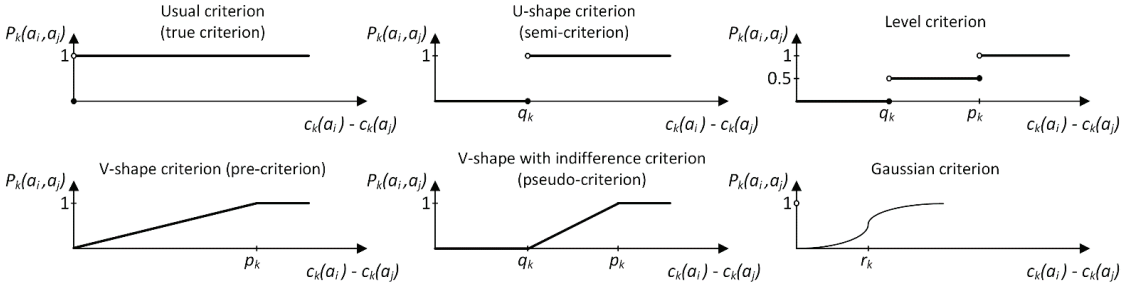

Figure 2. Preference functions used in the PROMETHEE method.

These functions are described by Formulas (3)–(8), where the following thresholds are used in selected functions: q_k—indifference, p_k—preference, r_k—Gaussian.

1. Usual criterion (true criterion) (3):

$$P_k(a_i, a_j) = \begin{cases} 0, \text{ for } d_k(a_i, a_j) \leq 0 \\ 1, \text{ for } d_k(a_i, a_j) > 0 \end{cases} \tag{3}$$

2. U-shape criterion (semi-criterion) (4):

$$P_k(a_i, a_j) = \begin{cases} 0, \text{ for } d_k(a_i, a_j) \leq q_k \\ 1, \text{ for } d_k(a_i, a_j) > q_k \end{cases} \tag{4}$$

3. V-shape criterion (pre-criterion) (5):

$$P_k(a_i, a_j) = \begin{cases} 0, & \text{for } d_k(a_i, a_j) \leq 0 \\ \frac{d_k(a_i, a_j)}{p_k}, & \text{for } 0 < d_k(a_i, a_j) \leq p_k \\ 1, & \text{for } d_k(a_i, a_j) > p_k \end{cases} \tag{5}$$

4. Level criterion (6):

$$P_k(a_i, a_j) = \begin{cases} 0, & \text{for } d_k(a_i, a_j) \leq q_j \\ \frac{1}{2}, & \text{for } q_k < d_k(a_i, a_j) \leq p_k \\ 1, & \text{for } d_k(a_i, a_j) > p_k \end{cases} \tag{6}$$

5. V-shape with indifference criterion (pseudo-criterion) (7):

$$P_k(a_i, a_j) = \begin{cases} 0, & \text{for } d_k(a_i, a_j) \leq q_k \\ \frac{d_k(a_i, a_j) - q_k}{p_k - q_k}, & \text{for } q_k < d_k(a_i, a_j) \leq p_k \\ 1, & \text{for } d_k(a_i, a_j) > p_k \end{cases} \tag{7}$$

6. Gaussian Criterion (8):

$$P_k(a_i, a_j) = \begin{cases} 0, & \text{for } d_k(a_i, a_j) \leq 0 \\ 1 - exp\left(\frac{-d_k(a_i, a_j)^2}{2{r_k}^2}\right), & \text{for } d_k(a_i, a_j) > 0 \end{cases} \tag{8}$$

Step 3. Calculating net outranking flows for individual criteria.

Based on the preference value P_k, the net outranking flow of alternative a_i over each other alternative for the k-th criterion is calculated, using Formula (9):

$$\phi_k(a_i) = \frac{1}{m-1} \sum_{j=1}^{m} \left[P_k(a_i, a_j) - P_k(a_j, a_i) \right], \forall i = 1, \ldots, m, \ \ \forall k = 1, \ldots, n \tag{9}$$

The ϕ_k values allow you to order the alternatives separately for each criterion.

Step 4. Calculating the global net outranking flow.

The global net outranking flow for each of the alternatives is determined on the basis of Formula (10):

$$\phi_{net}(a_i) = \sum_{k=1}^{n} \phi_k(a_i) \, w_k, \forall i = 1, \ldots, m \tag{10}$$

where w_k is the weight of the k-th criterion. Weights are normalized ($\sum_{k=1}^{n} w_k = 1$). The obtained values of ϕ_{net} are the final solution according to the PROMETHEE II method, and in the PROSA GDSS method they are the results obtained by each of the decision makers separately. Therefore, for each k-th decision-maker and for the i-th alternative, there is an assignment of $\varsigma^{dm_k}(a_i) = \phi_{net}(a_i)$.

3.3. PROSA-C Method for GDSS

The last, third stage is to use the PROSA-C method [35] in order to identify alternatives that represent the best compromise between decision makers. At this stage, the set of criteria $C = \{c_1, c_2, \ldots, c_n\}$ is replaced by the sequence set $R = \{Rdm_1, Rdm_2, \ldots, Rdm_K\}$. Each k-th sequence corresponds to the results of the evaluation of alternatives by the k-th decision-maker and is composed of the values $\varsigma^{dm_k}(a_i)$ determined in the second stage, i.e., $Rdm_k = \left\{ \varsigma^{dm_k}(a_1), \varsigma^{dm_k}(a_2), \ldots, \varsigma^{dm_k}(a_m) \right\}$. The performance table $E = R(A)$ is built on the basis of the sets A and R. The PROSA-C method for GDSS consists of eight steps, with the initial four steps being based on the PROMETHEE II method.

Step 1. Calculating deviations based on pair-wise comparisons.

The results obtained in the second stage by the individual alternatives are compared for each k-th decision maker. For each comparison, the deviation $d_k(a_i, a_j)$ is determined, according to Formula (11):

$$d_k(a_i, a_j) = \varsigma^k(a_i) - \varsigma^k(a_j), \ \ \forall i, j = 1, \ldots, m, \ \ \forall k = 1, \ldots, K \tag{11}$$

Step 2. Calculating the value of the preferences.

To transform the deviation d_k into the normalized preference value $P_k \in [0, 1]$, the V-shaped criterion is used (12):

$$P_k(a_i, a_j) = \begin{cases} 0, & \text{for } d_k(a_i, a_j) \leq 0 \\ \frac{d_k(a_i, a_j)}{p_k}, & \text{for } 0 < d_k(a_i, a_j) \leq 2 \\ 1, & \text{for } d_k(a_i, a_j) > 2 \end{cases}, \forall i, j = 1, \ldots, m, \ \ \forall k = 1, \ldots, K \tag{12}$$

The expression $d_k(a_i, a_j) > 2$ can only be true if the PROSA-C or PROSA-G method with the compensation factor $s > 0.3$ was used in the second PROSA GDSS stage.

Step 3. Calculating net outranking flows for individual criteria.

The net outranking flow of the alternative a_i over each other alternative for the k-th decision maker is calculated, based on Formula (13):

$$\phi_k(a_i) = \frac{1}{m-1} \sum_{j=1}^{m} \left[P_k(a_i, a_j) - P_k(a_j, a_i) \right], \forall i = 1, \ldots, m, \ \ \forall k = 1, \ldots, K \tag{13}$$

Step 4. Calculating the global net outranking flow.

For each alternative, a global net outranking flow is computed. The calculations are based on the individual outranking flows of each k-th decision-maker and its weight ω_k, according to Formula (14):

$$\phi_{net}(a_i) = \sum_{k=1}^{K} \phi_k(a_i)\ \omega_k, \forall i = 1, \ldots, m \tag{14}$$

Step 5. Analysis of the criteria compensation relationship.

Determining the values $\phi_k(a_i)$ and $\phi_{net}(a_i)$ allows investigating the compensation relations that exist between the alternatives.

1. The balance relation ($\approx$)—occurs when $\phi_k(a_i) \approx \phi_{net}(a_i)$ and means that the evaluation of the alternative a_i by the k-th decision maker is balanced in relation to the other decision makers.
2. The relation of being compensated (Cd)—occurs when $\phi_k(a_i) \ll \phi_{net}(a_i)$ and means that the low evaluation of the alternative a_i by the k-th decision maker is compensated for by the remaining decision makers ($\exists \phi_{k'}(a_i) : \phi_k(a_i)\ Cd\ \phi_{k'}(a_i)$).
3. Compensation relation (Cs)—occurs when $\phi_k(a_i) \gg \phi_{net}(a_i)$ and means that the high evaluation of the alternative a_i by the k-th decision maker compensates for the assessments of other decision makers ($\exists \phi_{k'}(a_i) : \phi_k(a_i)\ Cs\ \phi_{k'}(a_i)$).

The occurrence of the Cd or Cs relation means that the evaluation of the alternative a_i by the k-th decision maker is not balanced in relation to the other decision makers. The << and >> operators denote the contractual relations as "much less than" and "much greater than", expressing a subjective view of a large difference between the compared values. The $\approx$ operator expresses the subjective view that the values on both sides of the operator can be considered "approximately equal". The analysis of the compensation relation may be a hint regarding the expected values of the compensation factor s. If the decision-maker wants to increase the influence of the balance on the obtained solution, then higher values s can be assumed.

Step 6. Calculating absolute deviations for decision makers' assessments.

The value of the absolute deviation is determined separately for each decision maker and for each alternative, according to Formula (15):

$$AD_k(a_i) = |\phi_{net}(a_i) - \phi_k(a_i)|s_k, \forall i = 1, \ldots, m,\ \ \forall k = 1, \ldots, K \tag{15}$$

where s_k is the compensation factor for the k-th decision maker. In practice, s_k is a specific weight, and $AD_k(a_i)$ is the weighted distance of the global net outranking flow $\phi_{net}(a_i)$ from the net outranking flow obtained for the k-th decision maker $\phi_k(a_i)$.

Step 7. Calculating individual PROSA values for decision makers' evaluations.

Individual PROSA values are determined on the basis of Formula (16):

$$PSV_k(a_i) = \phi_k(a_i) - AD_k(a_i), \forall i = 1, \ldots, m,\ \ \forall k = 1, \ldots, K \tag{16}$$

Step 8. Calculating the global net PROSA values.

The net value of PROSA is determined using Formula (17):

$$PSV_{net}(a_i) = \sum_{k=1}^{K} PSV_k(a_i)\ \omega_k, \forall i = 1, \ldots, m \tag{17}$$

3.4. GAIA Analysis

An important aspect related to the application of the PROMETHEE and PROSA methods is the GAIA analysis. Formally, it is a method of multi-criteria decision analysis, dealing

with descriptive issues [36]. GAIA aims to provide a complete graphic representation of a decision problem, thanks to which it enables the analysis of the obtained solution and indication of directions for its possible improvement. Therefore, GAIA allows for grasping the decision problem and its solution from a descriptive perspective. It gives the decision maker a clear description of decision alternatives and their consequences [34,37].

In the PROSA GDSS method, the GAIA analysis can be used in stages two and three. In this study, in the second stage, it is based on the values of $\phi_k(a_i)$ (PROMETHEE GAIA) and is used to analyze alternatives in terms of criteria. In the third stage, the GAIA analysis is based on the values of $PSV_k(a_i)$ (PROSA-C GAIA), and the analysis concerns the assessments of decision makers. Both PROMETHEE GAIA and PROSA-C GAIA are based on the same procedure and differ only in the input data [38]. The GAIA method can be divided into six steps.

Step 1. Construction of the performance matrix.

In the performance matrix M with dimensions $M_{m\times n}$ (for criteria) or $M_{m\times K}$ (for decision makers), the alternative a_i is represented by the row α_i. Each row α_i corresponds to a point A_i in space $\mathbb{R}^n$ (in the case of criteria) or $\mathbb{R}^K$ (in the case of decision makers), so the row α_i contains the coordinates of the point A_i. The performance matrix for PROMETHEE GAIA is presented in expression (18), and for PROSA-C GAIA it is presented in expression (19):

$$M = \begin{pmatrix} \phi_1(a_1) & \phi_2(a_1) & \cdots & \phi_n(a_1) \\ \phi_1(a_2) & \phi_2(a_2) & \cdots & \phi_n(a_2) \\ \vdots & \vdots & \ddots & \vdots \\ \phi_1(a_m) & \phi_2(a_m) & \cdots & \phi_n(a_m) \end{pmatrix} = \begin{pmatrix} \alpha_1 \\ \alpha_2 \\ \vdots \\ \alpha_m \end{pmatrix} \tag{18}$$

$$M = \begin{pmatrix} PSV_1(a_1) & PSV_2(a_1) & \cdots & PSV_K(a_1) \\ PSV_1(a_2) & PSV_2(a_2) & \cdots & PSV_K(a_2) \\ \vdots & \vdots & \ddots & \vdots \\ PSV_1(a_m) & PSV_2(a_m) & \cdots & PSV_K(a_m) \end{pmatrix} = \begin{pmatrix} \alpha_1 \\ \alpha_2 \\ \vdots \\ \alpha_m \end{pmatrix} \tag{19}$$

Step 2. Calculating the variance-covariance matrix and determining the GAIA plane.

The calculation of the variance-covariance matrix is intended to reduce the space $\mathbb{R}^n$ ($\mathbb{R}^K$) to a 2-dimensional plane. In this operation, Formula (20) is used:

$$tC = M^T * M \tag{20}$$

where t is the coefficient with a positive integer value, C is the variance-covariance matrix, and T is the transportation of the M matrix. For matrix C, the set of eigenvalues $\lambda = \{\lambda_1, \ldots, \lambda_n\}$ or $\lambda = \{\lambda_1, \ldots, \lambda_K\}$ is determined. The plane $\mathbb{R}^2$ is marked by the eigenvectors $u \perp v$, corresponding to the two largest eigenvalues from the set λ (λ_u and λ_v).

Step 3. Finding coordinates of alternatives.

Each point $A_i = (u_i, v_i)$ represents the i-th alternative in the plane $\mathbb{R}^2$. The coordinates of these points are determined according to Formula (21):

$$\begin{cases} u_i = \alpha_i * u \\ v_i = \alpha_i * v \end{cases} \tag{21}$$

Step 4. Determining the coordinates of the criteria/decision makers' vectors.

For criteria, each vector $\overrightarrow{C_k} = \left[u_k^c, v_k^c\right]$ represents the k-th criterion on the $\mathbb{R}^2$ plane. In turn, in the case of decision makers, each vector $\overrightarrow{DM_k} = \left[u_k^{dm}, v_k^{dm}\right]$ represents the views of

the k-th decision maker. The tails of these vectors are at the origin of the coordinate system. The vector coordinates are determined according to Formulas (22) and (23):

$$\begin{cases} u_k^c = e_k * u \\ v_k^c = e_k * v \end{cases} \tag{22}$$

$$\begin{cases} u_k^{dm} = e_k * u \\ v_k^{dm} = e_k * v \end{cases} \tag{23}$$

where e_k is the k-th row of the identity matrix with dimensions $n \times n$ (for criteria) or $K \times K$ (for decision makers).

Step 5. Determining the direction of searching for a compromise solution.

The vector $\vec{\pi} = [u^\pi, v^\pi]$ determining the compromise solution is calculated according to Formula (24):

$$\begin{cases} u^\pi = W * u \\ v^\pi = W * v \end{cases} \tag{24}$$

where W is the vector of the normalized weights of criteria (w) or decision makers (ω).

Step 6. Calculating information loss.

Reducing the dimensionality of the space $\mathbb{R}^n$ ($\mathbb{R}^K$) to the plane $\mathbb{R}^2$ causes that some information about alternatives and criteria or the views of decision makers is lost. The amount of information transferred to the 2-dimensional space is represented by the δ value calculated using Formula (25) or Formula (26), for criteria or decision makers, respectively:

$$\delta^c = \frac{\lambda_u + \lambda_v}{\sum_{k=1}^{n} \lambda_k} \tag{25}$$

$$\delta^{dm} = \frac{\lambda_u + \lambda_v}{\sum_{k=1}^{K} \lambda_k} \tag{26}$$

The GAIA plane provides graphical information on alternatives and criteria or views of decision makers. If the criteria vectors $\vec{C_k}$ (or decision makers vectors $\vec{DM_k}$) point in the same direction, it means that the criteria they represent (views of decision makers) similarly affect the global assessment of alternatives. While the opposite turns of vectors indicate a contradiction of preferences or views. On the other hand, the orthogonal arrangement of vectors means a lack of dependence. The length of a vector is the strength of the influence of a given criterion (decision maker) on the global assessment of alternatives. The further in the plane the point A_i representing the i-th alternative is in the direction defined by the vector, the more the criterion (decision-maker) represented by the vector supports this alternative. The same principle applies to the vector $\vec{\pi}$ representing a compromise solution.

4. Results

4.1. Collection of Alternatives and Criteria, Performance Table of Alternatives

The first stage of the study was to select decision alternatives and evaluation criteria. The considered alternatives were the most popular e-scooters in Poland. The vehicles for analysis were selected on the basis of information about the most frequently purchased e-scooters. This information was obtained from the three largest stores on the Polish market offering electronic products [39]. The ten most popular vehicles were selected from each store. As some vehicles were included in the top 10 in more than one store, the result was a list of 21 e-scooters that created a set of decision-making alternatives A. It is worth noting that the selection of vehicles takes into account the specificity of the Polish market, because e-scooters include three vehicles by Polish manufacturers (Motus and Skymaster).

The selection of criteria was based on literature sources. As the literature shows a shortage of research on the multi-criteria price of e-scooters, the criteria used in similar decision

problems concerning e-bikes and e-micromobility in general were analyzed [15,31,32,40,41]. Moreover, publications on a similar problem of choosing an electric car [42–46]. As the criteria in the articles cited are not strictly aligned with the evaluation of e-scooters, only selected criteria were considered in this study. Table 2 contains the criteria selected for the evaluation of e-scooters along with references to the literature.

Table 2. Criteria selected for the evaluation of e-scooters.

No	Criterion	Unit	Direction	Reference
C_1	Battery capacity	Ampere hours [Ah]	Max	[31,32,40–43,45,46]
C_2	Battery charging time	Hours [h]	Min	[15,32,41–43,45,46]
C_3	Engine power	Watts [W]	Max	[32,40,42,43,45]
C_4	Max gradient	Percent [%]	Max	[31]
C_5	Number of gears	Units	Max	[32]
C_6	Weight	Kilograms [kg]	Min	[31,32,40,41,45]
C_7	Load capacity	Kilograms [kg]	Max	[42,43,45,46]
C_8	Range	Kilometers [km]	Max	[15,31,32,40–46]
C_9	Tires diameter	Inches [inch]	Max	
C_{10}	Mobile app	True/False	Max	
C_{11}	Cruise control	True/False	Max	
C_{12}	Pedestrian mode	True/False	Max	
C_{13}	KERS	True/False	Max	
C_{14}	e-ABS	True/False	Max	
C_{15}	Suspension	True/False	Max	[15]
C_{16}	Brakes	Points	Max	
C_{17}	Protection rating	Points	Max	[31]
C_{18}	Price	Polish new zloty [PLN]	Min	[31,32,41–46]

KERS—Kinetic Energy Recovery System, e-ABS—Electric Anti-lock Braking System.

The analysis of Table 2 shows that not all criteria are based on the literature. In particular, Table 2 defines several criteria closely tailored to the evaluation of e-scooters and related to their specific characteristics. These are criteria for tire diameter, vehicle communication with the mobile application, cruise control, pedestrian mode, presence of a Kinetic Energy Recovery System (KERS) and Electric Anti-lock Braking System (e-ABS), used suspension and braking systems, as well as hill climbing ability and the number of gears (speed modes). Some of the criteria are binary, so they refer to whether a given system/feature is present in the vehicle. Binary criteria occur when, on the basis of information from vehicle manufacturers, it would be difficult to determine which vehicles have for a given system, one that is developed more or less than another. The selected criteria are described using a point scale—these are the criteria for which the quality can be differentiated on the basis of information provided by manufacturers. For example, the braking system can be based on fender, electric, drum, or disk brakes. Depending on the components used in the braking system, it was assigned an appropriate score. In the same way, the use of disk and drum brakes was rewarded, as each of these types of brakes has certain advantages. Disk brakes are more efficient and have more stopping power, but wear faster and require more maintenance than drum brakes. A point scale is also used for the protection rating, depending on the level of protection of the vehicle against solids and liquids. In the case of the price, the lowest amount was selected from among the prices in the three stores from which information on vehicle popularity was obtained. Temporary trade promotions were not taken into account, taking into account only base prices. The underlying criteria (e.g., price, battery charging time, etc.) are described in terms of natural values. Most of the criteria are stimulants, so they are profit criteria [47]. Destimulants, i.e., cost criteria are battery charging time, weight, and price. It should be clarified that the literature often uses the criterion of maximum speed, which, however, was abandoned in this study. The resignation from this criterion is a result of the legal provisions in force in Poland, limiting the maximum permissible speed of e-scooters to 20 km/h [48]. All vehicles under consideration reach this speed and are equipped with a lock that prevents them from

reaching a higher speed. Therefore, the use of the maximum speed criterion in the current legal situation in Poland does not make sense. In this way, a list of 18 evaluation criteria constituting the set of C criteria was obtained and is shown in Table 2.

Table 3 presents the basic information about the e-scooters included in the study and their assessments. Table 3 can also be interpreted as a performance table $E = C(A)$ that is the basis for aggregating the criteria scores.

Table 3. Parameters and evaluations of e-scooters.

Criterion	A1—APRILIA eSR2	A2—BLAUPUNKT ESC608	A3—BLAUPUNKT ESC808	A4—BLAUPUNKT ESC90X	A5—DUCATI PRO-I EVO 2022	A6—DUCATI PRO-III 2022	A7—FIAT F500-F85P	A8—JEEP 2xe Urban Camou	A9—Kaabo Mantis 8	A10—Kaabo Mantis 10 ECO800	A11—Kaabo Sky -walker 8H ECO 500	A12—Motus PRO 8.5 Lite	A13—Motus PRO 10 Sport 2021	A14—Red Bull Racing RTEEN10-10	A15—Red Bull Racing RTEEN85-75	A16—Segway KickScooter AIR T15E	A17—SKYMASTER Nexos	A18—XIAOMI Mi 1S	A19—XIAOMI Mi 3	A20—XIAOMI Mi Essential	A21—XIAOMI Mi Pro2 2022
Popularity ranks	-/2/-	-/-/2	-/8/-	-/-/9	-/3/-	-/6/-	-/-/4	-/4/-	8/-/-	6/-/-	9/-/-	4/-/5	2/7/10	5/5/-	10/-/-	7/-/-	-/-/7	-/-/8	3/9/1	-/1/3	1/10/6
Battery capacity [Ah]	8	6	5	10	7.8	13	7.5	9.6	18.2	18.2	13	10.4	18.2	10.4	7.5	4	6	7.65	7.65	5.1	12.4
Battery charging time [h]	5	5	2	6	4	9	4	5	8.5	8	7	8	9	8	5	4	5	5.5	5.5	3.5	8.5
Engine power [W]	350	250	350	350	350	350	350	500	1600 *	800	500	350	2000 **	350	350	300	350	250	300	250	300
Max gradient [%]	23	15	18	15	15	20	15	26	30	30	20	20	30	15	10	15	10	14	16	10	20
Number of gears	3	3	3	4	4	4	3	4	4	4	3	3	3	3	3	4	3	3	3	3	3
Weight [kg]	16.5	15	13.5	14.5	12	17.5	14	19	26.5	26	18	17	29	17.3	14	10.5	14.2	12.5	13.2	12	14.2
Load capacity [kg]	100	120	120	120	100	100	140	100	120	120	100	120	150	100	120	100	120	100	100	100	100
Range [km]	25	20	20	40	25	50	20	45	56	54	45	35	65	35	20	15	25	30	30	20	45
Tires diameter [inch]	10	8.5	8.5	10	8.5	10	8.5	10	8	10	8	8.5	10	10	8.5	7.5	10	8.5	8.5	8.5	8.5
Mobile app	1	0	0	1	1	1	0	1	0	0	0	0	0	0	0	1	0	1	1	1	1
Cruise control	0	1	1	1	0	0	0	1	0	0	0	1	0	0	0	1	0	0	0	0	0
Pedestrian mode	1	0	0	1	1	1	0	1	0	0	0	0	0	1	0	1	0	1	1	1	1
KERS	1	0	0	0	1	1	0	1	1	1	0	0	0	0	0	1	0	1	1	1	1
e-ABS	0	1	1	1	0	0	0	0	1	1	0	0	0	0	0	0	0	1	1	1	1
Front & rear suspension	1	0	0	0	0	0	0	1	1	1	1	1	1	1	0	0	0	0	0	0	0
Brakes [points]	3	2	1	2	2	3	1	3	3	3	2	1	3	1	1	0	1	2	2	2	2
Protection rating [points]	3	0	0	0	2	3	3	3	0	0	0	1	1	0	0	3	0	2	2	2	2
Price [PLN]	4080	1600	2480	2790	2700	5500	1600	5200	7500	6000	4000	2700	7000	2500	2000	3060	1700	2060	2290	1750	2700
Front (FB) and rear brake (RB)	FB–D RB–C	FB–E RB–C	RB–C,F	FB–E RB–C,F	FB–E RB–C	FB–C RB–C	RB–C	FB–C RB–C	FB–C RB–C	FB–C RB–C	FB–E RB–D	RB–D	FB–C RB–C	RB–C	RB–C	FB–E RB–F	RB–C,F	FB–E RB–C	FB–E RB–C	FB–E RB–C	FB–E RB–C
Protection rating	IPX4	-	-	-	IP54	IPX4	IPX4	IPX4	-	-	-	IP44	IP44	-	-	IPX4	-	IP54	IP54	IP54	IP54
Reference	[49]	[50]	[51]	[52]	[53]	[54]	[55]	[56]	[57]	[58]	[59]	[60]	[61]	[62]	[63]	[64]	[65]	[66]	[67]	[68]	[69]

Brakes: 0—FB–E, RB–F; 1—RB–C,F; RB–C; RB–D; 2—FB–E, RB–C; FB–E, RB–D; FB–E, RB–C,F; 3—FB–C, RB–C; FB–D, RB–C; Protection rating: 0—No; 1—IP44; 2—IP54; 3—IPX4; Front (FB) and rear brake (RB): D—Drum, C—Disk, F—Fender; * 2 × 800 W; ** 2 × 1000 W.

4.2. Models of Stakeholder Preferences

As noted in Section 3.1, the two stakeholders were, respectively:

1. dm_1—VSS customer, i.e., a potential e-scooter user,
2. dm_2—VSS owner, making e-scooters available to users.

Of course, the interests and views of these stakeholders are in conflict. The user who rents an e-scooter is primarily interested in safety and comfort when using the vehicle. Therefore, the criteria directly affecting the safety and comfort of driving are of great importance to users: the braking system (including brakes and e-ABS), suspension, or, to a lesser extent, the diameter of the tires. The braking system allows you to stay safe in sudden, unexpected situations while driving. In turn, the suspension system and the diameter of the tires affect the comfort of driving and negotiating unevenness as well as the ability to climb curbs. Equally important are criteria regarding the comfort of use, such as sufficient range, gradeability, number of gears, and cruise control. The range should be sufficient for the needs of a typical user. According to various studies published in the literature, shared e-scooters users cover about 2–4 km in one trip [70,71], and according to other studies, it may even be more than 8 km [72,73]. Taking into account that sometimes you still need to return (e.g., travel from home to work, and then home from work), it may even be over 16 km. It should also be taken into account that as the battery degrades or at lower temperatures, the range will decrease. The ability to climb steep slopes relieves users from having to push the e-scooter uphill when it has too little power to climb the hill. More gears and cruise control allow you to set the right speed and lock it, so that the user can focus on the road and any obstacles. Criteria such as vehicle weight and pedestrian mode are slightly less important. The weight of the vehicle is related to the ease of riding, e.g., in the pedestrian mode. Technical criteria such as battery capacity, engine power, load capacity (assuming that this will be a value greater than the weight of the potential user), the presence of KERS, or protection rating are much less important for the user. However, these criteria are to some (slightly) degree significant, as they are indirectly related to the gradeability, range and failure-free operation of the vehicle. Access to the e-scooter setup via the mobile app is of very little importance, as in the case of a rented e-scooter, only a few users will want to use this feature, and most often the feature will be blocked by the VSS owner. However, battery charging time and price are irrelevant to the VSS customer. The price is irrelevant as the cost of purchasing the vehicle is borne by the owner of the VSS, not the customer. Likewise, the owner of the VSS is responsible for recharging the battery and the customer will not charge it when the battery is depleted, but will simply take another vehicle.

On the other hand, for the VSS owner, the most important criteria are directly related to his actions regarding the handling of e-scooters. From this perspective, criteria such as battery capacity and charging time, KERS, as well as load capacity and protection rating are important. The greater the battery capacity, the less frequently the e-scooter needs to be delivered to the base station and charged. In turn, the longer the charging time, the longer the vehicle is out of use in VSS. For this reason, KERS is to some extent useful as it increases the time intervals between successive charges.

The load capacity should be large enough not to limit the possibility of using the vehicle to obese people, of whom there are, unfortunately, relatively many in Polish society. In turn, the protection rating is a very important criterion determining whether the vehicle must be additionally protected against unfavorable weather conditions. E-scooters are usually left outdoors and are exposed to, for example, rainfall. Therefore, an appropriate degree of protection against liquids ensures their stability of operation, regardless of rainfall. One of the most important criteria for a VSS owner is, of course, the price of the e-scooter. The criteria most important to users are also relatively important, as they are responsible for driving comfort and thus the loyalty and retention of VSS users. Engine power is much less important, which is reflected indirectly in other criteria, and a mobile app is a completely redundant function.

In addition to the weights of criteria, an important aspect of preference modeling is the selection of appropriate preference functions and associated thresholds. The use of a pre-criterion, pseudo-criterion or Gaussian criterion is recommended for quantitative criteria. However, for low grade or quality criteria, consider using a true criterion, semi-criterion, or level criterion [74]. In turn, the thresholds q_k, p_k and r_k should be between the reliable values of the minimum and maximum of the k-th criterion [74,75]. Taking into account the cited guidelines, the usual preference function was used for the binary criteria and the two-fold number of gears criteria. The level criterion was used for the four-valued tire diameter and load capacity criteria and for the criteria expressed on the 4-point scales (brakes and protection rating). For the remaining criteria, the V-shaped preference functions (pre-criterion and pseudo-criterion) were used. The stakeholder preference models are presented in Table 4.

Table 4. Stakeholder preference models.

No	Criterion	Unit	Preference Direction	Weight [%]		Preference Function	Thresholds	
				VSS Client (dm_1)	VSS Client (dm_2)		q	p
C_1	Battery capacity	Ampere hours [Ah]	Max	3	11	pre	-	6
C_2	Battery charging time	Hours [h]	Min	0	11	pre	-	4
C_3	Engine power	Watts [W]	Max	3	1	pre	-	200
C_4	Max gradient	Percent [%]	Max	11	3	pseudo	2	6
C_5	Number of gears	Units	Max	7	3	usual	-	-
C_6	Weight	Kilograms [kg]	Min	5	2	pre	-	5
C_7	Load capacity	Kilograms [kg]	Max	3	5	level	0	30
C_8	Range	Kilometers [km]	Max	11	3	pseudo	2	15
C_9	Tires diameter	Inches [inch]	Max	8	3	level	0	1.5
C_{10}	Mobile app	True / False	Max	1	0	usual	-	-
C_{11}	Cruise control	True / False	Max	7	3	usual	-	-
C_{12}	Pedestrian mode	True / False	Max	5	2	usual	-	-
C_{13}	KERS	True / False	Max	3	6	usual	-	-
C_{14}	e-ABS	True / False	Max	8	3	usual	-	-
C_{15}	Suspension	True / False	Max	11	3	usual	-	-
C_{16}	Brakes	Points	Max	11	3	level	0	2
C_{17}	Protection rating	Points	Max	3	18	level	0	2
C_{18}	Price	Polish new zloty [PLN]	Min	0	20	pseudo	40	1000

4.3. Results of E-Scooters Assessment Using the PROSA GDSS Method

Based on the models of stakeholder preferences and the table of alternative performance, individual stakeholder rankings and group rankings were generated. The value $s_1 = s_2 = 1$ was adopted as the compensation factor for the results of the individual assessment in the group procedure. In turn, the weights of the stakeholders were set equal ($\omega_1 = \omega_2 = 0.5$). Table 5 presents the values of $\phi_{net}(a_i)$ and ranks obtained in individual rankings, as well as the ranks and values of $PSV_{net}(a_i)$ obtained in the GDSS procedure.

The analysis of individual rankings in Table 5 shows significant differences in the assessment of e-scooters based on the preferences of individual stakeholders. This is clearly visible on the example of the alternatives A7, A9, A13, A20, which depending on the stakeholder, occupy leading or final positions in the rankings. There is also a significant discrepancy in the case of alternatives A5, A10, A11, A14, A16, and A18, for which the difference between the ratings of the VSS owner and the VSS customer is at least eight positions. These differences are of course due to different stakeholder preferences. One can also observe alternatives that rank similarly or the same in both individual rankings. These are the alternatives A1, A3, A8, and A21. It is easy to notice that the alternatives A1, A8 and A21 occupy the leading positions in the group ranking. Moreover, the A3 and A21 alternatives in the GDSS procedure were ranked higher than it would result from their

position in the individual rankings. This effect is directly related to the PROSA method, which rewards well-balanced alternatives and penalizes unbalanced ones. An example of an alternative which position has been significantly lowered in the group ranking due to a very large discrepancy in individual ranks is A7. The confirmation of most of the indicated observations can be found on the PROMETHEE GAIA plane generated for individual rankings. Due to the fact that both individual rankings are based on the same performance table, the GAIA plant with identically distributed criteria vectors and alternative points is obtained for each of the individual rankings. These solutions differ only in the vector $\vec{\pi} = [u^{\pi}, v^{\pi}]$ which determines a compromise solution between the criteria. For this reason, both individual solutions are presented on the common PROMETHEE GAIA plant, shown in Figure 3.

Table 5. Assessments of alternatives aggregated in individual and PROSA GDSS group rankings.

Alternative	VSS Client (dm_1) (PROMETHEE II)		VSS Owner (dm_2) (PROMETHEE II)		Group (PROSA GDSS)	
	$\phi_{net}(a_i)$	**Rank**	$\phi_{net}(a_i)$	**Rank**	$PSV_{net}(a_i)$	**Rank**
A1	0.1123	7	0.0609	7	0.0320	2
A2	−0.1534	16	0.0047	11	−0.0805	15
A3	−0.1353	15	−0.0516	14	−0.0710	13
A4	0.1596	6	−0.0076	12	−0.0040	5
A5	−0.0753	14	0.0661	6	−0.0395	10
A6	0.1712	5	0.0056	10	0.0029	4
A7	−0.2750	19	0.2003	1	−0.1444	19
A8	0.3952	1	0.1453	2	0.0763	1
A9	0.3110	3	−0.1255	19	−0.0659	12
A10	0.3861	2	−0.0437	13	−0.0229	6
A11	−0.0361	10	−0.2110	21	−0.1108	18
A12	0.0019	9	−0.0532	15	−0.0279	8
A13	0.2503	4	−0.1181	18	−0.0620	11
A14	−0.0662	12	−0.1380	20	−0.0724	14
A15	−0.3765	21	−0.0996	17	−0.1977	21
A16	−0.1590	17	0.0466	9	−0.0835	16
A17	−0.3217	20	−0.0634	16	−0.1689	20
A18	−0.0674	13	0.1097	4	−0.0354	9
A19	−0.0451	11	0.0828	5	−0.0237	7
A20	−0.1642	18	0.1379	3	−0.0862	17
A21	0.0876	8	0.0518	8	0.0272	3

When analyzing the GAIA plane, it should be noted that not all information was transferred from the $\mathbb{R}^{18}$ to $\mathbb{R}^2$ space. The value of $\delta^c = 0.655$, so only 65% of the information has been preserved in the two-dimensional space. Nevertheless, some valuable information can be obtained from the figure. On the GAIA plane, the support of criteria for alternatives is clearly visible. For example, criterion C_1 strongly supports the alternatives A9, A10, A13 (these vehicles have a very high battery capacity), and criterion C_{18} supports the alternatives A2, A7, A15, A17, and A20 (these e-scooters have the lowest prices). In addition, it is possible to indicate the solutions most supported by individual stakeholders. The decision maker dm_1 strongly supports the alternatives A6, A8, A9, A10, and A13 (the points representing these alternatives are most advanced in the direction indicated by the vector $\vec{\pi}(dm_1)$). In turn, the decision-maker dm_2 strongly supports, among others, alternatives A5, A18, A19, A20. On the GAIA plane, the dashed line marks the extension of the vectors $\vec{\pi}(dm_1)$ and $\vec{\pi}(dm_2)$ thus delineating the space of solutions strongly supported by both stakeholders. These solutions include A1, A6, A8 and A21, the four top group ranking alternatives. This analysis shows that the GAIA plane is a valuable carrier of descriptive information about the solution of the decision problem, even if only part of the information was transferred to the plane.

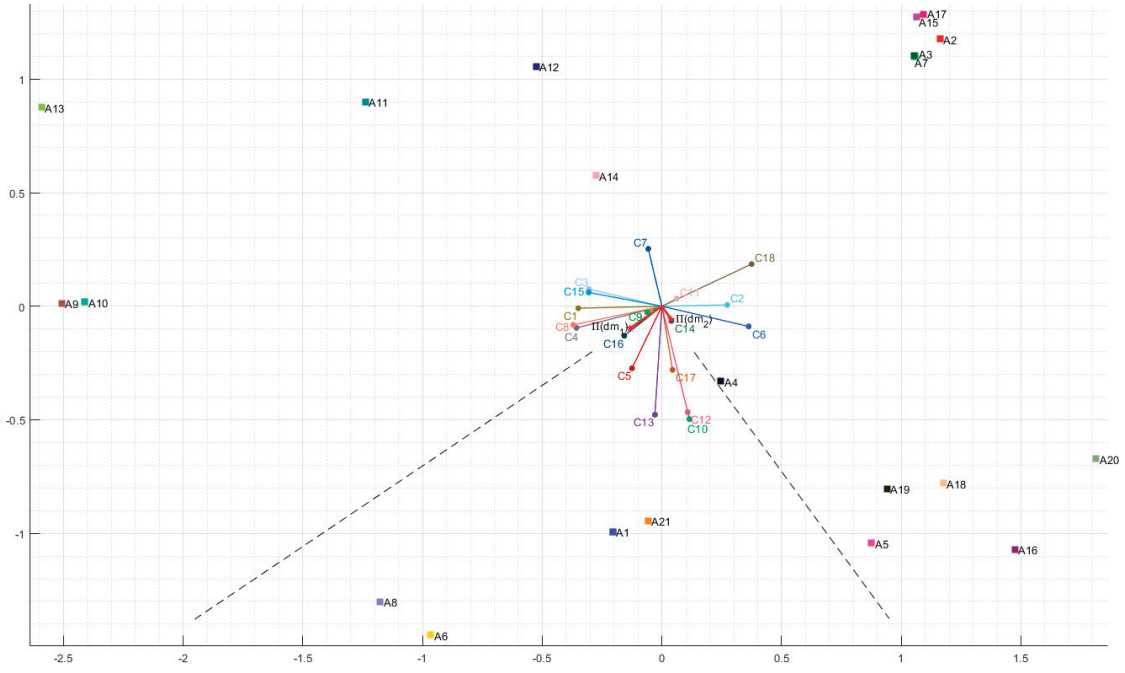

Figure 3. PROMETHEE GAIA plane obtained for individual stakeholder rankings.

5. Discussion

5.1. Comparison of the Results of the PROSA GDSS and PROMETHEE GDSS Methods

As noted earlier, the PROSA method favors well-balanced (or sustainable) alternatives and penalizes unbalanced ones. In other words, it limits the compensation of factors (criteria, decision makers) in the decision problem. In particular, the PROSA GDSS method limits the compensation of decision makers' assessments at the stage of aggregating individual assessments into group assessments. In this way, PROSA GDSS favors balanced alternatives, assessed at a similar level by all stakeholders.

To analyze the impact of the balance-based approach on solving the decision problem, the results of the PROSA GDSS and PROMETHEE GDSS methods were compared. In accordance with the research procedure presented in Section 3.1, each of these methods was used separately at the stage of aggregating individual assessments into group assessment (PROMETHEE GDSS uses the PROMETHEE II procedure with V-shaped criterion and threshold $p_k = 2$ at this stage). Table 6 presents the results of the PROMETHEE GDSS method and the results for the PROSA GDSS method, previously quoted in Table 5. On the other hand, Figure 4 contains the GAIA GDSS planes obtained using the PROMETHEE and PROSA methods (for both planes $\delta^{dm} = 1$ was obtained).

A comparison of the PROMETHEE GDSS and PROSA GDSS rankings indicates that taking into account the balance between decision makers and limiting compensation significantly changes the rankings of alternatives. Alternative A1, which was ranked second in the PROSA GDSS ranking, without balance (PROMETHEE GDSS ranking), was ranked fifth. In turn, alternative A21 fell from third to seventh, and A4 lost one position (from fifth to sixth). Of the top alternatives, the A8 and A6 retained their ranks. As for the other alternatives, which were penalized for the lack of balance in the PROMETHEE GDSS ranking included unbalanced alternatives, which were penalized for lack of balance in the PROSA GDSS ranking.

Table 6. PROMETHEE GDSS and PROSA GDSS groups rankings.

Alternative		A1	A2	A3	A4	A5	A6	A7	A8	A9	A10	A11	A12	A13	A14	A15	A16	A17	A18	A19	A20	A21
PROMETHEE GDSS	$\phi_{net}(a_i)$	0.0454	−0.039	−0.0491	0.0399	−0.0024	0.0464	−0.0196	0.1419	0.0487	0.0899	−0.0648	−0.0134	0.0347	−0.0536	−0.125	−0.0295	−0.1011	0.0111	0.0099	−0.0069	0.0366
	Rank	5	16	17	6	11	4	14	1	3	2	19	13	8	18	21	15	20	9	10	12	7
PROSA GDSS	$PSV_{net}(a_i)$	0.032	−0.0805	−0.071	−0.004	−0.0395	0.0029	−0.1444	0.0763	−0.0659	−0.0229	−0.1108	−0.0279	−0.062	−0.0724	−0.1977	−0.0835	−0.1689	−0.0354	−0.0237	−0.0862	0.0272
	Rank	2	15	13	5	10	4	19	1	12	6	18	8	11	14	21	16	20	9	7	17	3

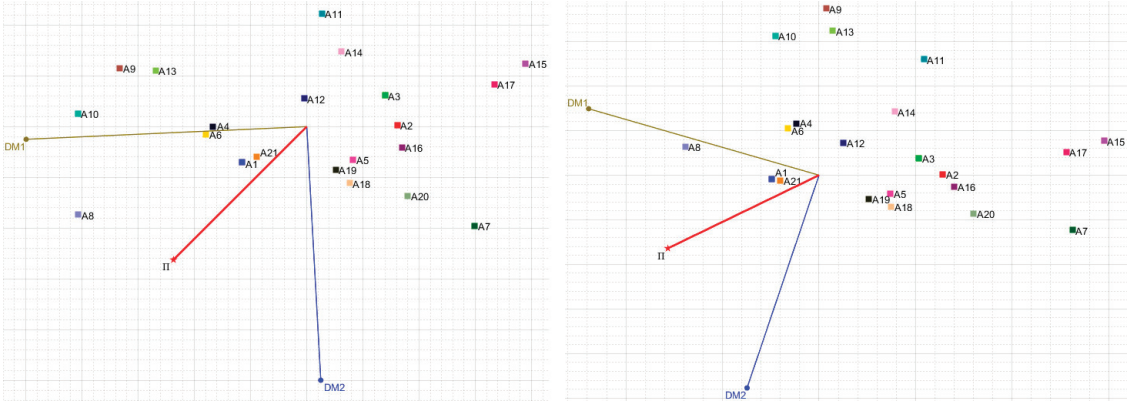

(**a**) (**b**)

Figure 4. GAIA planes obtained for group rankings by aggregating individual rankings using the following methods: (**a**) PROMETHEE GDSS, (**b**) PROSA GDSS.

The differences in the rankings are clearly visible on the GAIA planes based on the PROMETHEE GDSS and PROSA GDSS methods (Figure 4). The vector $\vec{\pi}$ determining the order of alternatives indicates that in the case of the PROMETHEE GDSS GAIA plane, the leading alternatives are: A8, A10, A9, A1, A6, etc., respectively. On the PROSA GDSS plane, the best alternatives are: A8, A1, A21, A6, A4, etc., respectively. On both GAIA planes, the $\vec{\pi}$ vectors also correctly indicate the order of the other alternatives. Although the differences in the position of points representing alternatives on both planes of GAIA are small, the position of these points precisely describes the order of alternatives in the rankings and the support of individual alternatives by decision makers. Both GAIA planes indicate that the preferences of decision-makers are independent of each other (they are not supportive, but also not strongly conflicted), as shown by the orthogonal arrangement of the vectors dm_1 and dm_2. These vectors, through their orthogonal arrangement, define the space of solutions constituting a compromise between the two decision-makers. In the case of PROMETHEE GDSS GAIA, this area includes the balanced alternatives A1, A8, A21, and the unbalanced alternative A6, while on the PROSA GDSS GAIA plane, this area covers

only the balanced alternatives A1, A8, A21. This observation confirms that PROSA is able to capture the balance of decision alternatives. It should be noted that the area defined by the vectors dm_1 and dm_2 is very similar to the area marked in Figure by the extension of the vectors $\vec{\pi}(dm_1)$ and $\vec{\pi}(dm_2)$, which confirms that capturing two individual rankings and their compromise solutions $\vec{\pi}$ on the GAIA plane can provide relatively precise information about the group solution.

5.2. PROSA GDSS Sensitivity Analysis

The sensitivity analysis of the PROSA GDSS ranking was considered from two perspectives. We analyzed how the solution of the decision problem changes with linear changes (1) of criteria weights and (2) of the compensation coefficient s_k. In the first study, the weight of the selected criterion was linearly changed, proportionally increasing or decreasing the initial weights of the remaining criteria. Criterion weights given in Table 4 were used as initial values. Stability ranges of criterion weights were determined on the basis of the sensitivity analysis. Due to the large number of alternatives and the frequent reordering of further positions in the ranking, the stability ranges were derived from the top five alternatives. This makes it possible to determine the stability of the best alternatives without introducing information noise in a situation where changes occur in the last places in the ranking. The stability intervals for each criterion are presented in Table 7. The analysis presented in Table 7 shows that the stability intervals are much wider for the weights defined by the decision maker dm_1 than for the weights of the decision maker's criteria dm_2. This means that the leading alternatives are more sensitive to changes in the weights of the decision maker's criteria dm_2, while in the case of weight changes by the decision maker dm_1, the solution is more stable. Table 7 is supplemented by Figure 5 that allows observing the ranking position with linear changes in the weights of individual criteria.

Table 7. Stability ranges and sensitivity for the top five positions in the PROSA GDSS ranking.

Criteria	VSS Client (dm_1)—Criteria Weights					VSS Owner (dm_2)—Criteria Weights				
	Stability Interval		Sensitivity		Nominal Weight	Stability Interval		Sensitivity		Nominal Weight
	Min	Max	Min-Nominal	Max-Nominal		Min	Max	Min-Nominal	Max-Nominal	
C_1	0	21	-	18	3	8	12	3	1	11
C_2	0	11	-	11	0	11	12	0	1	11
C_3	0	21	-	18	3	0	4	-	3	1
C_4	0	50	-	39	11	1	5	2	2	3
C_5	0	15	-	8	7	0	7	-	4	3
C_6	0	12	-	7	5	0	4	-	2	2
C_7	0	23	-	20	3	0	7	-	2	5
C_8	0	21	-	10	11	0	7	-	4	3
C_9	0	43	-	35	8	2	10	1	7	3
C_{10}	0	7	-	6	1	0	15	-	15	0
C_{11}	0	22	-	15	7	0	4	-	1	3
C_{12}	0	11	-	6	5	0	18	-	16	2
C_{13}	0	9	-	6	3	5	9	1	3	6
C_{14}	0	13	-	5	8	0	3	-	0	3
C_{15}	1	25	10	14	11	3	6	0	3	3
C_{16}	0	58	-	47	11	1	11	2	8	3
C_{17}	0	21	-	18	3	17	25	1	7	18
C_{18}	0	9	-	9	0	17	21	3	1	20

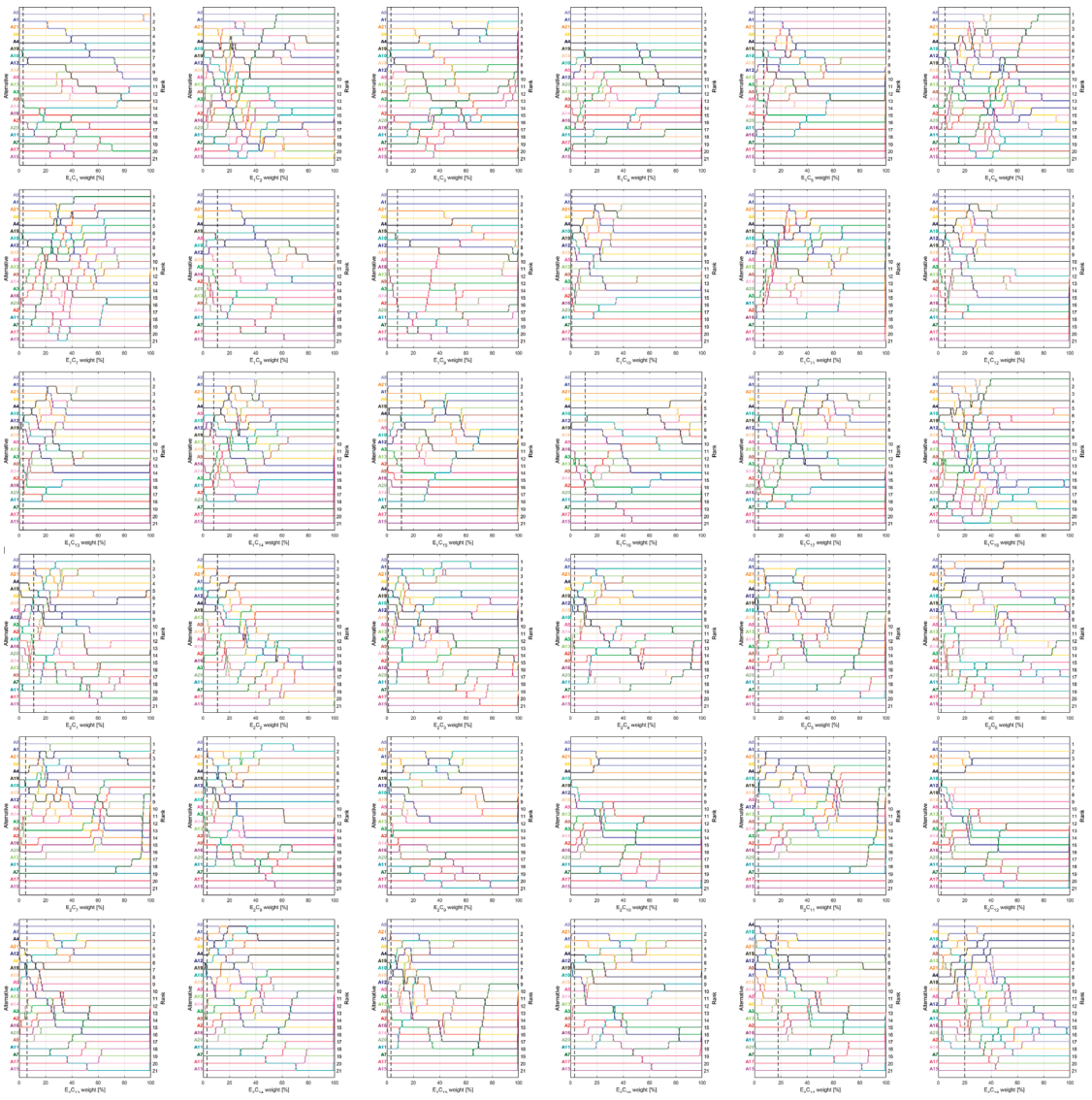

Figure 5. Changes in the PROSA GDSS ranking depending on changes in the weights of the criteria.

The second sensitivity study consisted of a linear change of the value of the compensation coefficient s_k, separately for decision-makers dm_1 and dm_2. For one of the decision makers, the value of s_k was changed in the range [0, 1], while for the other stakeholder $s_k = 1$ was left. It should be explained that in the case of two-decision makers with equal weights, the change of the coefficient s_k for $k = 1$ and $k = 2$ gives the same solution. In other words, regardless of the decision-makers for which the s_k coefficient is changed, the solution will change exactly the same. This is due to the specificity of the PROSA method, because in the case of two decision-makers with the same weights, the solution $\phi_{net}(a_i)$ is simply an average. In turn, the distance of both solutions $\phi_k(a_i)$ from the solution $\phi_{net}(a_i)$ is the same ($AD_1(a_i) = AD_2(a_i)$), which results from Formulas (14) and (15). This is confirmed by Figure 6 showing changes in the PROSA GDSS ranking depending on the

linear change in the value of the s_k coefficient separately for each of the stakeholders. In this figure, it can be seen that the top five positions in the ranking are stable. The order of the five best alternatives only changes when the value of s_k for one of the stakeholders drops < 0.5, and for the best three alternatives, when $s_k = 0$ for one of the decision makers, bearing in mind that for the other stakeholder $s_k = 1$.

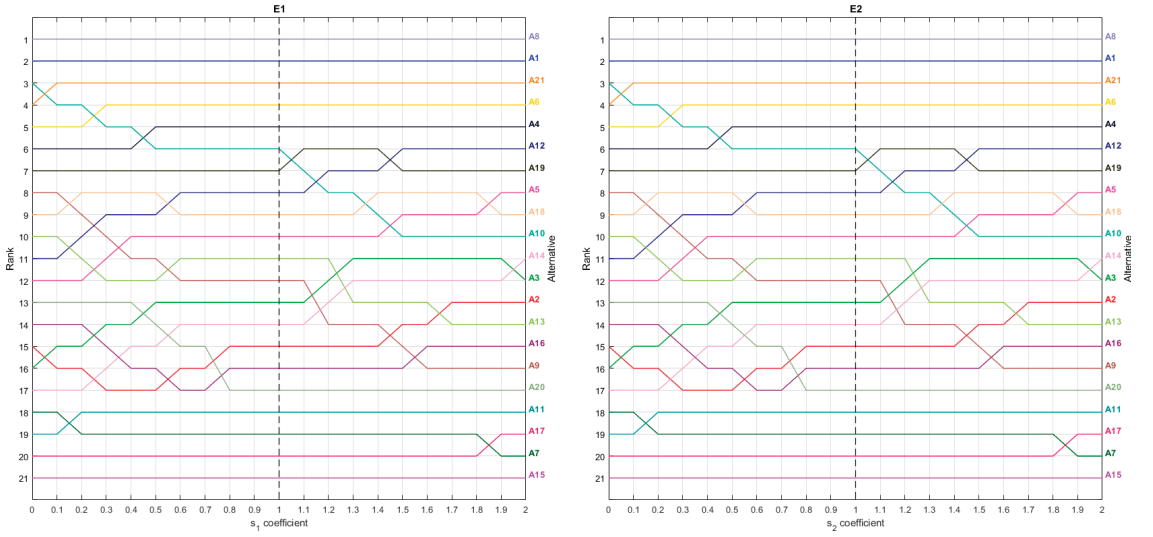

Figure 6. Changes in the PROSA GDSS ranking depending on changes in the weighting of the criteria.

6. Managerial and Environmental Implications

The results of the research show that the best compromise between the needs of the VSS owner and the needs of potential users of such a service is the A8—JEEP 2xe Urban Camou. It occupies the leading positions in the individual rankings of both stakeholders, which means that it almost perfectly meets the needs of each of them. Choosing the next good e-scooter is not an obvious decision. If we take into account the need to balance the needs of stakeholders and rely on the methodology taking into account the balance (PROSA GDSS), then the second and third places in the ranking will be occupied by: A1—APRILIA eSR2 and A21—XIAOMI Mi Pro2 2022. However, if we apply the compensation methodology (PROMETHEE GDSS) and we will look for a solution that will be a resultant of the views of both decision makers, without taking into account the balance between them, then the second and third places in the ranking will be occupied by A10—Kaabo Mantis 10 ECO800 and A9—Kaabo Mantis 8. Other good vehicles identified by both methodologies are A6—DUCATI PRO-III 2022, A4—BLAUPUNKT ESC90X and the A1 and A21 vehicles already mentioned in the context of good balance, as well as the A10 previously indicated as a very good solution, although less balanced. All these vehicles largely meet the needs of both the entrepreneur and his customers.

Looking at the problem of choosing e-scooters for VSS in Poland from a broader perspective, one should notice the great potential of business activities related to the provision of this type of service. The introduction of comfortable and eco-friendly e-micromobility vehicles is an opportunity to reduce the unfavorable patterns of daily commuting observed in Poland and the extremely high ratio of private transport [76]. Based on the Recovery and Resilience Plan for Poland (the so-called national recovery plan), it should be noted that from the perspective of the next few years, legal regulations are planned in Poland, which will certainly contribute to an increase in the popularity of e-micromobility and e-mobility. Namely, in the Annex to the Recovery and Resilience Plan for Poland [77] one see that in 2025 in Poland, low-emission transport zones are to be introduced in cities with over

100,000 inhabitants and which exceed pollution standards. In addition, the same annex contains information about new taxes that will be imposed on internal combustion vehicles from 2024 and 2026. Together with the dynamically growing gasoline prices in Poland, these activities will certainly force some vehicle users to give up owning a car and buy their own e-micromobility vehicle or use the VSS.

The development of e-mobility has been supported in Poland for several years, but recently there are also programs promoting the development of e-micromobility. For example, the program of government subsidies for the purchase of electric vehicles ('My electrician') introduced in 2021 in Poland includes co-financing for the purchase of e-cars, but also electric mopeds, motorcycles, and all-terrain vehicles (quads). For vehicles in the L1-L7 categories, a subsidy in the amount of PLN 4000 is planned [78]. In addition, recently Gdynia was the first city in Poland to introduce co-financing for the purchase of e-bikes by residents. The maximum amount of funding is PLN 2500 (not more than 50% of the purchase price) [79].

The basic justification for the indicated trends is the need to reduce environmental pollution, because electric vehicles do not emit exhaust fumes. However, the environmental impact of electric vehicles depends on the country's energy mix. Meanwhile, over 70% of the Polish energy mix is based on carbon [6], which makes the argument about environmental protection lose its sense. According to plans for the Polish energy policy, in the coming years, the Polish energy mix should change to renewable energy sources (mainly offshore wind farms and photovoltaics) and nuclear energy [80], but for now these are mainly plans. Therefore, even if the planned legal regulations and the incentive system were already in force and contributing to an increase in the popularity of electric vehicles in a short time, they can only bring positive environmental effects over a longer time span.

7. Conclusions

The aim of the article was to analyze selected e-scooters available on the Polish market and to identify vehicles of this type that are most useful from two slightly opposing perspectives—the owner of the VSS and a potential customer of such services. The solution to the given decision problem is of practical value in the presented research. On the other hand, the scientific contribution of the article included the use of the PROSA GDSS method to search for a compromise between the stakeholders of the decision-making process. The results of the PROSA GDSS method were compared with the results of the application of the PROMETHEE GDSS method, which does not take into account the balance between stakeholders, and allows for a strong compensation of decision makers' assessments. Graphical representations of PROSA GDSS and PROMETHEE GDSS solutions on the GAIA plane were also compared. Additionally, an analysis of the sensitivity of the PROSA GDSS ranking, changes in criteria weights, and changes in compensation coefficients was performed. The basic PROSA GDSS solution identified the e-scooter A8—JEEP 2xe Urban Camou as the optimal choice. Both the sensitivity analysis and the solution obtained using the PROMETHEE GDSS method confirmed that it is the optimal alternative, the least sensitive to changes in criteria weights and changes in compensation factors. E-scooters are interesting vehicles, which took a few more places in the PROSA GDSS ranking, because they are vehicles well-balanced between the needs of users and entrepreneurs running VSS.

During the research work, no significant limitations were encountered that could significantly affect the obtained results. There was a problem with obtaining reliable data on individual vehicles, as not all e-scooters manufacturers and suppliers provide complete technical information about vehicles on their websites. Therefore, part of the information was obtained on the basis of an analysis of vehicle operating instructions or reviews of e-scooters posted on the Internet. As for methodological limitations, it should be noted that not all the obtained data were precise and reliable. Therefore, in several cases, an average was entered in the performance table based on information from various sources. Therefore, an interesting direction for further methodological work would be to develop

the PROSA family of methods for fuzzy representations so that they could better capture the uncertainty of the data.

Author Contributions: Conceptualization, P.Z.; data curation, P.Z. and I.G.; investigation, P.Z.; methodology, P.Z.; resources, I.G.; supervision, P.Z.; visualization, P.Z.; writing—original draft, P.Z. and I.G.; writing—review & editing, P.Z. All authors have read and agreed to the published version of the manuscript.

Funding: This research was funded by the National Science Centre, Poland, grant number 2019/35/D/HS4/02466.

Institutional Review Board Statement: Not applicable.

Informed Consent Statement: Not applicable.

Data Availability Statement: Data are contained within the article.

Conflicts of Interest: The authors declare no conflict of interest.

References

1. OPEC. *World Oil Outlook*; OPEC: Vienna, Austria, 2012; ISBN 978-3-9502722-4-6.
2. Intergovernmental Panel on Climate Change. *Climate Change 2007: Mitigation of Climate Change*; Cambridge University Press: Cambridge, UK, 2007; ISBN 978-0-511-54601-3.
3. Ortega-Cabezas, P.-M.; Colmenar-Santos, A.; Borge-Diez, D.; Blanes-Peiró, J.-J. Can Eco-Routing, Eco-Driving and Eco-Charging Contribute to the European Green Deal? Case Study: The City of Alcalá de Henares (Madrid, Spain). *Energy* **2021**, *228*, 120532. [CrossRef]
4. EMEP/EEA Air Pollutant Emission Inventory Guidebook 2019—European Environment Agency. Available online: https://www.eea.europa.eu//publications/emep-eea-guidebook-2019 (accessed on 26 March 2022).
5. Nowelizacja Ustawy o Elektromobilności i Paliwach Alternatywnych z Podpisem Prezydenta RP—Ministerstwo Klimatu i Środowiska—Portal Gov.pl. Available online: https://www.gov.pl/web/klimat/nowelizacja-ustawy-o-elektromobilnosci-i-paliwach-alternatywnych-z-podpisem-prezydenta-rp (accessed on 17 March 2022).
6. Lis, A.; Szymanowski, R. Greening Polish Transportation? Untangling the Nexus between Electric Mobility and a Carbon-Based Regime. *Energy Res. Soc. Sci.* **2022**, *83*, 102336. [CrossRef]
7. Macaudière, P.; Rocher, L.; Naschke, W. Diesel Particulate Filters. *MTZ Worldw.* **2004**, *65*, 11–13. [CrossRef]
8. Meijering, J.V.; Kern, K.; Tobi, H. Identifying the Methodological Characteristics of European Green City Rankings. *Ecol. Indic.* **2014**, *43*, 132–142. [CrossRef]
9. Salmeron-Manzano, E.; Manzano-Agugliaro, F. The Electric Bicycle: Worldwide Research Trends. *Energies* **2018**, *11*, 1894. [CrossRef]
10. Lin, H.-H.; Shen, C.-C.; Hsu, I.-C.; Wu, P.-Y. Can Electric Bicycles Enhance Leisure and Tourism Activities and City Happiness? *Energies* **2021**, *14*, 8144. [CrossRef]
11. Sandoval, R.; Van Geffen, C.; Wilbur, M.; Hall, B.; Dubey, A.; Barbour, W.; Work, D.B. Data Driven Methods for Effective Micromobility Parking. *Transp. Res. Interdiscip. Perspect.* **2021**, *10*, 100368. [CrossRef]
12. Shamshiripour, A.; Rahimi, E.; Shabanpour, R.; Mohammadian, A. (Kouros) How Is COVID-19 Reshaping Activity-Travel Behavior? Evidence from a Comprehensive Survey in Chicago. *Transp. Res. Interdiscip. Perspect.* **2020**, *7*, 100216. [CrossRef]
13. Felipe-Falgas, P.; Madrid-Lopez, C.; Marquet, O. Assessing Environmental Performance of Micromobility Using LCA and Self-Reported Modal Change: The Case of Shared E-Bikes, E-Scooters, and E-Mopeds in Barcelona. *Sustainability* **2022**, *14*, 4139. [CrossRef]
14. Storme, T.; Casier, C.; Azadi, H.; Witlox, F. Impact Assessments of New Mobility Services: A Critical Review. *Sustainability* **2021**, *13*, 3074. [CrossRef]
15. Bajec, P.; Tuljak-Suban, D.; Zalokar, E. A Distance-Based AHP-DEA Super-Efficiency Approach for Selecting an Electric Bike Sharing System Provider: One Step Closer to Sustainability and a Win–Win Effect for All Target Groups. *Sustainability* **2021**, *13*, 549. [CrossRef]
16. Hamerska, M.; Ziółko, M.; Stawiarski, P. Assessment of the Quality of Shared Micromobility Services on the Example of the Electric Scooter Market in Poland. *IJQR* **2022**, *16*, 19–34. [CrossRef]
17. Ziemba, P. Multi-Criteria Group Assessment of E-Commerce Websites Based on the New PROSA GDSS Method–the Case of Poland. *IEEE Access* **2021**, *9*, 126595–126609. [CrossRef]
18. Marques, D.L.; Coelho, M.C. A Literature Review of Emerging Research Needs for Micromobility—Integration through a Life Cycle Thinking Approach. *Future Transp.* **2022**, *2*, 135–164. [CrossRef]
19. Boglietti, S.; Barabino, B.; Maternini, G. Survey on E-Powered Micro Personal Mobility Vehicles: Exploring Current Issues towards Future Developments. *Sustainability* **2021**, *13*, 3692. [CrossRef]

20. Tian, Z.; Wang, J.; Wang, J.; Zhang, H. A Multi-Phase QFD-Based Hybrid Fuzzy MCDM Approach for Performance Evaluation: A Case of Smart Bike-Sharing Programs in Changsha. *J. Clean. Prod.* **2018**, *171*, 1068–1083. [CrossRef]
21. Karolemeas, C.; Vassi, A.; Tsigdinos, S.; Bakogiannis, E. Measure the Ability of Cities to Be Biked via Weighted Parameters, Using GIS Tools. The Case Study of Zografou in Greece. *Transp. Res. Procedia* **2022**, *62*, 59–66. [CrossRef]
22. Kurniadhini, F.; Roychansyah, M.S. The Suitability Level of Bike-Sharing Station in Yogyakarta Using SMCA Technique. *IOP Conf. Ser. Earth Environ. Sci.* **2020**, *451*, 012033. [CrossRef]
23. Kabak, M.; Erbaş, M.; Çetinkaya, C.; Özceylan, E. A GIS-Based MCDM Approach for the Evaluation of Bike-Share Stations. *J. Clean. Prod.* **2018**, *201*, 49–60. [CrossRef]
24. Eren, E.; Katanalp, B.Y. Fuzzy-Based GIS Approach with New MCDM Method for Bike-Sharing Station Site Selection According to Land-Use Types. *Sustain. Cities Soc.* **2022**, *76*, 103434. [CrossRef]
25. Guler, D.; Yomralioglu, T. Bicycle Station and Lane Location Selection Using Open Source GIS Technology. In *Open Source Geospatial Science for Urban Studies: The Value of Open Geospatial Data*; Mobasheri, A., Ed.; Springer International Publishing: Cham, Switzerland, 2021; pp. 9–36. ISBN 978-3-030-58232-6.
26. Fazio, M.; Giuffrida, N.; Le Pira, M.; Inturri, G.; Ignaccolo, M. Planning Suitable Transport Networks for E-Scooters to Foster Micromobility Spreading. *Sustainability* **2021**, *13*, 11422. [CrossRef]
27. Psarrou Kalakoni, A.M.; Christoforou, Z.; Farhi, N. A Novel Methodology for Micromobility System Assessment Using Multi-Criteria Analysis. *Case Stud. Transp. Policy* **2022**, *10*, 976–992. [CrossRef]
28. Torkayesh, A.E.; Deveci, M. A MulTi-NoRmalization MUlti-Distance ASsessmenT (TRUST) Approach for Locating a Battery Swapping Station for Electric Scooters. *Sustain. Cities Soc.* **2021**, *74*, 103243. [CrossRef]
29. Tang, Y.; Yang, Y. Sustainable E-Bike Sharing Recycling Supplier Selection: An Interval-Valued Pythagorean Fuzzy MAGDM Method Based on Preference Information Technology. *J. Clean. Prod.* **2021**, *287*, 125530. [CrossRef]
30. Deveci, M.; Gokasar, I.; Pamucar, D.; Coffman, D.; Papadonikolaki, E. Safe E-Scooter Operation Alternative Prioritization Using a q-Rung Orthopair Fuzzy Einstein Based WASPAS Approach. *J. Clean. Prod.* **2022**, *347*, 131239. [CrossRef]
31. Wankmüller, C.; Kunovjanek, M.; Sposato, R.G.; Reiner, G. Selecting E-Mobility Transport Solutions for Mountain Rescue Operations. *Energies* **2020**, *13*, 6613. [CrossRef]
32. Sałabun, W.; Palczewski, K.; Wątróbski, J. Multicriteria Approach to Sustainable Transport Evaluation under Incomplete Knowledge: Electric Bikes Case Study. *Sustainability* **2019**, *11*, 3314. [CrossRef]
33. Ziemba, P.; Gago, I. Uncertainty of Preferences in the Assessment of Supply Chain Management Systems Using the PROMETHEE Method. *Symmetry* **2022**, *14*, 1043. [CrossRef]
34. Brans, J.-P.; De Smet, Y. PROMETHEE Methods. In *Multiple Criteria Decision Analysis: State of the Art Surveys*; Greco, S., Ehrgott, M., Figueira, J.R., Eds.; International Series in Operations Research & Management Science; Springer: New York, NY, USA, 2016; pp. 187–219. ISBN 978-1-4939-3094-4.
35. Ziemba, P. Multi-Criteria Stochastic Selection of Electric Vehicles for the Sustainable Development of Local Government and State Administration Units in Poland. *Energies* **2020**, *13*, 6299. [CrossRef]
36. Ishizaka, A.; Nemery, P. General Introduction. In *Multi-Criteria Decision Analysis: Methods and Software*; Wiley: Chichester, UK, 2013; pp. 1–9. ISBN 978-1-118-64489-8.
37. Mareschal, B.; Brans, J.-P. Geometrical Representations for MCDA. *Eur. J. Oper. Res.* **1988**, *34*, 69–77. [CrossRef]
38. Ziemba, P. Towards Strong Sustainability Management—A Generalized PROSA Method. *Sustainability* **2019**, *11*, 1555. [CrossRef]
39. Statista Poland: Most Popular Electronics Stores. 2021. Available online: https://www.statista.com/statistics/1242536/poland-most-popular-electronics-stores/ (accessed on 26 May 2022).
40. Apostolou, G.; Reinders, A.; Geurs, K. An Overview of Existing Experiences with Solar-Powered E-Bikes. *Energies* **2018**, *11*, 2129. [CrossRef]
41. Timmermans, J.-M.; Matheys, J.; Lataire, P.; Van Mierlo, J.; Cappelle, J. A Comparative Study of 12 Electrically Assisted Bicycles. *World Electr. Veh. J.* **2009**, *3*, 93–103. [CrossRef]
42. Ziemba, P. Multi-Criteria Approach to Stochastic and Fuzzy Uncertainty in the Selection of Electric Vehicles with High Social Acceptance. *Expert Syst. Appl.* **2021**, *173*, 114686. [CrossRef]
43. Ziemba, P. Selection of Electric Vehicles for the Needs of Sustainable Transport under Conditions of Uncertainty—A Comparative Study on Fuzzy MCDA Methods. *Energies* **2021**, *14*, 7786. [CrossRef]
44. Biswas, T.K.; Das, M.C. Selection of Commercially Available Electric Vehicle Using Fuzzy AHP-MABAC. *J. Inst. Eng. India Ser. C* **2019**, *100*, 531–537. [CrossRef]
45. Ecer, F. A Consolidated MCDM Framework for Performance Assessment of Battery Electric Vehicles Based on Ranking Strategies. *Renew. Sustain. Energy Rev.* **2021**, *143*, 110916. [CrossRef]
46. Sonar, H.C.; Kulkarni, S.D. An Integrated AHP-MABAC Approach for Electric Vehicle Selection. *Res. Transp. Bus. Manag.* **2021**, *41*, 100665. [CrossRef]
47. Piwowarski, M.; Borawski, M.; Nermend, K. The Problem of Non-Typical Objects in the Multidimensional Comparative Analysis of the Level of Renewable Energy Development. *Energies* **2021**, *14*, 5803. [CrossRef]
48. Ustawa z Dnia 30 Marca 2021 r. o Zmianie Ustawy—Prawo o Ruchu Drogowym Oraz Niektórych Innych Ustaw. Available online: https://isap.sejm.gov.pl/isap.nsf/DocDetails.xsp?id=WDU20210000720 (accessed on 30 May 2022).
49. Aprilia ESR2. Available online: https://www.apriliasmartmovement.it/en/product/aprilia-esr2/ (accessed on 30 May 2022).

50. Blaupunkt ESC608. Available online: https://blaupunkt.com/cpl/produkt/esc608/ (accessed on 30 May 2022).
51. Blaupunkt ESC808. Available online: https://blaupunkt.com/cpl/produkt/esc808/ (accessed on 30 May 2022).
52. Blaupunkt ESC90X. Available online: https://blaupunkt.com/cpl/produkt/esc90x/ (accessed on 30 May 2022).
53. Ducati PRO-I EVO. Available online: https://www.ducatiurbanemobility.com/electric-mobility/pro-i-evo/ (accessed on 30 May 2022).
54. Ducati PRO-III. Available online: https://www.ducatiurbanemobility.com/electric-mobility/pro-iii/ (accessed on 30 May 2022).
55. FIAT F500-F85P. Available online: https://4cv.pl/wp-content/uploads/2021/03/F500-F85_manual_EN_PL.pdf (accessed on 30 May 2022).
56. Jeep 2xe Camou Electric Scooter Review. Available online: https://scooter.guide/jeep-2xe-camou-electric-scooter-review/ (accessed on 30 May 2022).
57. Kaabo Mantis 8 PLUS Electric Scooter. Available online: https://kaaboeurope.com/products/kaabo-mantis-8-plus-electric-scooter (accessed on 30 May 2022).
58. Kaabo Mantis 10 ECO 800 (Lite Plus) Electric Scooter. Available online: https://kaaboeurope.com/products/kaabo-mantis-10-lite-plus-electric-scooter (accessed on 30 May 2022).
59. Kaabo Skywalker 8H ECO500. Available online: https://kaabostore.eu/product/skywalker-8h (accessed on 30 May 2022).
60. Motus PRO 8.5 Lite 350W 35 km/h. Available online: https://motusxd.pl/hulajnogi-za-miasto/20-190-hulajnoga-elektryczna-motus-pro-85-lite-350w-35kmh-5901821995450.html (accessed on 30 May 2022).
61. Motus PRO 10 sport 2021 2 × 1000 W 66 km/h. Available online: https://motusxd.pl/hulajnogi-za-miasto/28-553-hulajnoga-elektryczna-motus-pro-10-sport-2021-2x1000w-66kmh-5901821995474.html (accessed on 30 May 2022).
62. Red Bull Racing RTEEN10-10. Available online: https://www.mediaexpert.pl/products/files/37/3735110/instrukcja-obslugi-RED-BULL-Racing-10-Pro.pdf (accessed on 30 May 2022).
63. Red Bull Racing RTEEN85-75. Available online: https://www.mediaexpert.pl/products/files/37/3735102/instrukcja-obslugi-red-bull-rteen85-75.pdf (accessed on 30 May 2022).
64. Segway T15D. Available online: https://pl-pl.segway.com/products/ninebot-kickscooter-air-t15e-powered-by-segway-1 (accessed on 30 May 2022).
65. Skymaster Nexos. Available online: https://skymaster24.pl/sklep/hulajnogi/212--hulajnoga-elektryczna-skymaster-nexos.html (accessed on 30 May 2022).
66. Mi Electric Scooter 1S. Available online: https://www.mi.com/global/mi-electric-scooter-1S/ (accessed on 30 May 2022).
67. Mi Electric Scooter 3. Available online: https://www.mi.com/global/product/mi-electric-scooter-3/ (accessed on 30 May 2022).
68. Mi Electric Scooter Essential. Available online: https://www.mi.com/global/mi-electric-scooter-essential/ (accessed on 30 May 2022).
69. Mi Electric Scooter Pro 2. Available online: https://www.mi.com/global/mi-electric-scooter-Pro2/ (accessed on 30 May 2022).
70. Wang, K.; Qian, X.; Fitch, D.T.; Lee, Y.; Malik, J.; Circella, G. What Travel Modes Do Shared E-Scooters Displace? A Review of Recent Research Findings. *Transp. Rev.* **2022**, *102*, 103134. [CrossRef]
71. Yang, H.; Bao, Y.; Huo, J.; Hu, S.; Yang, L.; Sun, L. Impact of Road Features on Shared E-Scooter Trip Volume: A Study Based on Multiple Membership Multilevel Model. *Travel Behav. Soc.* **2022**, *28*, 204–213. [CrossRef]
72. Cao, Z.; Zhang, X.; Chua, K.; Yu, H.; Zhao, J. E-Scooter Sharing to Serve Short-Distance Transit Trips: A Singapore Case. *Transp. Res. Part A Policy Pract.* **2021**, *147*, 177–196. [CrossRef]
73. Chicco, A.; Diana, M. Understanding Micro-Mobility Usage Patterns: A Preliminary Comparison between Dockless Bike Sharing and e-Scooters in the City of Turin (Italy). *Transp. Res. Procedia* **2022**, *62*, 459–466. [CrossRef]
74. Deshmukh, S.C. Preference Ranking Organization Method Of Enrichment Evaluation (Promethee). *Int. J. Eng. Sci. Invent.* **2013**, *2*, 28–34.
75. Roy, B. The Outranking Approach and the Foundations of Electre Methods. *Theory Decis.* **1991**, *31*, 49–73. [CrossRef]
76. Połom, M. E-Revolution in Post-Communist Country? A Critical Review of Electric Public Transport Development in Poland. *Energy Res. Soc. Sci.* **2021**, *80*, 102227. [CrossRef]
77. European Commission. *Annex to the Proposal for a Council Implementing Decision on the Approval of the Assessment of the Recovery and Resilience Plan for Poland*; European Commission: Brussels, Belgium, 2022.
78. Polishnews Surcharges for Electric Cars. My Electrician Program Start. Available online: https://polishnews.co.uk/surcharges-for-electric-cars-my-electrician-program-start/ (accessed on 10 July 2022).
79. Bates, K. Subsidies for Electric Bikes in the First City in Poland! GAMINGDEPUTY 2022. Available online: https://www.gamingdeputy.com/subsidies-for-electric-bikes-in-the-first-city-in-poland/ (accessed on 10 July 2022).
80. Kudełko, M. Modeling of Polish Energy Sector—Tool Specification and Results. *Energy* **2021**, *215*, 119149. [CrossRef]

MDPI
St. Alban-Anlage 66
4052 Basel
Switzerland
www.mdpi.com

Energies Editorial Office
E-mail: energies@mdpi.com
www.mdpi.com/journal/energies

Academic Open
Access Publishing

mdpi.com

ISBN 978-3-0365-8909-1